

American University in Cairo

AUC Knowledge Fountain

Theses and Dissertations

6-1-2016

Fabrication of polyvinyl alcohol / chitosan / bidens pilosa composite electrospun nanofibers and their enhanced antibacterial activities

Kegere James

Follow this and additional works at: <https://fount.aucegypt.edu/etds>

Recommended Citation

APA Citation

James, K. (2016). *Fabrication of polyvinyl alcohol / chitosan / bidens pilosa composite electrospun nanofibers and their enhanced antibacterial activities* [Master's thesis, the American University in Cairo].

AUC Knowledge Fountain.

<https://fount.aucegypt.edu/etds/249>

MLA Citation

James, Kegere. *Fabrication of polyvinyl alcohol / chitosan / bidens pilosa composite electrospun nanofibers and their enhanced antibacterial activities*. 2016. American University in Cairo, Master's thesis. AUC Knowledge Fountain.

<https://fount.aucegypt.edu/etds/249>

This Thesis is brought to you for free and open access by AUC Knowledge Fountain. It has been accepted for inclusion in Theses and Dissertations by an authorized administrator of AUC Knowledge Fountain. For more information, please contact mark.muehlhaeusler@aucegypt.edu.



THE AMERICAN UNIVERSITY IN CAIRO
الجامعة الأمريكية بالقاهرة

School of Sciences and Engineering

Fabrication of Polyvinyl alcohol / Chitosan / *Bidens Pilosa* Composite Electrospun Nanofibers and their Enhanced Antibacterial Activities

A Thesis Submitted to
The Nanotechnology Master's Program
In partial fulfilment of the requirements for
The degree of Master of Science

By:

Kegere James

Under the supervision of:

Dr. Wael Mamdouh (Supervisor)

Department of Chemistry, The American University in Cairo

&

Dr. Rania Siam (Co-supervisor)

Department of Biology, The American University in Cairo

February 09, 2016

Acknowledgements

I would like to thank my thesis advisor Dr. Wael Mamdouh who provided me with solid support at every time I needed it and he worked around the clock to ensure the work in this research was steered in the right direction and yet consistently allowed it to be my own.

I extend my sincere thanks to my thesis Co-advisor Dr. Rania Siam for providing me with knowledge and support on how to carry out some crucial tests. Dr. Rania's door was always open whenever I needed help and she ensured I received the right assistance where I need specialized help.

I would like to register special appreciation to Dr. Adam Ramadan for the tremendous support he has rendered me in this work. Dr. Adam always had solutions to my problems even before I uttered them to him. He provided me with the vital support to secure my studies and research at AUC and enabled this work to progress smoothly even when it all looked difficult.

I thanks Sawsan Mardini the director graduate studies services and fellowships for providing me with the facilitation and ensuring all went well regarding my welfare and studies. Ms Sawsan worked tirelessly to ensure I got the necessary requirements and also provided me with the opportunity to discuss my progress and Challenges at every time I talked to her.

I salute my Family for standing with me from the inception of this program to its completion. With their backing, it was easier to work harder and achieve this result. In particular I thank Charles Muthuthi, Charles Sendaaza, Fahad Kimera, Josephine Kwagala and Julia Kegere for providing me with support and care that enabled me to do my tasks at ease.

I finally wish to thank all my colleagues and Friends in the research team (Sara, Mona, Habiba, Lila, Raneem, Sandra, Rua, Nada, and Ghada), Chemistry Department Assistant Ahmed Omia for the support they provided me since joining them in the research team until the time this work reached completion and also Amged Ouf from the biology deartment for the antibacterial tests.

Abstract

Given the current Challenges faced by the increasing rate of drug resistant bacteria, a lot of attention has been shifted from synthetic antibiotic products to natural products that are eco friendly and have a wide spectrum of activity when exposed to pathogens.

The main objective of this research was to successfully fabricate electrospun nanofibers from polyvinyl alcohol, polyvinyl alcohol blended with Chitosan, *Bidens pilosa* (Both distilled and crude extract) composite blends and investigate their potential antibacterial activities against *E. coli* and *S. aureus*. Fabrication of nanofibers was performed by the electrospinner technique which applies high voltage on the polymer forcing it to spinoff as a spray onto a collector. Characterization of the nanofibers was successfully performed by Scanning electron microscopy (SEM), Fourier Transform infrared (FT-IR) spectroscopy technique. To study anti bacterial effect, *E.coli* and *S. aureus* were cultured in Luria Broth liquid media for 24 hrs at 37 °C after which nanofibers from different composite blends were exposed to the bacteria in three well plate. Hourly measurements of optical density using a spectrophotometer were carried out. Results obtained show enhanced antibacterial activity of composite nanofibers obtained from combinations containing either crude extract or Chitosan. Whereas Chitosan nanofibers are already well researched and its anti microbial property vastly known, *Bidens pilosa* although known to possess biomedical properties, its anti bacterial properties in nanofiber form have not been reported in literature.

Table of Contents

List of Abbreviations.....	ii
List of Figures.....	vii
List of Tables	X
Chapter 1 Introduction and Literature Review.....	1
1.1 Bacterial infections.....	2
1.1.1 Existing methods used in treating bacterial infections.....	3
1.1.2 Draw backs in the current methods used in treating bacterial infections.....	4
1.1.3 Biofilm formation process.....	7
1.2 Nanotechnology and Nanomaterials.....	7
1.2.1 Nanotechnology in biomedical industry.....	9
1.2.2 Nanoscale vs bulk scale materials.....	11
1.2.3 Biology at nanoscale.....	13
1.2.4 Nanotechnology in wound care.....	15
1.2.5 Nano-composites and scaffolds.....	18
1.2.6 Applications of nanofibers.....	20
1.2.6.1 Methods of fabricating nanofibers.....	20
1.2.6.3 Fabrication of Nanofibers with natural extracts.....	21
1.2.6.3 .1 Polyvinyl alcohol (PVA) Nanofibers.....	21
1.2.6.3 .2 Chitin and Chitosan.....	23

1.2.6.3	.3	Anti-microbial activity of Chitosan.	25
1.3		Herbal extracts	27
1.3.1		Bidens pilosa	28
1.4		Electrospinning technique	29
1.4.1		Parameters controlling the electrospinning process.	30
1.4.1.1		Solution Parameters	30
1.4.1.1.1		Concentration	30
1.4.1.1.2		Molecular Weight	31
1.4.1.1.3		Viscosity	32
1.4.1.1.4		Conductivity/Surface Charge Density	33
1.4.1.2		Processing Parameters	34
1.4.1.2 .1		Voltage	34
1.4.1.2 .2		Flow rate	34
1.4.1.2 .3		Distance (H) Between the Syringe tip and the collector	35
1.4.1.2.4		Type of Collector	35

1.4.1.2	.5	Ambient
factors.....	35	
1.5	Aim	of
work.....	36	the
Chapter	2	Materials
Methods.....	37	and
2.1 Materials.....	38	
2.2 Synthesis procedures.....	38	
2.2.1 Synthesis of composite Nanofibers.	38	
2.2.1.1 In-situ Blends.....	38	
2.2.1.2		In-situ/Ex-situ
Blends.....	39	
2.2.1.3 Ex-situ Blends.....	39	
2.3		Characterization.
.....	39	
2.3.1 Scanning Electron Microscope (SEM).	39	
2.3.1.1 Background.....	39	
2.3.1.2 Theoretical background of SEM	40	
2.3.1.3	Preparation	.of
test.....	40	samples
		for
		SEM
2.3.2 Fourier Transformation Infra-Red Spectroscopy.....	41	
2.3.2.1 Background.....	41	
2.3.2.2 Operation principle of FTIR Spectrometer.....	41	

2.3.2.3 Preparation of samples for FTIR.....	42
2.3.3 Cross linking.....	43
2.3.3.1 Swelling and weight loss tests.....	43
2.3.3.1.1 Test procedure.....	43
2.3.3.1.2 Calculating degree of swelling.....	43
2.3.4 Anti-Bacterial tests.....	43
2.3.4.1 Luria Broth liquid media method.....	43
2.3.4.2 Media preparation.....	44
2.3.4.3 Bacteria culture.....	44
2.3.4.4 Preparation of bacteria culture.....	45
2.3.4.5 Preparation of the samples.....	45
Chapter 3 Results and Discussion – Part I.....	48
3.1 SYSTEM VALIDATION.....	49
3.2 Composite Nanofibers.....	49
3.2.1 Cold extract Bidens pilosa distilled Bidens pilosa and Chitosan Nanofibers.....	50
3.2.2 Insitu Composite mixtures.....	50
3.2.2.1 PVA Nanofibers.....	50
3.2.2.2 PVA dissolved in Distilled Bidens pilosa (PVADBP) Nanofibers.....	51

3.2.2.3	PVA	in	extract	Bidens	pilosa	(PVAEXT)	
Nanofibers.....							51
3.2.3		In-situ		mixtures		with	
Chitosan.....							53
3.2.3.1			PVA			and	
Chitosan.....							53
3.2.3.2	PVA	in	distilled	Bidens	pilosa	and	Chitosan PVADBP:
CS.....							53
3.2.3.3	PVA	in	crude	extract	Bidens	pilosa	and
PVAEXT:CS.....							53
3.2.4 Ex-situ mixtures.....							54
3.2.4 .1 Polyvinyl alcohol and distilled Bidens pilosa PVA: DBP.....							54
3.2.4 .2 PVA and Cold extract Bidens pilosa (PVA: EXT).....							55
3.2.5		Ex-situ		mixtures		with	
Chitosan.....							56
3.2.5.1 PVA, Distilled Bidens pilosa and Chitosan Nanofibers (PVA: DBP: CS).....							56
3.2.4.2 PVA, Crude Extract Bidens pilosa and Chitosan Nanofibers (PVA: E XT: CS).....							57
3.3	Effect	of	working	parameters	on	the	morphology
of Nanofibers.....							58
3.3.1	Effect	of	Voltage	on	In	situ	mixtures.
.....							58
3.3.2 Effect of flow rate on Nano fiber morphology.							59
3.3.3		Effect		of		Collector	
distance.....							62
3.3.4 Effect of solution concentration.....							64

3.3.5	Effect	of	ratio	adjustments.	66								
3.3.6	Effect	of	differences	in the	molecular	weight	of	Chitosan.	68				
3.4	Discussion.								69				
3.5	Water	Immersion	tests.							75			
3.6	Fourier transform infra-red spectroscopy.								76				
3.7	Discussion.								80				
Chapter 4 Results and Discussion – Part II									81				
4.	Anti-bacterial	tests	results.							82			
4.1	Effect	of	Pure	extract	PVA	on	test	bacteria.	82				
4.2	Effect	of	Pure	extract	and	Pure	distilled	Bidens	pilosa	on	test	bacteria.	83
4.3	Effect	of	PVADBP	and	PVAEXT	nanofibers	on	test	bacteria.	85			
4.4	Effect	of	PVA: CS	and	PVA: DBP: CS	nanofibers	on	test	bacteria.	86			
4.5	Effect	of	PVADBP: CS,	and	PVAEXT: CS	nanofibers	on	test	bacteria.	87			

4.6 Discussion	89
Chapter 5 Conclusion and Future work.....	91
CONCLUSION & FUTURE WORK.....	92
Chapter 6	6
References.....	94
References.....	95

List of Figures

Figure 1.1 Leading causes of death in 2014 and ARM projection in 2050 (1).	2
Figure 1.2 List of antibiotics developed since original discovery (6).	4
Figure 1.3 Showing a decline in antibiotic development since 1980 (8).	5
Figure 1.4 (a) Stages of bacterial colonization. (b) SEM image of biofilm (11).....	6
Figure 1.5 Factors involved in the biofilm formation (14).	7
Figure 1.6 Image of the Lycurgus cup which shines red when illuminated from the front (right) and green when illuminated from the back (left) (18).....	8
Figure 1.7 Increase in surface area with decrease in size towards nanoscale (36).....	13
Figure 1.8 Structure of DNA Nano-cages with capacity for multiple applications (35).....	14
Figure 1.9 Structure of PVA unit (63).....	21
Figure 1.10 SEM micrograph of PVA Nanofibers diluted in DI water obtained at a voltage of 13KV and flow rate of 3mL/hr and scale bar 40µm (64).....	22
Figure 1.11 SEM image of antimicrobial (a) PVA/Chitosan and (b) PVA/ AgNO ₃ nanofibers (X50000 magnification) performed at a voltage 5KV and 15KV respectively. (65).....	23
Figure 1.12 Structure of Chitin in (a) worms, (b, c and d) insects and (e) crustaceans (66).....	24
Figure 1.13 Chemical structure of (a) Chitin, (b) Chitosan, and (c) De-acetylation of chitin to form chitosan (66).....	25
Figure 1.14 Different forms of Chitosan for biomedical applications (a) films, (b) gels, (c) microspheres, (d) tubes, (e) sponges and (f) powder (67).....	26
Figure 1.15 SEM micrographs of <i>S. simulans</i> cells (a), control, then (b), (c), and d which are treated with chitosan for: 5 mins, 20 mins, and 60 mins respectively. Insets show magnified single cells. Bars, 2 µm (a to d) and 200 nm (for magnified cells (a) to (d)) (67).....	27

Figure 1.16 Schematic of a typical electrospinning system. While the polymer solution is pushed through the orifice, the electrostatic forces must be greater than the surface tension of the solution at which stage the polymer forms a Taylor cone and subsequently (62). 30

Figure 1.17 SEM images showing the effect of concentration scale bar 100µm, with voltage fixed at 15KV, (a) 5 wt%, (b) 10wt %, (c) 25wt% and (d) 40 wt % (72).....31

Figure 1.18 SEM Images of typical structure in the electrospun polymer for various molecular weights. (a) 9000–10,000 g/mol; (b) 13,000–23,000 g/mol; and (c) 31,000–50,000 g/mol (solution concentration 25 wt. %) (72).....32

Figure 1.19 SEM images showing the effect of viscosity, obtained by adjusting the concentration of the solution (Molecular weight of PAN is 150000) (a) low viscosity (1.3%) and (b) higher viscosity (15%) (72).....33

Figure 1.20 SEM images of PSF solution in DMAC/acetone solution with differing voltages as indicated inside the micrographs (a), (b) and (c). The average diameter for (a), is 344, 331 for (b) and 323 for case (c). The average diameters of (a), (b), and (c) are 344 ± 51 , 331 ± 26 , and 323 ± 22 nm, respectively (72).....34

Figure 1.21 SEM images of PSF nanofibers at different flow rates. (a) 0.4mL/hr and (b) 0.66mL/hr at a fixed voltage of 10kv (72).....35

Figure 1.22 Illustration of the composite materials synthesis.....36

Figure 2.1 Scheme showing the working principle of SEM (73).....40

Figure 2.2 FTIR Spectroscopy (74). 42

Figure 2.3 Images of E. coli (A) and S. aureus (B) (79). 44

Figure 2.4 A schematic presentation illustrating the sample preparation steps for anti-bacterial tests.....46

Figure 3.1 SEM Images of (A) PVADBP, (B) PVADBP: CS (C) PVAEXT and (D) PVAEXT: CS Nanofibers at WD6 (x30000 magnification) obtained at a voltage of 16KV, flow rate of 1mL/hr and collector distance of 13cm49

Figure 3.2 SEM images of PVA (a), PVADBP (b) and PVAEXT (c) at WD6, (x30000 magnification), and their histograms (d), (e), and (f) at 16kv, 1mL/hr and 13cm collector distance.....52

Figure 3.3 SEM image of PVA: CS (a), PVADBP: CS (b) and PVAEXT: CS (c) nanofibers at WD6, histograms (d), (e) and (f) for fiber diameter distribution, at 4:1 ratio, a flow rate of 1.5mL/hr. and collector distance of 12cm. The arrow in the Figure points to the formed beads.....54

Figure 3.4 SEM images of PVA: DBP (a) and PVA: EXT (b) nanofibers at WD6, (x30000 magnification) with their fiber diameter distribution histograms (c) and (d) obtained at a voltage of 16KV and 1mL/hr. of flow rate.....56

Figure 3.5 SEM images of PVA: DBP (a) and PVA: EXT (b) nanofibers with Chitosan of concentration 3% at WD6 (x30000 magnification) with their fiber diameter distribution histograms (c) and (d) obtained at a voltage of 16KV and 1mL/hr. of flow rate.....57

Figure 3.6 SEM images of PVADBP nanofibers with effect of voltage (a) (16kv), (b) (18kv) and (c) (21kv) on 8% at WD6 (x30000 magnification), flow rate 1mL/hr., distance of 12cm with their histogram (d), (e) and (f) for fiber diameter distribution.....59

Figure 3.7 SEM images of PVADBP nanofibers with effect of flow rate (a) (0.8mL/hr), (b) (1mL/hr) and (c) (1.2mL/hr) on 8% at WD6, (x30000 magnification), obtained at 16KV and collector distance of 12cm with their histogram (d), (e) and (f) for fiber diameter distribution.....61

Figure 3.8 SEM images of Insitu composite nanofibers investigating effect of collector distance (a) 12cm, (b) 13cm and (c) 14cm at WD6, (x30000 magnification), with histograms (d), (e), and (f) for fiber diameter distribution at voltage of 16kv.....63

Figure 3.9 SEM images of PVADBP nanofibers electrospun at WD6, (x30000 magnification), flow rate 1mL/min and voltage 16kv from PVA solutions concentration (w/w): (a) 6%, (b) 8%, (c) 10%, and (d) 12%, (w/w), respectively.....65

Figure 3.10 Changes in viscosity with Change in concentration of PVADBP.....66

Figure 3.11 SEM images showing the Effect of solution Ratio for PVA: CS ((A) 3:1, (B) 4:1) and PVA: DBP: CS ((C) 4:1:1, (D) 5:1:1) nanofibers at WD6, voltage of 16kv, flow rate of 1mL/h and collector distance of 13cm.....67

Figure 3.12 Viscosity of the different molecular weights of chitosan.....69

Figure 3.13 Effect of voltage on nanofiber diameter on Polysulfone nanofibers at a fixed flow rate of 4mL/hr. and distance of 150mm. (81)70

Figure 3.14 Effect of feed rate on Polysulfone nanofibers morphology obtained at a fixed voltage of 20KV and collector distance of 150mm (81).....71

Figure 3.15 SEM images of PVA and Chitosan blend electrospun nanofibers with different weight at varying ratios of PVA/CS; (A) 90/10, (B) 80/20, (C) 75/25, and (D) 70/30 (83) obtained at a constant voltage of 15KV (81).....73

Figure 3.16 Average diameter of the electrospun PVA and Chitosan nanofibers as a function of the weight ratio (PVA/CS) (84).74

Figure 3.17 Size distribution of diameters in nanofibers electrospun from polyethylene oxide PEO/water solutions: (a) 7 wt%; and (b) 10 wt% (84).....74

Figure 3.18 Water Immersion test for weight loss and swelling capacity of the nanofibers.....75

Figure 3.19 FTIR Charts for (a) Chitosan (b) PVA and (c) PVA: CS blend at a ratio of 4:177

Figure 3.20. FTIR Charts for crude extract and distilled extract *Bidens pilosa* showing detailed composition of their individual functional groups.....78

Figure 3.21 FTIR Charts for Crude extract (a) distilled *Bidens pilosa* in PVA nanofibers (PVADBP), (b) crude extract *Bidens pilosa* in PVA nanofibers (PVAEXT) Showing changes that occur in their blends and (c) distilled *Bidens pilosa* in PVA nanofibers and Chitosan.....79

Figure 4.1 Growth curves for *E. coli* and *S. aureus* with PVA nanofibers.....83

Figure 4.2 Growth curves for *E. coli* and *S. aureus* with (a) PVA dissolved in extract *Bidens pilosa* nanofibers (PVAEXT), and (b) PVA dissolved in distilled *Bidens pilosa* nanofibers (PVADBP).....84

Figure 4.2 Growth curves for *E. coli* and *S. aureus* with (a) PVA dissolved in extract *Bidens pilosa* nanofibers (PVAEXT), and (b) PVA dissolved in distilled *Bidens pilosa* nanofibers (PVADBP).....85

Figure 4.3 Growth curves for *E. coli* and *S. aureus* with (a) PVA and chitosan nanofibers, (b) PVA, Distilled *Bidens pilosa*, and Chitosan.....87

Figure 4.4 Growth curves for *E. coli* and *S. aureus* with (a) PVA dissolved in distilled *Bidens pilosa* and chitosan Nanofibers, and (b) PVA dissolved in crude extract and chitosan nanofibers.....89

List of Tables

Table 1.1 Different types of nanocomposites (54).....	19
Table 1.2 Classification of <i>Bidens pilosa</i> (70).....	28
Table 2.1 Preparation of composite materials and parameters for their electrospun nanofibers.....	38
Table 2.2 Summary of differences between gram positive and gram negative bacteria (79).....	45
Table 2.6 Samples for anti-bacteria tests are summarized.....	47
Table 3.1 Viscosity of the PVADBP solution at different concentrations.....	66
Table 3.2 Results of the water immersion test.....	76
Table 4.1 Materials tested against <i>E.coli</i> and <i>S. aureus</i>	83

List of Abbreviations.

PVA: Polyvinyl alcohol

CS: Chitosan

DBP: Distilled *Bidens pilosa*

EXT: Crude extract *Bidens pilosa*.

O.D: Optical Density

PVADBP: Polyvinyl alcohol dissolved in distilled *Bidens pilosa*.

PVAEXT: Polyvinyl alcohol dissolved in crude extract *Bidens pilosa*.

FTIR: Fourier Transform Infrared spectroscopy.

SEM: Scanning electron microscopy.

HMWC: High molecular weight Chitosan.

MMWC: Medium molecular weight Chitosan.

LMWC: Low molecular weight Chitosan.

WHO: World Health Organization.

NPs: Nanoparticles.

List of equations

Equation 2.1 Fourier transform.....	42
Equation 2.2 Degree of swelling.....	43
Equation 2.3 Weight lose test.....	43

Chapter 1

Introduction and Literature Review

1. Introduction

1.1 Bacterial infections

Pathogenic micro-organisms had been a total menace to human populace for very long time and by the early 19th century, bacterial infections in particular comprised some of the leading killers. After the penicillin discovery however the trend changed owing to the developments that took place to enhance the functionality of antibiotics and by the second half of the 19th century, the threat posed by pathogenic bacterial was contained and there was relative ease albeit a few isolated cases. The hope of eradicating microbial infections through antibiotics has however been eroded by the development of "super bugs" that exhibit resistance to antibiotics and adversely affected the development of antibiotics as depicted in Figure 1.1 (1).

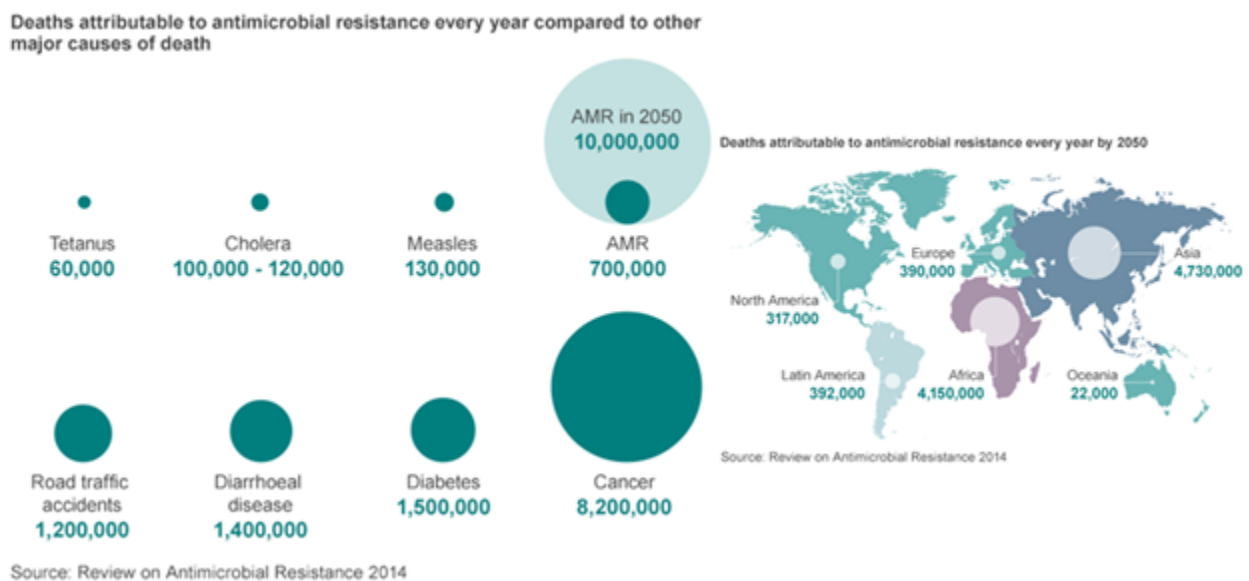


Figure 1.1 Leading causes of death in 2014 and ARM projection in 2050 (1).

As archeological findings indicate, infections have been part of human history since ancient ages. At some points of human existence, infection caused by viruses, bacteria, and to some extent protozoa have threatened and endangered human existence. Plaques like the “bubonic plaque”, ‘black death’, the great white plaque among others are some of those well documented human catastrophes that were caused by deadly microbial infections (2). Despite the technological edge in the modern history, especially the medical sector, pandemics caused

by microbial infections continue to cause uncertainty. With the rate of anti-biotic resistance being developed by bacteria which has stunned the world the scientific community and policy makers alike are engaging a protracted search for remedies to give humanity a modicum of hope (3). Bacterial infection are ubiquitous in our world today especially in the developing world where access to disinfection is not possible for every person and although in the developed world antibiotics are easy to access, bacterial infections are proving difficult to contain due to the evolving antibiotic resistance exhibited by a wide range of pathogenic bacteria (3, 4).

Bacterial infections generally fall into two classes i.e. acute and chronic infections with classification based on the virulence products due to differences in gene expression along with the bacterial infection style and duration. Acute infections are characterized by a brief infection period that is carried out by single planktonic cells which are known for their cruelty and efficiency. They normally occur through tissue damage and production of a huge amount of virulence factors (molecules produced by pathogens). Clinical symptoms associated with these kinds of infections are usually treated by a single or limited number of antibiotics. On the other hand, chronic infections are caused by biofilms which are bacterial aggregates covered by a matrix made of, proteins, exopolysaccharides, DNA and fatty acids. These kinds of infections are difficult to treat as they persist despite administration of anti-biotics (4, 5).

1.1.1 Existing methods used in treating bacterial infections

Bacterial infections have been treated by the use of antibiotics since 1940 and through the 20th century. So far, anti-biotics offer the first line of defense against diseases attributed to bacteria. Discovery of antibiotics remains one of the milestone achievements of medicine in modern era and has saved millions of lives from deaths that characterized the 19th century. Antibiotics act by manipulating the biochemistry of the invading bacteria and not human biochemistry (6).

Many different classes of antibiotics, as shown in Figure 1.2, have been developed since the original discovery to those that are in use today.

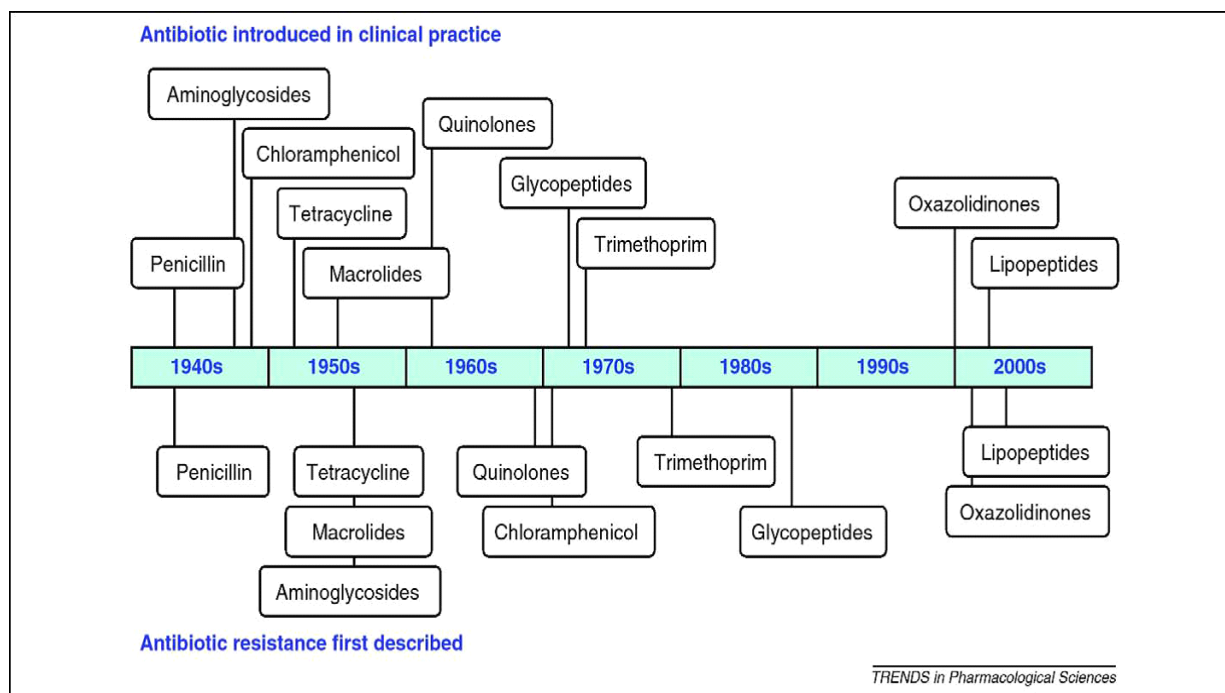


Figure 1.2 A list of antibiotics developed since original discovery (6).

1.1.2 Draw backs in the current methods used in treating bacterial infections.

Challenges of antibiotics appeared almost as soon as the penicillin was identified by Alexander Fleming in 1928. Earlier years before penicillin discovery, as therapeutic agent, members of the penicillin research team discovered an enzyme penicillinase that cleaves penicillin and thus render it ineffective. Once the antibiotic was established, despite initial breakthroughs, strains capable of rendering the drug ineffective soon appeared and thus necessitated measures to reinvigorate the active ingredient of the penicillin and be able to overcome penicillinase activity. Discovery of penicillinase before the use of penicillin drug is currently being revisited with keen interest as challenges of antibiotic after studies of penicillinase from bacteria opened new insights into a group of *r* genes as components of the natural microbial populations. So the question of whether resistance to antibiotics came before the drug have been investigated since 1944 when “streptomycin”, a drug for Tuberculosis, developed resistance during the treatment of the disease caused by mycobacterium tuberculosis.

In 1950, the genetic transfer of anti-biotic resistance was discovered in Japan, and was first received with doubt in the west. That was a milestone into the understanding the concept of

transfer of r gene (resistance genes) for resistance in bacteria by conjugation (7). Consequently, many drugs were developed to counter this resistance. Bacterial infections were quickly controlled at the onset of antibiotic administration, however with time, these microbes developed drug resistance to these active compounds. This new dilemma enlisted further research to alter a given drug after exposure to bacteria and this became the norm (7). The trend above has thus characterized the emergence of several kinds of antibiotics against bacterial infections. Bacterial resistance to drugs took a different course during the last few decades and the impact on anti-bacterial drug research was drastic as depicted in Figure 1.3 below (8).

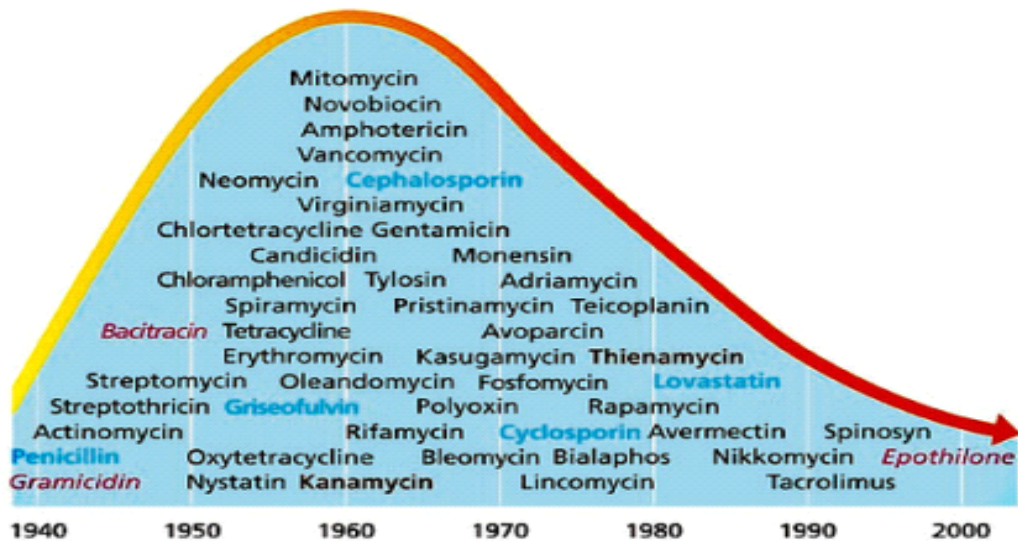


Figure 1.3 Showing a decline in antibiotic development since 1980 (8).

Several factors have been proposed for this phenomena and among them include climate change which has created a conducive environment for microorganisms to thrive where previously weather conditions could not permit. Such changes also facilitate targeted mutations which enable bacteria develop resistance against antibiotics have also been of recent enhanced partly due to changes in the microclimate of their hosts in nature and also emergency of new pathogens as conditions become conducive for their survival. This is enhanced by the formation of biofilms at the sites of infection which make it very hard for the drug to penetrate the defense barrier to reach the bacterial cells. A biofilm is composed of multiple cells clustered together and function as a single unit and is the first event that occurs in the process of site

colonization by invading bacteria. Biofilm formation is similar in other unicellular organisms which despite the ability to survive independently, prefer to aggregate to form clusters that is covered by a membrane and offers member cells the following benefits: Improved cell attachment to their hosts, enhanced access to nutrients and ultimately provides protection from adverse environment. A good example of a biofilm favoring bacteria is the *Caulobacter crescentus*, which lives in nutrient deficient environment and by forming a biofilm enhances its accessibility to organic matter (9, 10, and 11).

In general, biofilms account for more than 80% of bacterial infections in humans and the process of biofilm formation creates bacteria that is 1000 times more resistant to antibiotics in relation to planktonic bacterial cells. For instance, *S. aureus*, *E. coli*, and *P. aeruginosa* are very virulent and cause high morbidity due to creation of persistent biofilms at infections sites. This is the same with *vibrio cholera* which causes diarrhea in order to survive in water and in the gut of humans (11, 12). Other bacterial biofilms are beneficial to humans for example those of *Bacillus sp* in root nodules are very important in nitrogen fixation in plants. The process through which bacteria form biofilms is shown in Figure 1.4 (11).

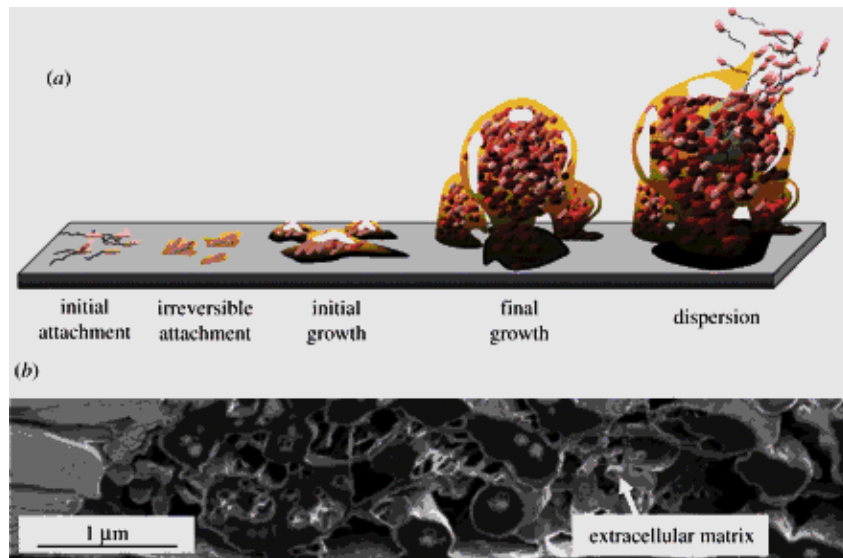


Figure 1.4 (a) Stages of bacterial colonization. (b) SEM image of biofilm (11).

1.1.3 Biofilm formation process

Initiation of biofilm formation by planktonic cells is still to be fully elucidated, however extra cellular matrix in bacteria plays a critical role in biofilm development just like regulation of cellular activities in multicellular organisms. Most important initial step in biofilm formation in bacteria is accumulation of cyclic dinucleotide (c-di-NMPs) in the environment surrounding cells. This event triggers signals that lead to the activation of interferon 1 immune response type which is well known response in case of bacterial infection (9,13, 14, 15). The process of biofilm formation is summarized in Figure 1.5 (14).

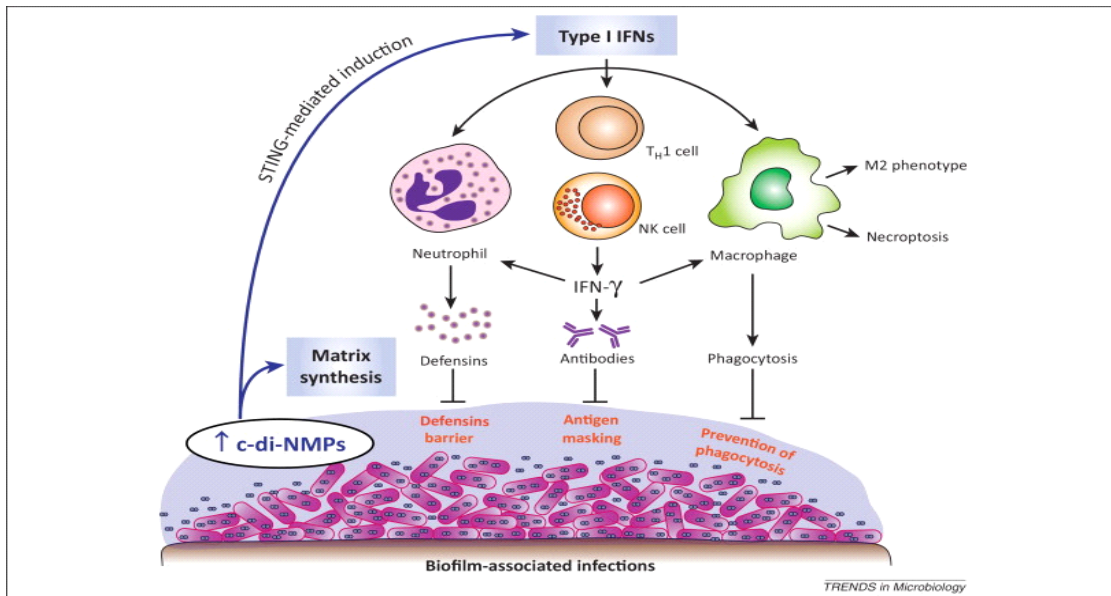


Figure 1.5 Factors involved in the biofilm formation (14).

1.2 Nanotechnology and Nanomaterials

Nanotechnology has been in existence for many centuries although, real ground breaking discovery into the potential of materials at the bottom was made in the 20th century. NPs were in use in ancient times in spite of lack of evidence to prove existent knowledge on exactly the science of these materials but the technology was in existence. Ancient Egyptians for example used nanomaterials in their monumental clay works in which clay works containing particles at nanoscale that preserved the glossy appearance and quality for thousands years. Another way

in which NPs were used is evidenced in the Roman Lycurgus cup depicted in the Figure 1.6 that changes color when exposed to light of different wave lengths (18).



Figure 1.6 Image of Lycurgus cup which shines red color when light is illuminated from the front (right) and shows green when illuminated from the back (left) (18).

Although Nanotechnology was exploited in ancient times, the full knowledge of nanoscale properties were not developed largely because lack of capacity to manipulate nature as advanced as it is in modern times. First insights into nanoscale science was published in Albert Einstein paper in 1905 when he postulated the size of sugar molecule (19). The birth of modern nanotechnology is traced back to the famous lecture by Richard Feynman “There is plenty of room at the bottom” (19). This lecture opened a new thinking into potential of miniaturizing materials and have bulk volumes of material for example encyclopedia volumes to house in a small pin. This lecture focused on references derived from cells which despite their small size are very active and produce enormous substances in form of products. The invention of Atomic force microscope by Gerd binning and Heinrich Rohrer and the building of the first Scanning electron microscope SEM by IBM, further reinforced Dr. Feynman’s dream (19). This ground breaking discovery was followed by the first publication of nanotechnology by Eric Drexler in 1986 titled “Engines of creation” which highlighted the manipulation of matter at nanoscale through self-assembly of these particles. Currently nanotechnology is the engine of new technological age and multiple applications are currently being developed in different sectors among which include, biomedical, plastics, aerospace, electronics and construction industries. Some good examples of such products of nanotechnology in these sectors include carbon

nanotubes, fullerenes their products, quantum dots, NPs, and nanocomposite materials (20). Recent developments in physical sciences, biotechnology, medicine and biology and molecular sciences have all incorporated nanotechnology and thus created an interface between all these fields with one denominator as nanotechnology (21, 22). With this enormous attention, nanotechnology has attracted attention from both research and policy making. Governments and non-government organizations around the world have embarked on promotion and fostering of new nanoinspired technologies and by 2012 the funding for nanotechnology was over 1 trillion dollars (20, 21). The United States of America alone has got 23 Federal nanotechnology research fostering organizations with a multibillion dollar budget (22).

1.2.1 Nanotechnology in Biomedical industry.

Biomedical applications of nanotechnology are some of the most evolved and intensively researched areas of Nanotechnology. These applications range from drug delivery to specific tissues in the body, ultra filtration to eliminate even the finest contaminant, anti-microbial properties among others. Nanotechnology has therefore revolutionized the biomedical industry in all aspects and this has given medical scientists unique abilities. The charges of this technology is engrained in its unique and novel physical, chemical and biological properties as the size of a material approaches the nanoscale i.e. 10^{-7} to 10^{-9} m in size (22). One of the rapidly expanding biomedical frontiers of nanotechnology is the development of nanosensors for biological processes and conditions. Inroads into the nanosensor research has led scientists to believe that nanates (nanomaterials) and nanites (nanomachines) will soon be employed in human body to monitor metabolic changes as early warning systems to defend against disease developments and also monitor disease progress in tissues, and finally metabolism in the body. These biosensors would provide scientists with a video or a quick “snap shot” of the biochemical processes taking place in cells at a given time. Nanotechnology is also actively being exploited in the development of multifunctional delivery vehicles for drugs and other substances directly into cells or tissues (23). Nanomaterials used in drug delivery, are tailored around viruses like adenoviruses or nanocages or particles and fibrous materials, for example; dendrimeric materials, magnetic NPs, nanofibers, and nonporous materials (24, 25). The

unique ability of engineered NPs to deliver customized drugs and other therapeutic agents directly to the tissues enable medical practitioners to target specific infected cells or tissues and be able to alter the biochemistry of these cells, and create balance in biomolecules (hormones, cytokines, receptors, enzymes etc.) and gene therapy that involves introduction of new genes or altering the existing genes to be able to amend biochemical disorders and diseases. Beyond drug and gene delivery, Researchers have been investigating the possibility of exploiting drug and gene delivery nanates as weapons against a diseased tissue by engineering them as “smart bombs” which do both targeting and destroying diseased or damaged tissues or cells a condition that would bear semblance to the natural programed cell death also known as apoptosis (26). This approach would be very important in the treatment of cancers and viral infections.

Nanotechnology has so far been successfully employed in the treatment of diseases like diabetes (27). Studies by Yamuguchi *et, al* revealed the use of NPs coated with calcium carbonate could contribute to regeneration of beta cells in vivo which is very important in the treatment of diabetes. Some pharmaceutical companies have also picked keen interest in the use of Nano controlled delivery of insulin to diabetic patients so as to control the release of insulin to be delivered only when it's necessary along with monitoring of blood glucose levels (28).

This application is very useful in scientific research in mutation analysis, DNA diagnosis, Haplotyping, study of protein expression, Single nucleotide Polymorphism analysis, immunoassay, and as a disease marker detection tool (29).

Nanotechnology is also being investigated with keen intensity to be employed in cancer therapy. Cancer cells are characterized by uncontrolled proliferation (30). Because of this uncontrolled cell division, certainly cancer cells develop with abnormalities which provides scientists with the ease of targeting them since they develop with unique intracellular and extra cellular signaling events. Through use of materials on which cell division is dependent, it's possible to identify and target exclusively cancer cells. So by incorporating anticancer agents with these materials targeting of cancer cells is enhanced and scientists can then develop

cancer specific drugs that will not affect healthy cells or tissues unlike current remedies like thermotherapy, chemotherapy, and radiotherapy which destroy all cells including health cells. Although these technologies are still largely in theory, the reality that they promise has invigorated research agencies, and policy agencies to invest intensively in this highly coveted technology with hope of having rare diseases remedied.

Nanotechnology has also proven promising in separation technology. Biomolecules like DNA, RNA, proteins (peptides and poly peptides), glycoproteins and polysaccharides are separated by use of Nanotechnology (31). Regenerative medicine is another area which has under gone a major metamorphosis with the discovery of nanotechnology. Researchers have been able to isolate single cells from tissues grown in temperature sensitive conditions when carried out at temperature below 32 °C and thus opens possibilities of tissue reconstruction for example the corneal regeneration (32). In this regard, researchers have identified soft and wet materials like hydrogels with important applications like cartilage replacement and they believe nanoengineered hydrogels possess similar or even more powerful properties to the cartilage yet without harmful properties that were associated with the traditional cartilage replacement methods which is normally limited to use of dry and hard substances which are susceptible to friction and bacterial invasion.

Synthetic bone and nerve tissue engineering is another tissue engineering field that has been boosted by the advances in nanotechnology. Nanoengineered bones are by far stronger than their natural counterparts and yet have similar functional properties and thus limited harmful effects (33). Future research is set to focus on generating complete organs of any system in human body and in the process alleviate the challenges associated with organ transplant as well as complications that arise from infections, rejections and also scarcity of organ donors. In cell and tissue engineering, nano materials are used as media to encourage regeneration and division of cells and tissues

1.2.2 Nanoscale vs. bulk scale materials

Recent development in microscopy has enabled scientists to discover and understand the behavior of matter at nanoscale which occurs naturally. Most fundamental chemical and biological processes in nature occur at nanoscale. This phenomena is critical as it provides insights into how nature best applies the concept for effective and unfettered biochemical control and systems coordination. This concept is in turn used to develop systems that mimic what happens at nanoscale for example scientists are able to use this knowledge to enhance processes like catalysis, computing , printing, material synthesis, medicine, imaging, and many others. Nanotechnology is not just concerned with small dimensions but rather building systems or materials that will utilize a scale that enables them have superior physical, mechanical biological, optical and chemical properties (33). When particles are compared between their bulk scale and light microscopic properties, there is no noticeable difference in their properties. However, when materials are compared between bulk and nanoscale, there is a big difference in their properties. This can be done by using powerful microscopes like the scanning electron microscope and Transmission electron microscope. This is the scale or size at which quantum effects rules on properties of materials (33). As a material approaches nanoscale, properties like conductivity mechanical, magnetism, permeability, fluorescence, chemical reactivity, and thermo properties change dramatically (33).

One example of such materials is Gold. At bulk scale Gold comes in yellow color, however, at nanoscale, Gold shows a range of colors that include purple and red due to confinement of its electron motion. This is because as electrons are restricted in movement, their interaction with light will differ with the way they do at bulk scale (33). These properties can be exploited to human advantage as gold nanoparticles selectively accumulate in tumors which helps scientists carry out precision laser destruction of the tumor (33).

The main property that rules the behavior of nano materials is the expanded surface area as the material approaches nanoscale. To illustrate what this means, consider a solid cube of a given material with 1 centimeter on one side and 6 square centimeters of surface area almost one side of a gum stick. If 1 cubic centimeters are to be filled with 1 mm cubes on one side, there would be 1000 mm cubes i.e. 10 by 10 by 10 each with a surface area of 6 sq. mm leading to a

total area of 60 cm which is equivalent to area of a card. If the same one cubic centimeter is filled with micro sized cubes the a trillion of them would align with a surface area of 6 sq. mm each thus total surface area becomes 6 sq. meters equivalent to an area of a bathroom. Furthermore, if the same 1 cubic centimeter is filled with 1 nm sized cubes this would result in one Sextillion i.e. 10 to the charges of 21 of them and the total surface area would be about 6000 square meters thus a single cubic centimeter filled with NPs contains a surface larger than a football field as in Figure 1.7 (36).

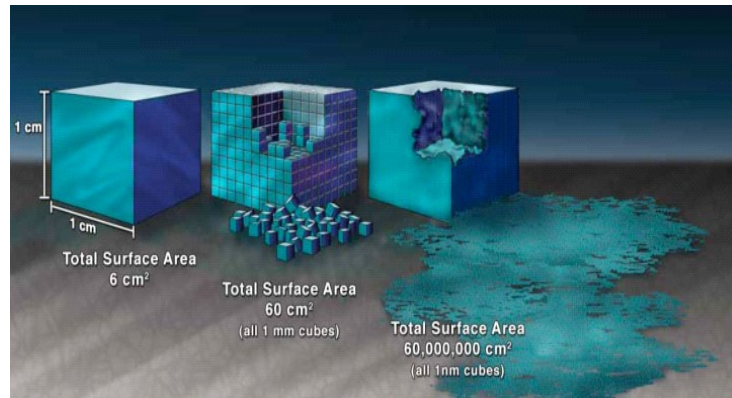


Figure 1.7 Increase in surface area with decrease in size towards nanoscale. (36)

These nanoscale properties have inspired a plethora of scientific applications including catalysis and chemical reactions, anti-microbial reactions and interactions and many others (35, 36).

1.2.3 Biology at Nanoscale.

Over thousands of years nature has progressed through a myriad of changes and perfections through biological processes at nanoscale. Most of the cell biochemistry carefully occurs and is controlled at nanoscale for example hemoglobin is about 5.5nm in diameter and is responsible for transportation of blood oxygen, the strands of DNA which is the building block of life making up what is called central Dogma are 2 nm in diameter (34). With insights drawn from biological process, scientists have been inspired to design molecular systems that mimic these systems and produce lifesaving products that are otherwise very difficult to achieve without Nanotechnology. Through this research, personalized medicines are being developed, early detection and warning system in our bodies for example the bio-barcode assay, a diagnostic

tools that monitors and detects even the slightest changes associated with a given disease and thus help get medicine or prevention before the actual disease stage develops. This tool is vital in the fight against chronic illnesses like cancer, diabetes, heart disease among others (34). One such system that relies on the attachment of recognition particles on DNA and its subsequent amplifications was first demonstrated by a group of Researchers at Northwestern University to develop a test for prostate cancer after prostatectomy.

Discerning nanoscale bio-molecular structures and functioning has enabled scientist to exploit the natural phenomena that happens in systems for example molecular self-assembly of DNA is being developed by scientists in what we know as DNA Nanotechnology to develop unrivaled capacities to deliver therapeutic agents as well diagnosis. A team of Danish Researchers at Aarhus University (Center for DNA Nanotechnology) successfully developed DNA nano cages with a controllable lid as shown in Figure 1.8 which provides the platform to safely load drugs and deliver them directly to disease sites and minimize the side effects that comes with the conventional drug administration (34).

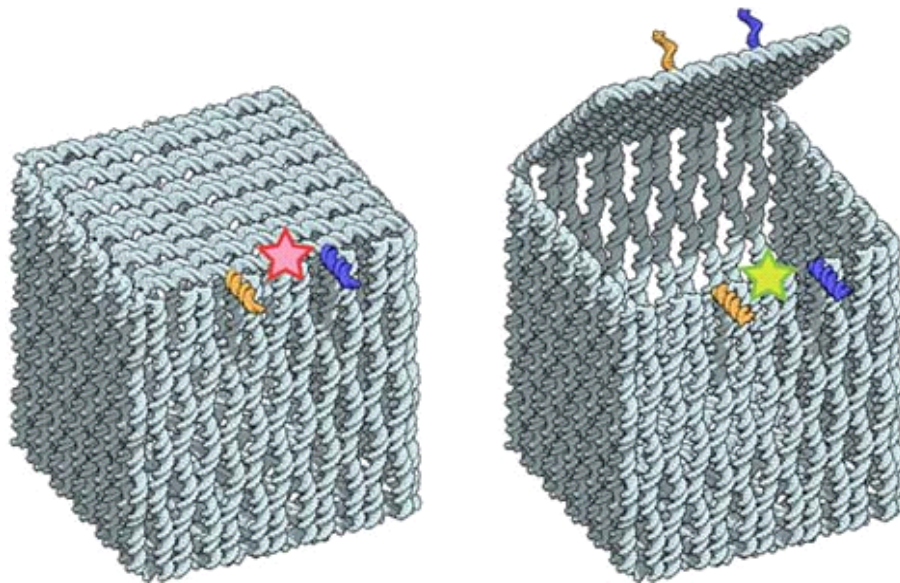


Figure 1.8 Structure of DNA nano Cages with capacity for drug delivery (35)

Energy scientists have been studying Photosynthesis phenomena in which molecules in green plants synthesis the energy required for their survival and they discovered that the energy plants absorb from the sunlight is quickly transferred to reaction centers and ensures that no

energy is wasted or lost as heat in the process thus achieving a near 100% efficiency and this reaction occurs at molecular (nanoscale) level. Drawing lessons from this natural reaction scientists are trying to devise a mechanism that mimics this process and ultimately increase the efficiency of harvesting the green energy in form of solar energy which is a clean and nonpolluting form of energy to tackle growing energy demands around the globe taking in account that solar energy alone has the capacity to generate over 60 terawatts of charges which is far above the 12 terra watts needed to fulfill energy demands for the modern technology driven economies (36).

As mentioned earlier, nanoscale materials are mainly governed by large surface area to volume ratio in comparison to similar materials in bulk state. Increase in surface area to volume ratio is directly proportional to the amount of material exposed to the surrounding environment i.e. other materials and thus their reactivity.

Silver is one such element whose anti-microbial properties at bulk scale are mildly powerful and as a result it has been used in history for preservation of food and treatment of wounds. However when silver approaches nanoscale its antimicrobial reactions explode by a factor similar to that of its surface area. Free radical silver is therefore being used in modern anti-microbial and different disinfectants to rid surfaces of pathogenic microorganisms.

Natural polymeric materials like chitosan follow the same pattern. Chitosan has got anti-microbial properties and its solutions have been used in different antimicrobial formulations. Recent conversion of bulk scale chitosan to nanoscale revealed the hidden potential of this compound to confront bacteria and viruses and thus offer a new line of defense against a scourge of infections since chitosan is a biological compound that is biocompatible with no side effects to humans.

1.2.4 Nanotechnology in anti-bacteria and wound treatment.

Silver and silver NPs are some of the first nanotechnology engineered anti-microbial materials with extensive use in biomedical industry. The use of silver in bulk form as an antimicrobial agent dates back to ancient times when it was used as a food preservative, wound treatment etc. Currently silver and silver nanoparticles are essential components of modern products like

shampoo, anti-fungal creams, textiles, some of the silver nanoparticle inspired wound dressing include the Acticoat. These materials are in circulation for the treatment of toxic epidermal necrotic wounds, burns, different ulcers, pemphigus wounds and steven-johnson disease. In this case the Nano crystalline particles are sprayed to the polyethylene to form a layer of between 10 to 15 nms which forms two layers sandwiching a polyester gauze. Trails with silver NPs have shown superior properties when compared with the bulk scale silver sulfadiazine and normal gauze dressings especially in the treatment of burns. When randomized clinical trials were carried out, they found out that nanoparticle inspired dressings shortened wound healing time by nearly half of the time it takes normal silver based dressings and also bacterial clearance was much enhanced as compared to the traditional methods. Following these successful tests scientists then sought to create a composite of nano materials including silver and chitosan and then tested them for the wound healing and bacteria clearance (37, 38). The result obtained shown 89% healing rate compared to the bulk scale silver which gave 68% and chitosan film which gave 74% healing rate. NPs in this case achieve superior results due to accelerated re-epithelization. Further research was carried out by Karla *et, al* 2010 to investigate the anti-inflammatory role of silver based NPs and also elucidate the mechanism of this activity if present. To study the anti-inflammatory activity, 1, 2-dinitrochlorobenzene was used to induce dermatitis in swine. The results obtained were compared with the control experiments of silver nitrate and saline soaked wound dressings. Anti-inflammatory superiority of silver NPs in comparison to the control was significantly higher. After 72 hrs of investigation with nano crystalline silver, histopathology of the pig shown near-normal epidermal structure (39, 40, 41).

Furthermore, immune histchemical staining test shown increased pro inflammatory cytokines TGF- β and TNF- α in the case of saline and silver nitrate solutions and while negative control samples had the same amount of pro inflammatory cytokines thus indicating the anti-inflammatory property of silver nanoparticles. This phenomenon was speculated to possibly result from reduction of cytokine release, inhibiting lymphocyte and mast cells from infiltrating the wounded site and also encouraging apoptosis of inflammatory cells. One known factor that impede healing of chronic wounds is the presence of matrix metalloproteinase enzyme (MMPs)

since their over expression is always associated with chronic ulcers and thus play a big role in prolonging the healing of chronic ulcers. However studies in porcine model revealed that nano crystalline silver significantly reduces the levels of MMP-9 and improved the wound healing rate although the exact mechanism has not yet been understood. Similar studies in human Chronic ulcers have shown nano structured silver accelerate their healing and this could largely be attributed to:

- 1- Ability to rid wounds of bacteria which infects these wounds and make the healing process very difficult since they develop resistance to the commonly used anti-biotic (40, 41, 42).
- 2- Ability to inhibit inflammatory response that typically follows any ulceration (43, 44).

Plethora of research into nano crystalline silver for anti-microbial properties has been done and continues to be done. Paladin F *et, al* 2013 reported the successful photochemical deposition of silver NPs on wound dressing materials for antimicrobial protection by surface modification of cotton gauze (45). Kim J *et, al* 2007 working on antimicrobial properties of silver NPs synthesized spherical silver NPs using the wet chemical technique and subsequent exposure to wound infecting bacteria *Staphylococcus sp* and *E.coli*. Results shown significant inhibition of bacterial growth in both species of bacteria (46). Palanisamy N.K. *et, al* 2014 investigated the anti-biofilm properties of silver NPs against *Pseudomonas sp* and reported positive results (47).

Citing numerous questions concerning metallic NPs to the environment and health systems, Nanocomposite materials have taken center stage in biomedical research. Composite material means that material is composed of more than one type or component and as such it's a heterogeneous material whose properties are dissimilar to the ones of the parent materials. Nanocomposites therefore mean a composite material composed of units in which at least one of the phases exists in nm range i.e. from 1nm to 100nm. These Nanocomposite materials have got better properties in regard to anti-microbial activity as different materials at nanoscale exhibit anti-microbial and anti-inflammatory activity and when combined, there is a synergistic effect that increases the property at the center stage by many folds (48). Synthesis and characterization of silver/montmorillonite/Chitosan bionanocomposites by Chemical reduction

technique using sodium borohydrate was carried by Shameli *et, al* (49). The resulting 2D structure of MMT-Chitosan complex with silver NPs embedded in their matrix was tested on gram positive bacteria *S. aureus* (49). Lee *et, al* reported synthesis of Chitosan having controlled levels of silver NPs through electrospinning technique (50). The resulting Chitosan-silver NPTs composite was tested for anti-bacterial action and produced positive results against *p. aeruginosa* (50). Carboxymethyl Chitosan/polyethylene oxide nanofibers embedded silver NPs for anti-bacterial properties have been reported by Fouad *et, al* (51). In their report the nanocomposite material were synthesized by electro spinner to create a mart of carboxymethyl Chitosan (CMCTS) mixed with Polystyrene oxide (PEO) and then tested for anti-microbial activity (51). Zhao *et, al* synthesized silver NPs in Chitosan and poly vinyl alcohol cross linked by glutaraldehyde vapor at 80 °C for 12 h to ensure controlled release of silver NPs for anti-microbial action (52).

The advance of nanotechnology research in biomedical industry has presented another alternative approach of tackling the existing microbial infections (53). Nanotechnology exploits materials when they approach nanoscale which results in novel properties like antimicrobial action (48). Such materials may not necessarily exhibit the same properties in bulk state, but due to the exponential increase in the surface area, the chemical groups are activated and reaction with the substrate is elevated thousands of times. One such material of enormous interest is chitosan synthesized by DE acetylation of chitin found in crustaceans and mollusks (48).

1.2.5 Nano-composites and scaffolds

Development of nanocomposites has been inspired by the Challenges and limitations encountered when using micro composite and monolithic materials since. Although they pose challenges in preparation due to the stoichiometric limitations in nanophase, nanocomposites generally offer superior and user friendly properties when compared with the micro composites and monoliths. Nanocomposite materials are reputed to be materials of the 21st century owing to uniqueness in property combination which are rare in conventional materials. Since the start of the 21st century, there has been exponential increase in the amount of research involving

nanocomposites and according to literature survey made by authors show that of the publications that have been made during this period about nanotechnology, over 30% have been specifically discussing nanocomposites. Similarly patents in nanotechnology show the same trend thus indicating unrivalled potential of nanocomposite materials in almost all fields of research. As explained in the previous section, the smaller the material becomes, the more efficient it becomes in exhibiting its inherent properties. This is the main reason why independent materials at nanoscale when joined to other materials produce novel combinations which are Cheaper and more effective. Nanocomposite research gained momentum after the discovery of carbon nanotubes in 1991 and then development of composites using these CNTs greatly improved mechanical and conductive properties of materials (54, 55, & 56). CNTs were spanned into composite products and textiles to provide strong properties for example in the development of armored materials for the defense sector. Micron and nanocomposite materials are classified into different categories are shown in table 1.1.

Table 1.1: Different types of Nanocomposites (54).

Class	Examples
Metal	Fe-Cr/Al ₂ O ₃ , Ni/Al ₂ O ₃ , Co/Cr, Fe/MgO, Al/CNT, Mg/CNT Ceramic Al ₂ O ₃ /SiO ₂ , SiO ₂ /Ni, Al ₂ O ₃ /TiO ₂ , Al ₂ O ₃ /SiC, Al ₂ O ₃ /CNT
Polymer	Thermoplastic/thermoset polymer/layered silicates, polyester/TiO ₂ , polymer/CNT, polymer/ layered double hydroxides.
Ceramic	TiN-Si ₃ N ₄ , SiC-Al ₂ O ₃ , SiC-SiC, Graphine/CNT + SiC and Carbon fiber + SiC

A number of review articles covering a wide range of nanocomposites have been published among them are: Ceramic Matrix nanocomposites, Carbon nanotube reinforced nanocomposites, Polymer Matrix nanocomposites, and metal matrix nanocomposites (54). For the polymer matrix nanocomposites, most research has been focused on layered silicates, conductive and biodegradable polymers, nano fiber reinforced, structure and the morphological aspect and then their applications and perspectives. Reviews have also been discussing the Challenges and key opportunities that are engrained in the fiber nanocomposite

technology. The sub area of conductive nanocomposites is a new and promising field that is aimed at producing polymer based nanocomposites with electrical conducting properties that are superior to the conventional conducting materials (54).

1.2.6 Applications of nanofibers

Development of nanofibers and their applications in various fields has attracted tremendous attention from Researchers in the last decade (55). This is a testament to the unique novel properties that come with reduction in size towards nanoscale and for the case of fibers comes with enviable benefits in both environment and biomedical fields. Nanofibers have got a large surface area to volume ratio, an easily bio functionalized surface, superior mechanical properties. These properties have made nanofibers versatile in application ranging from medical, environmental, and catalysis (56, 57, & 58).

1.2.6.1 Methods of fabricating nanofibers

The field of nanofiber synthesis has attracted tremendous attention in the last decades due to the versatility of these materials with a wide range of applications in sectors that are so crucial to human survival. Nanofibers are excellent in their applications because of the changes caused by reduction in size of material, for example the increase in surface area to volume ratio plays a key role in enhancing the properties of a material of which case nanofibers fit perfectly in the property. There are other properties that come along with the formation of nanofibers for example increased mechanical strength and the easiness of their surface modification, bio functionalization, and creation of tubelike structures for controlled delivery applications (58,).

Applications of nanofibers are numerous and cross nearly all sectors ranging from biomedical, pharmaceutical, water treatment, filtration, and catalysis. There are both chemical, electro-chemical and physical methods of synthesizing nanofibers among which include electrospinning, laser ablation, chemical vapor deposition, physical vapor deposition use of reverse micelles, explosion techniques for example cellulose nanofibers, and template guided synthesis among others. Lakshmi *et, al* reported successful synthesis of carbon nanotubes and nanofibers by the chemical vapor deposition technique while Meng *et, al* were able to synthesize semiconducting

nanofibers using physical vapor deposition method. Goux *et, al* using the template aided deposition method were able to synthesize polyaniline nanofibers. One of the most popular methods in synthesizing nanofibers for biomedical application is the electrospinning technique. This technique is dependent on the whipping of the polymer solution under electrostatic forces. Electrospinnable polymers include polyamides, polyolefin, polyesters, polyurethanes, polyvinyl alcohol, polysaccharides and polypeptide materials (59, 60, 61, & 62).

1.2.6.2 Fabrication of Nanofibers with natural extracts

1.2.6.3 .1 Polyvinyl alcohol (PVA) nanofibers

PVA is a hydrophilic synthetic colorless resin which is principally used in the treatment of textile and paper. PVA is a unique polymer from the rest since it's not made of monomer units but rather comes from another polymer, polyvinyl acetate (PVAc) in methanol or any other alcohol in the presence of an alkyl catalyst for example sodium hydroxide. Hydrolysis or acidosis reaction is then used to eliminate acetate groups from the PVAc without affecting the chain structure (63). The chemical structure of PVA is shown in Figure 1.9.

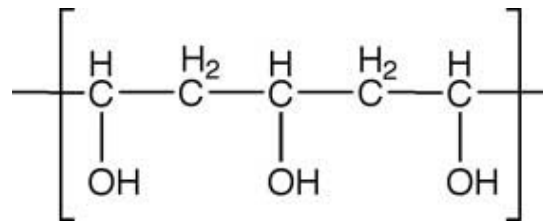


Figure 1.9 Structure of PVA unit (63)

PVA is a highly water soluble compound and insoluble in nearly all organic solvents and this is dependent on the degree of de acetylation of the chain groups. Any residual acetate groups will lower the solubility of the resins in water and make them soluble in organic solvents. In textile PVA is used to improve the strength of yarns and improve their resistance to oils and greases. PVA is also commonly used in emulsifiers, hydrophilic protective films and also as a starter for

the synthesis of other resins. When PVA is reacted with butyraldehyde and formaldehyde to form products polyvinyl butyral (PVB) and polyvinyl formal (PVF) of which PVB is a very important water resistant adhesive used in laminating safety glass for the automobile industry while PVF is used for the manufacture of insulators (63).

PVA is a well-known compound for its biocompatibility and biodegradability and these novel qualities exhibited have made it gain enormous attention in biomedical research for multiple applications ranging from drug delivery, antibiotic development and scaffolds for tissue engineering (63). PVA is excellent material used to develop hydrogels that are used for vascular cell culturing as well as implant and organ cultures which include arterial phantom, heart valves, corneal implants and cartilage replacements Hubbel, chu, jiang, vijayasekaran and stamnen. Vrana *et, al* have been focusing their efforts on the evaluation of vascular cells response to changes in the hydrogel structure while Hoffman was able use hydrogels to grow living cells because the extensive porosity and degradability of the hydrogels. Hydrogels are normally water swollen polymers that have been cross linked and poses properties such as tissue-like elasticity and appearance (64).

PVA based hydrogels have got properties that similar to natural arterial tissue and as result of near native like properties, PVA hydrogels are used in medical research to mimic natural tissues to assess the effect of therapeutic interventions and also to mimic surgical interventions. Another front of molding PVA into biomedically active material is the synthesis of PVA nanofibers. PVA Nanofibers are obtained by a number of techniques that range from Chemical and electro Chemical methods of which electrospiner technique (see SEM image in Figure 1.10) is most commonly used (64).

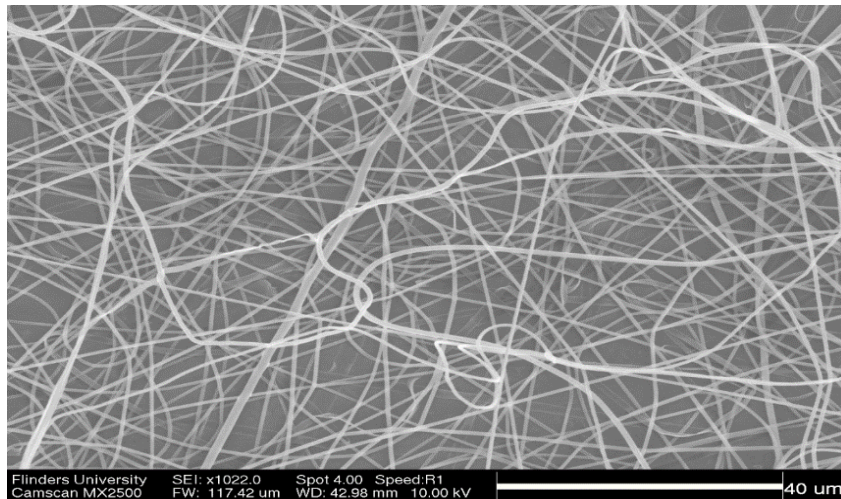


Figure 1.10 SEM micrograph of PVA nanofibers diluted in DI water obtained at a voltage of 13KV and flow rate of 3mL/hr. and scale bar 40μm (64).

PVA has been used to form nanocomposite fiber materials due to its good spinnability properties and thus the combination comes with improved chemical, mechanical and biological properties. Zille *et al* developed PVA/Chitosan nanofibers and reported successful synthesis of nanofiber mats that were free from beading and consistent in the fiber diameters as shown in Figure 1.11 (65).

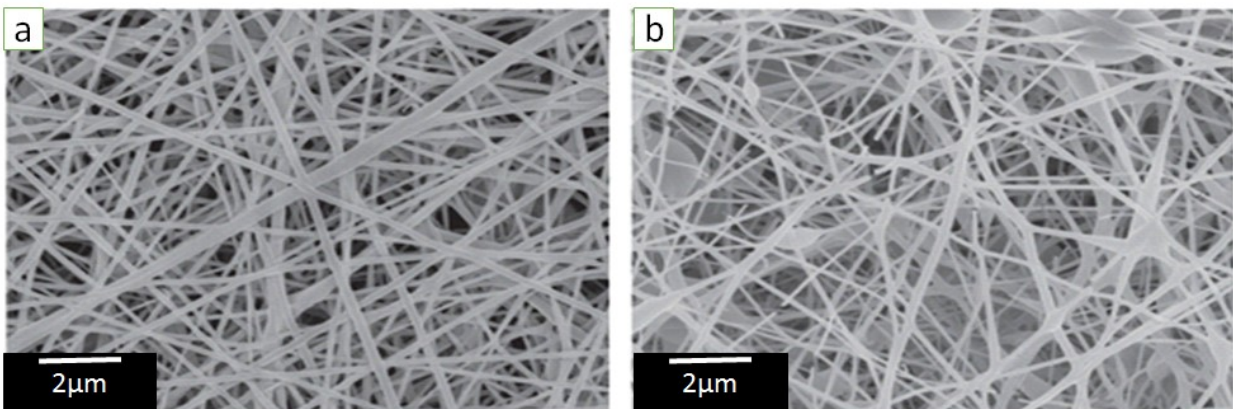


Figure 1.11 SEM images of antimicrobial (a) PVA/Chitosan and (b) PVA/AgNO₃ nanofibers (X50000 magnification) performed at a voltage 5KV and 15KV, respectively. (65).

PVA and chitosan nanofibers shown in Figure 1.11 have got distinct properties and are suitably applied to tissue engineering and anti-microbial activity. PVA nanofibers have also been used in filtration and reinforcement of materials, wound dressings drug deliver etc. (65).

1.2.6.3 .2 Chitin and Chitosan

Chitin is the second most abundant natural polymer in the world after cellulose and the second most important polymer given the numerous applications that employ chitosan (Figure 1.12 and 1.13) that is a direct derivative of chitin. The history of chitin is traced back to the start of life on earth and is thought to have been a crucial constituent of the first living cells about 2 billion years ago. Its existence goes well beyond the dinosaurs which lived around 200 million years ago. Dinosaurs are believed to have been exterminated by a comet that crashed into the Yucatan peninsula 65 million years ago however crabs and small animals were able to survive this catastrophe owing to the singular protection that was provided by chitin (Figure 1.12) that covered them (66, 67).

Existence of life has been sustained by two compounds chitin and cellulose for animals and plants respectively. Chitin is an English word derived from a French word chitine which is traced to 1836 when it first appeared and was derived from the Greek word chitosan that means mollusk. Chitin was first extracted from mushrooms by a French scientist Henri Brancconot in the year 1811. Chitin is a giant molecule made of beta 14 acetyl glucosamine monomers and it exists in α , β , and γ forms. Alpha form is the form extracted from prawn, shrimps, crabs, and other crustaceans. In the book that was published in 1977 a full list of organisms from which chitin is generated was published and among them are: Cnidarian, Fungi, Algae round worms, round worms (*Aschelminthes*), moss, horse worms, lamp shells segmented worm's mollusks, crustaceans, and anthropods. Chitin is found on the outer surface as well as lining of gut and other organs in some organisms for protection as depicted in Figure 1.12. The commercial type of Chitin is extracted from crustaceans (66, 67).

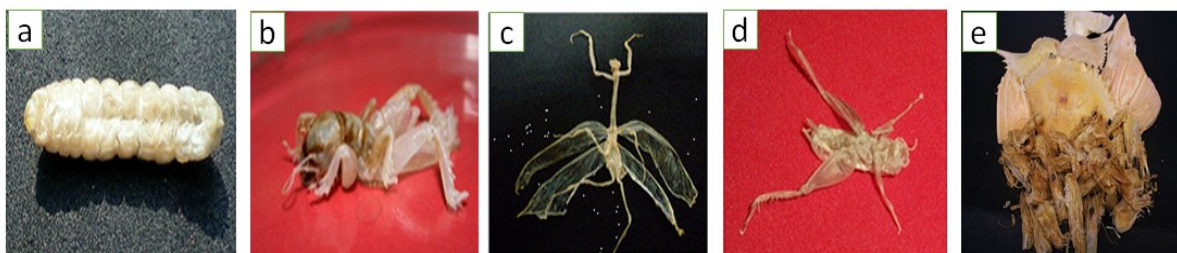


Figure 1.12 Structure of Chitin in (a) worms, (b, c and d) insects and (e) crustaceans (66).

Chitin was first discovered in 1884 and is an important material in a variety of living organisms. Chitosan is formed by de acetylation of chitin see figure 1.17. Chitin exists in nature as an ordered crystalline nanofibril which normally forms the structural components of exoskeleton for a variety of arthropods and cell walls microorganisms mainly yeasts and fungi. Lower plants and animals are also known to have chitin as a reinforcing material in parts that require reinforcement for mechanical strength (67).

Although chitin is abundant in many organisms, crabs and shrimp shells continue to provide commercially viable chitin. In crustaceans, chitin is extracted by dissolution of calcium carbonate through acid treatment followed by alkaline extraction to dissolve the proteins. Another important step is the decolonization step which is carried to remove any residual pigments. Due to differences in the sources of chitin, extraction conditions are adopted to each source so as to account for the differences and avoid destroying the chitin in the process. Partial de acetylation of chitin produces chitosan (shown in Figure 1.13) which is the most important derivative for a huge array of applications (66).

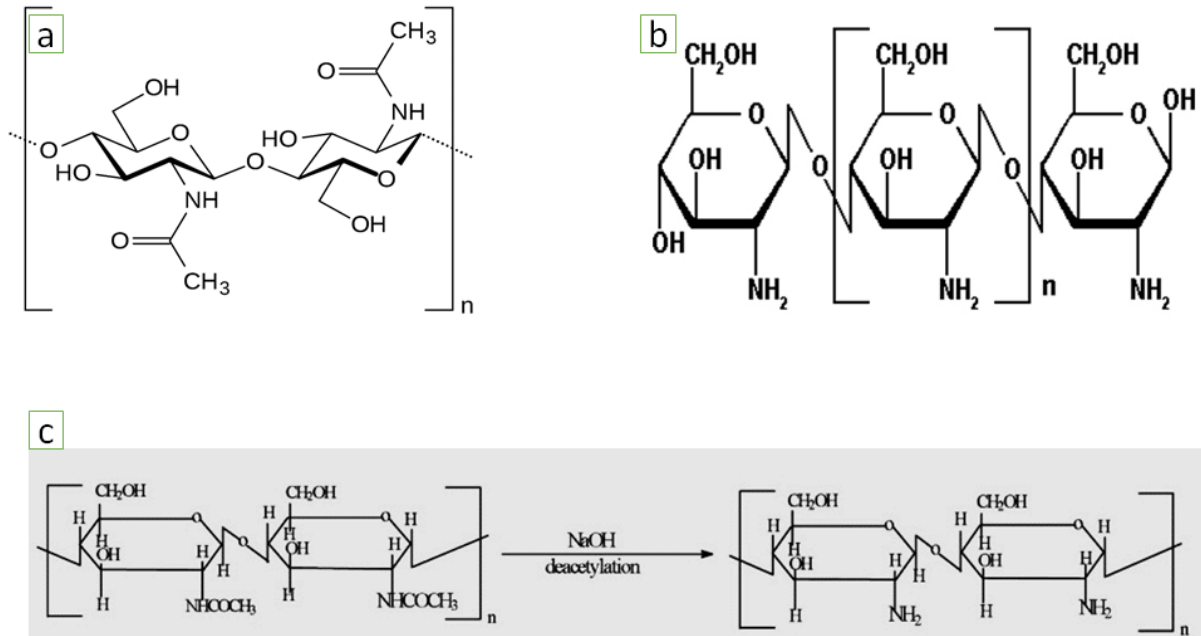


Figure 1.13 Chemical structure of (a) Chitin, (b) Chitosan, and (c) De-acetylation of chitin to form chitosan (66).

1.2.6.3 .2 Anti-microbial activity of Chitosan.

Chitosan is known to have strong anti-microbial activity against both gram positive and gram negative bacteria, viruses and fungi. It has attracted great attention in the last two decades for biomedical applications given the novelty chitosan has as pertains to its properties. The mechanism of chitosan anti-microbial action is still not clear, however research has linked the polycationic nature of the amine groups which in solution lowers PH below 6.5 as being one of the main factors behind its anti-microbial efficiency (66, 67). The cations on the biopolymer is therefore believed to interact with negatively charges on the cell membrane of microorganisms and thus affecting the physiological processes of the cell. Other findings indicate that lower molecular weight chitosan diffuses into the bacterial cells and attach to the DNA thereby inhibiting the process of RNA synthesis. Chitosan can be processed into different forms including films, particles, pellets, fibers, and powders (Figure 1.14)



Figure 1.14 Different forms of Chitosan for biomedical applications (a) films, (b) gels, (c) microspheres, (d) tubes, (e) sponges and (f) powder (67).

Chitosan has been proven to promote accelerated tissue repair and wound healing and its anti-microbial activities have been extensively tested against yeast molds and different strains of bacteria as shown in Figure 1.15 (68). Chitosan is also reported to have inherent osteoconductive properties which makes them suitable for applications in orthopedic medicine (5).

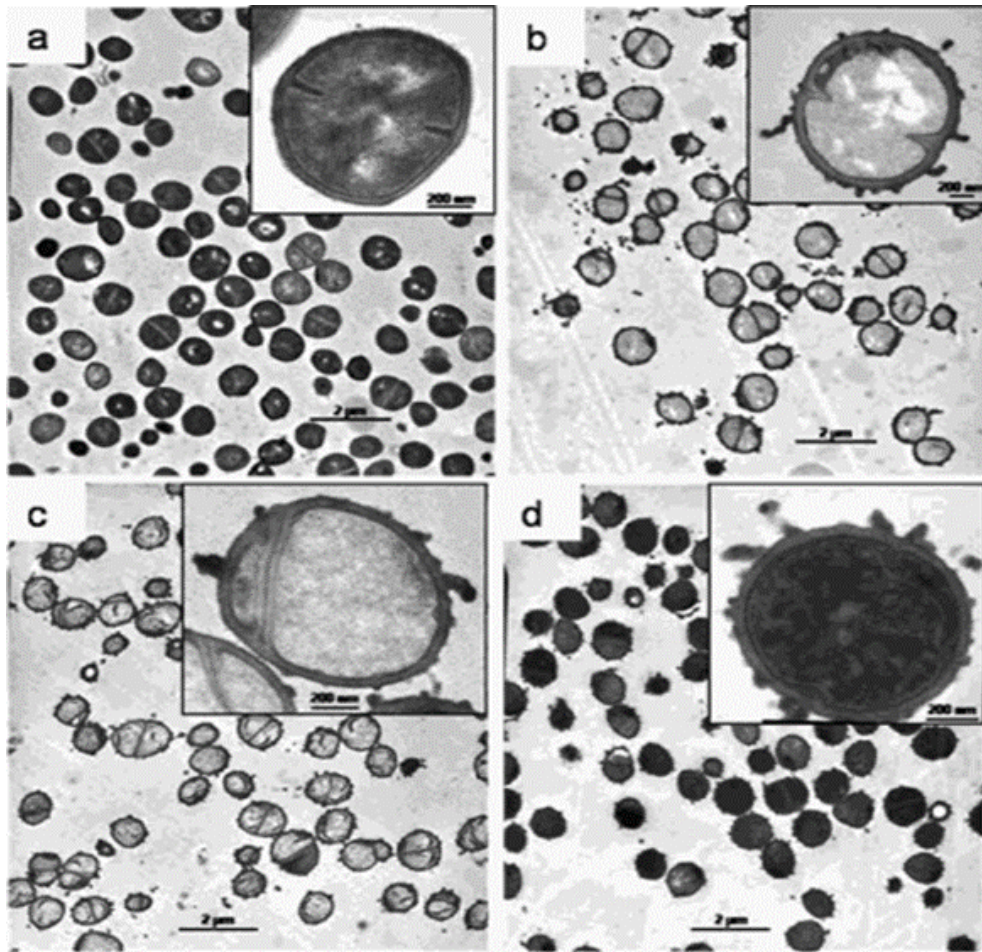


Figure 1.15 SEM micrographs of *S. simulans* cells (a), control, then (b), (c), and (d) which are treated with chitosan for: 5 mins, 20 mins, and 60 mins respectively. Insets show magnified single cells. Bars, 2 µm (a-d) and 200 nm (for magnified cells a-d) (67).

1.3 Herbal extracts

According to the United Nations, over 5.6 billion people which is approximately 80% of the entire human population use medicinal plants as the first line of defense in case of disease a

trend that has been around for thousands of years. Chinese and Indians have been heavily linked to the development of herbal medicine systems and since the 11th century BCE and Chinese and Ayurveda medicines are widely used today and are increasing finding their way into modern medicines (69).

1.3.1 *Bidens pilosa*

Bidens pilosa is a famous herbaceous plant commonly referred to as Spanish needle or black jack. *Bidens pilosa* originated in South America and is widely distributed around the world being used as a food and medicine in many communities in Africa, America, Asia and Oceania (70). *Bidens pilosa* is classified according to the table 2.2.

Table 2.2. Classification of *Bidens pilosa* (70).

Kingdom	Plantae
Sub-kingdom	Tracheobionta
Super division	Spermatophyta
Division	Magnoliophyta
Class	Magnoliopsida
Order	Asteridae
Family	Asterales
Genus	Asteraceae
Species	<i>Bidens pilosa</i>

Bidens pilosa has gained reputation for its rich reservoir of phytochemicals which give it unique properties in anti-microbial activity, anti-septic, anti-inflammatory, anti-oxidant, anti-cancer, and nutritional applications. Research done to profile the phytochemical found in *Bidens pilosa* concluded that it has got 201 compounds of which 34.8% are aliphatic compounds, 29.8% terpenoids, 9.45% phenylpropanoids, 6.4%, aromatics 3.9% porphyrins, and 2.9% other compounds. Each part of the world has adopted *Bidens*'s to a given function for example in Africa it is used for treatment of wounds, diarrhea, influenza, headache, stomachache, etc. while in Cuba the decoction (Boiled extract) of *Bidens pilosa* is used juice as well as anti-inflammatory, diabetes and Asthma, it is medicine for conjunctivitis, otitis, and colic, snake

bites in China. In Middle America *Bidens pilosa* is important in the treatment of eye infections and diuretic hypotensive. In Uganda *Bidens pilosa* has been explored in the treatment of malaria, wounds nasal bleeds and stomach ulcers. The list of applications in biomedical field is extensive (70).

The wound healing activity of *Bidens pilosa* has been utilized in many parts of the world and is being used for treatment of tissue injury in Africa and South America. Hassan *et, al* reported on the use of *B. pilosa* against a host of bacteria with two controls the positive one with neomycin sulfate and the negative control. Rats with wounded tissues were treated for 9 days with the three formulations.

Result shown a mirror comparison between neomycin positive controls and *Bidens pilosa* yet the negative control shown no improvement. Further analysis on this experiment revealed better collagen formation, angiogenesis, and tissue organization in the *B. pilosa* and also epithelialization and the healing time in *B. pilosa* was similar to that of neomycin sulfate samples thus indicating how *Bidens pilosa* could be a very good substitute for neomycin in wound treatment. Tan *et, al* also explored the wound healing activity of the methanol, cyclo hexane and methyl chloride extracts of *Bidens pilosa* in gastric wound treatment. Their results indicated a dose dependent lesion inhibition rate that ranged from 40 to 82% (70).

1.4 Electrospinning technique

Electrospinning is a technique in which materials in solution form are subjected to high voltage current to create fibers that are in micro and nano size range. The term electrospinning was coined in mid 1990s to replace the original name of electrostatic spinning. Electrospinning technique has gained momentous attention in research and industry owing to the novelty of the products it produces. In comparison with dry/wet spinning methods, electrospinning technique produces superior fibers with a much larger surface area as well as small fiber diameter. Electrospinning technique has developed unrivalled reputation in the synthesis of scaffolds in tissue engineering. In tissue engineering, developing cells emerge in fibrous form

and find nanofibers as the physical guides for their organized growth and multiplication (61, 62, 63, & 71).

For electrospinning process the following have to be in place: polymer solution, high voltage supply, and a collector plate (62, 71). The mechanism that leads to the formation of fibers here in is the stretching of the solution as it attempts to drop of the needle tip. This stretching is forced by the electrostatic forces that act on the polymer solution as a result of repulsion between like charges on the polymer solution and the current. The solution is forced to pass through a narrow highly orifice electrified by between 10 to 30 kilo volts which charges the solution and leads to the formation of a tailor cone that then provides a platform for the jet of the material to whip down violently towards the collector plate as shown in Figure 1.16 (62, 71).

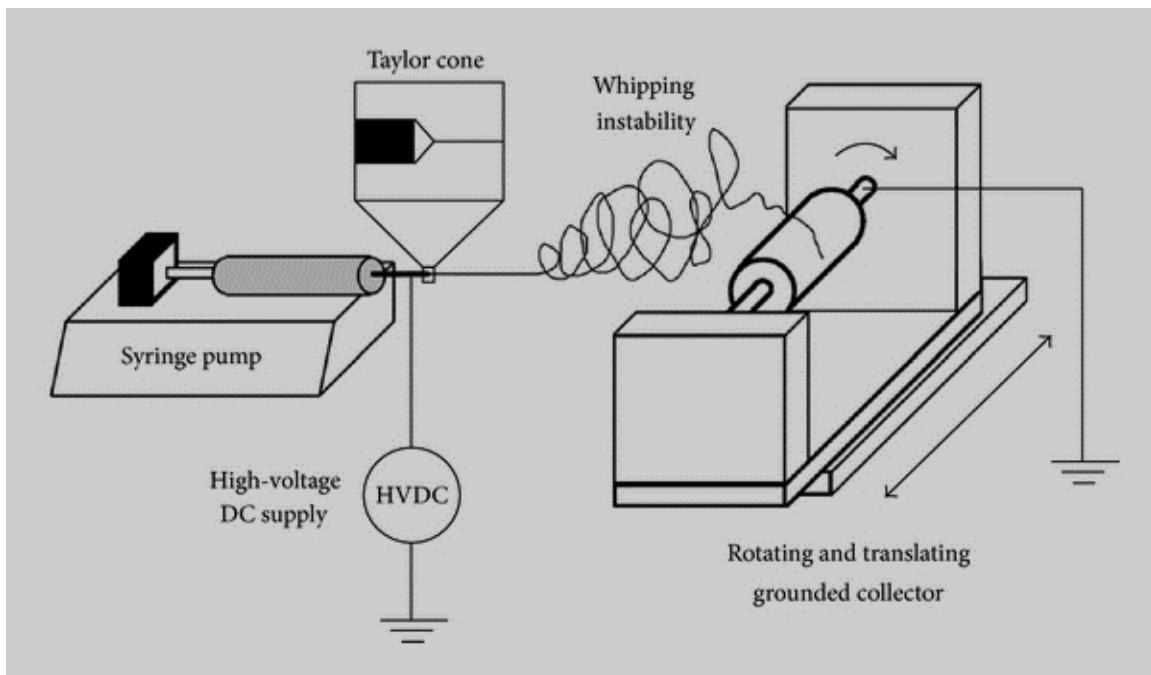


Figure 1.16 Schematic of a typical electrospinning system. While the polymer solution is pushed through the orifice, the electrostatic forces must be greater than the surface tension of the solution at which stage the polymer forms a Taylor cone and subsequently (62).

1.4.1 Parameters controlling the electrospinning process.

The process of electrospinning is affected by a number of parameters that are either solution parameters, process parameters, or ambient parameters. Each of the parameters has got a strong impact on the fiber morphology and sizes.

1.4.1.1 Solution Parameters

1.4.1.1.1 Concentration

Concentration of the polymer solution is a crucial factor in the formation of nanofibers during electrospinning. Note should be made that there are four critical concentrations which include

- Very low concentration (Between 5 to 10 wt. %) Leads to the creation of polymeric nanoparticles as a result of electro spray which substitute's electrospinning. This results from the low viscosity which results into higher surface tension of the solution (72).
- Low concentration (Between 10 to 15 wt. %) which is a concentration relatively higher than the first category and in this case the result is a fiber beads mixture
- Smooth/ideal concentration (20 to 25 wt. %) This concentration will lead to the formation of uniform fibers
- High concentration (30 to 40 wt. %) will lead to the helix shaped micro and not nano ribbons will be formed.

The four categories of concentration have been shown in SEM image in Figure 1.17.

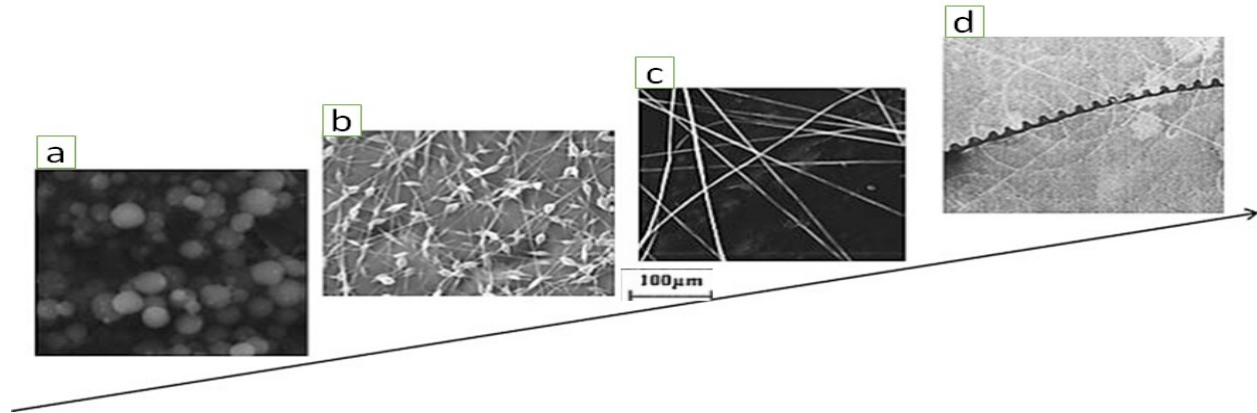


Figure 1.17 SEM images showing the effect of concentration. Scale bar 100µm, with voltage fixed at 15KV, (a) 5 wt%, (b) 10wt %, (c) 25wt% and (d) 40 wt % (72).

1.4.1.1.2 Molecular Weight

Just like concentration, molecular weight of the material being electrospun affects the resultant fiber morphologies as molecular weight of a material affects the degree of entanglement of the polymer chains in the solution and hence affect solution viscosity. At a fixed concentration, lowering molecular weight will result in the formation of beads and increasing the molecular weight, smooth beads shall be obtained (72). However further increase in molecular weight will lead to the formation of micro ribbons and at this point even lower concentrations of this molecular weight will produce ribbons. Very high molecular weight material will lead to the formation of patterned nanofibers. However not must be taken in that molecular weight of a material is not one of the fore front parameters that influence the process of electrospinning, especially if there is sufficient intermolecular interaction created by oligomers (72). The above effects of molecular weight are shown by the SEM images in Figure 1.18.

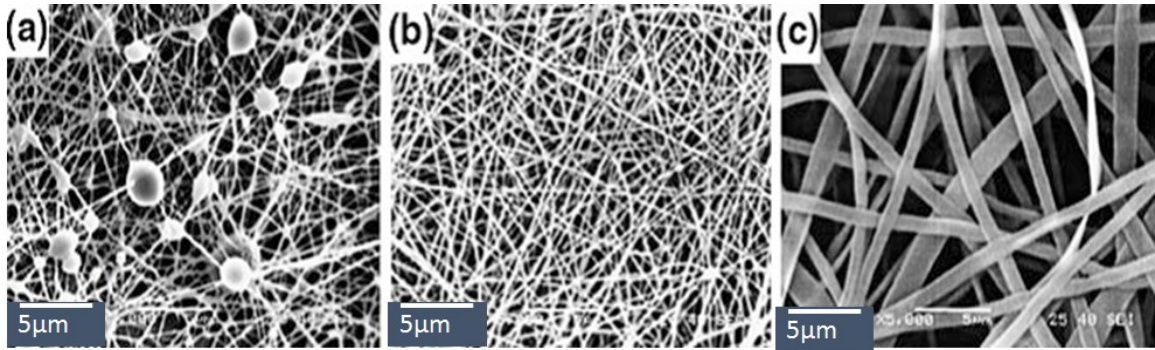


Figure 1.18 SEM Images of typical structure in the electrospun polymer for various molecular weights. (a) 9000–10,000 g/mol; (b) 13,000–23,000 g/mol; and (c) 31,000–50,000 g/mol (solution concentration: 25 wt. %). (72)

1.4.1.1.3 Viscosity

Viscosity is a key factor in the determination of fiber morphology and size. Experiments have shown that viscosity of a solution is directly responsible for the behavior and appearance of the fibers (72). Thus increase in viscosity leads to production of smooth fibers and vice versa as shown in Figure 1.19.

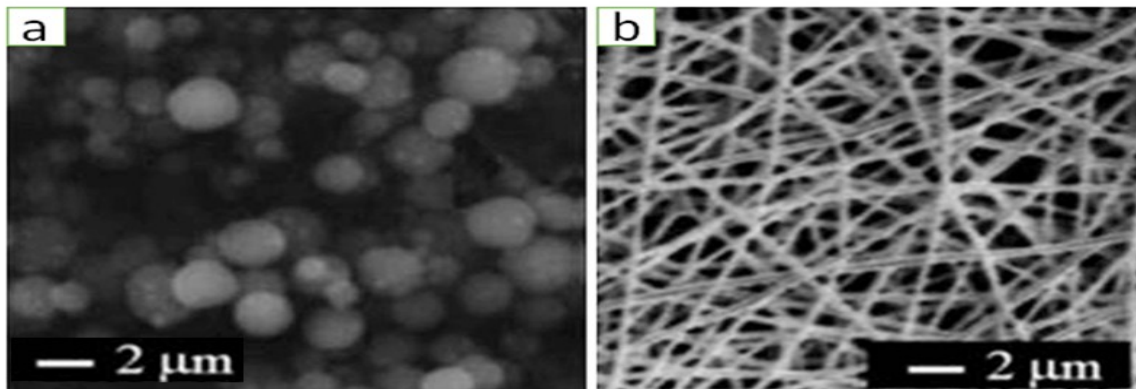


Figure 1.19 SEM images showing the effect of viscosity, obtained by adjusting the concentration of the solution (Molecular weight of PAN is 150000) (a) low viscosity (1.3%) and (b) higher viscosity (15%). (72)

Polymer viscosity is directly proportional to the degree of concentration and polymeric molecular weight. As was the case with low molecular weight, low viscosity is associated with high surface tension and thus favors formation of beads. On the other hand, higher viscosity is

accompanied with lowered surface tension and increased electrostatic forces while enables it to form well-formed stable fibers (72).

1.4.1.1.4 Conductivity/Surface Charge Density

Conductivity of the solution is generally dependent on the type of polymer, type of solvent, and type of the salt. Natural polymers are normally characterized by their polyelectrolyte nature and their ions increases their capacity to carry charges and thus the polymer jet is subjected to increased tension in an electric field which leads to poor formation of the electrospun fibers. On this note, it is therefore important to know the conductivity so appropriate adjustments using potassium hypo phosphate, sodium chloride etc. Addition of organic acid can increase solution conductivity while ethanol reduces conductivity of the solution and thus affect fiber formation.

1.4.1.2 Processing Parameters

1.4.1.2 .1 Voltage

Voltage is one of the most critical factors affecting the electrospinning process and the process will only occur when the threshold voltage is bypassed. Applied voltage effects on the fiber diameter is still a controversial subject. Some research finding have indicated that increase in applied voltage will result in increased fiber diameter. Zhang *et, al* researched the effect of applied voltage on fiber diameter of polyvinyl alcohol and found out that fiber diameter size was increased at higher voltages and narrowed at low voltage as shown in Figure 1.20 (72). However, other finding have indicated and actually reasoned that increase in voltage will increase the electrostatic repulsion on the charged jet and thus lead to formation of narrow fiber diameters. Yuan *et, al* reported similar findings with polysulfone.

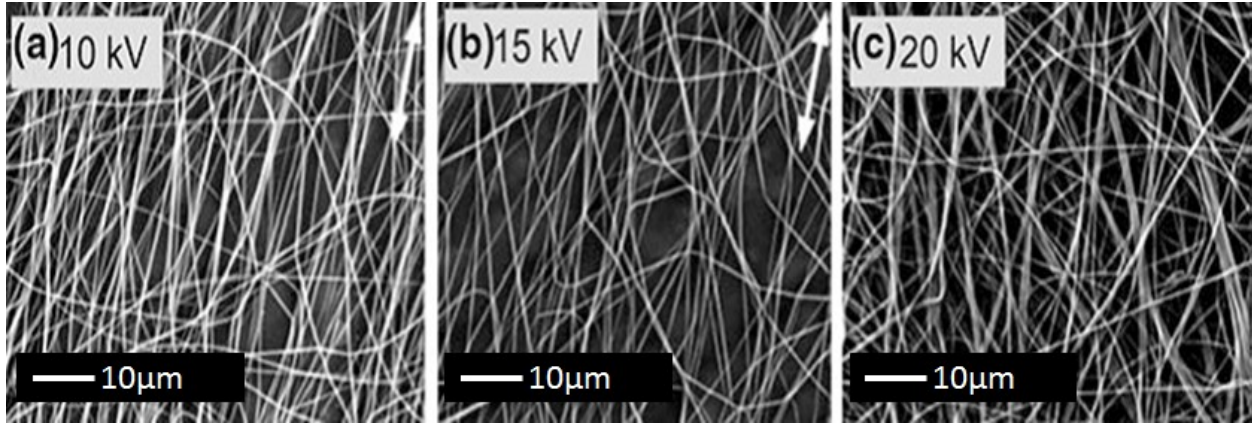


Figure 1.20 SEM images of PSF solution in DMAC/acetone solution with differing voltages as indicated inside the micrographs (a), (b) and (c). The average diameter for (a), is 344, 331 for (b) and 323 for case (c). The average diameters of (a), (b), and (c) are 344 ± 51 , 331 ± 26 , and 323 ± 22 nm, respectively (72).

1.4.1.2 .2 Flow rate

Flow rate affects the electrospinning process and its effect is much clear than that of voltage. Lower flow rate is generally recommended for smooth and good fiber formation while higher voltage will lead to the formation of beaded fibers with large diameters. This is explained by the fact that at low flow rate, the solution tailor cone will have enough time for polarization to take place before being released and evaporated. The effect of flow rate was reported by many Researchers among whom Yuan *et, al* investigated the effect of flow rate on the morphology of PSF fibers at a fixed voltage of 10kv and results are shown in Figure 1.21 (72).

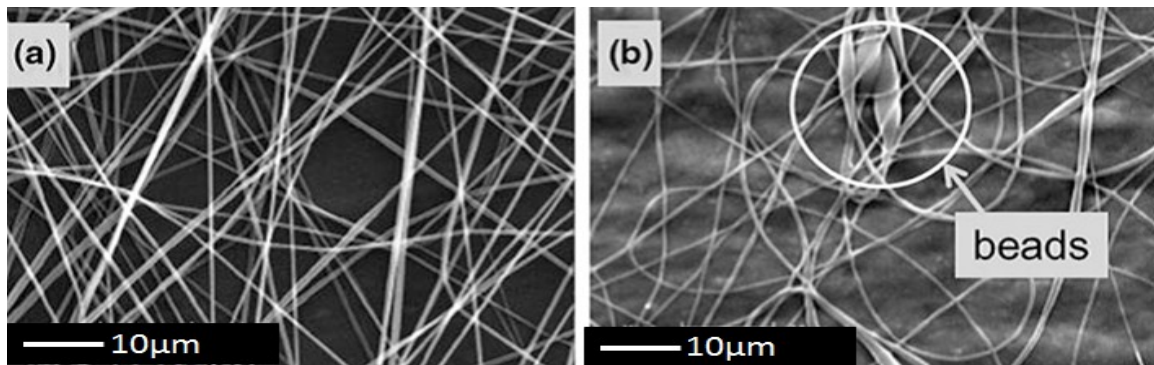


Figure 1.21 SEM images of PSF nanofibers at different flow rates. (a) 0.4mL/h and (b) 0.66ml/h at a fixed voltage of 10kv (72).

1.4.1.2 .3 Distance (D) Between the Syringe tip and the collector.

Collector-syringe tip distance is important in the determination of whether fibers will have beads or not. Too short collector-syringe tip distance will provide no room and time for the fibers to evaporate and dry up properly before landing on the collector. Conversely long collector distances will be long enough for the fibers to form beads as it takes them long to reach the collector and in the process entangle with the beads. Yuan *et, al* reported on the effect of distance (D) on the formed nanofibers. It is therefore to adjust the distance to the ideal parameter for a given polymer solution to obtain thinner and uniform fibers (72).

1.4.1.2.4 Type of Collector

Normally Aluminum foil is used for the collection of nanofibers but due to the difficulty in the removal of the fibers for the applications, a number of methods have been devised which include the following: wire mesh, grids, pins, guided or parallel bars, rotating wheel or rod, and liquid bath.

1.4.1.2 .5 Ambient factors

Finally ambient parameters are also crucial for the process of electrospinning to produce good fibers. Factors such as humidity and temperature affect fiber diameter. Research carried out by Mituppatham *et, al* shown that increase in temperature on polyamide 6 leads to formation of thinner fiber diameters. Humidity is known to affect the morphological characteristics of nanofibers in the way that low humidity enhances the velocity of the formed fibers thus forming narrow diameter nanofibers and increases the efficiency of the electro spinner process. High humidity will increase the diameter of the nanofibers which results from the neutralization of the charges on the jet thus diminishing the stretching forces.

1.5 Aim of this thesis work

The goal of this project was to synthesize PVA/*Bidens pilosa* (distilled and crude)/Chitosan composite nanofibers and investigate the effect of solution electrospinning parameters on the fabrication of these nanocomposites and their anti-bacterial properties. This plan as captured in figure 1.22, was based on the fact that composite materials have better anti-bacterial effect.

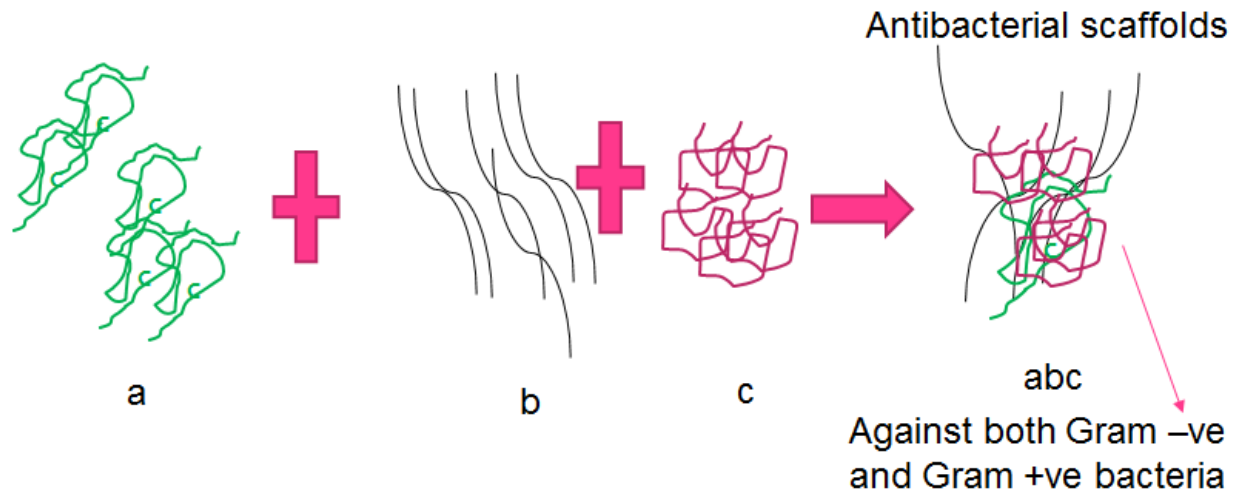


Figure 1.22 Illustration of the composite materials synthesis through electrospinning.

Nanocomposite materials as shown in figure 1.32 a, b, and c, combine parent properties of each component $a + b + c$ to result in the formation of a blend (abc) that has superior properties (chemical, mechanical and biological) as compared with individual polymers.

Chapter 2

Materials and Methods

2. Materials, synthesis and methods.

2.1 Materials

Polyvinyl alcohol (PVA MW 125000, 20-98% hydrolysis) and Chitosan (HMWC 1600 and MMWC 400) were purchased from Sigma Aldrich, Europe. *Bidens pilosa* (Crude and distilled extract) was purchased from SEFA organic for extracts Kampala Uganda. *Staphylococcus aureus* and *Escherichia Coli*.

2.2 Synthesis procedures

2.2.1 Synthesis of composite Nanofibers.

To synthesis composite electrospun nanofibers, materials were prepared both in situ and ex-situ and then the materials were then mixed at an adjusted ratio so as to enable smooth electrospinning. A number of parameters that range from ambient, solution and process parameters were adjusted as shown in table 2.1.

Table 2.1. Preparation of composite materials and parameters for their electrospun nanofibers.

Sample	% (w/w) PVA (EXT/DBP) With/without chitosan in 1 % acetic acid	Voltage/KV	Flow rate / mL/hr.
1	6 or (6%PVA to 3% CS)	16-21	0.8-1.2
2	8 or (8% PVA to 3% CS)	16-21	0.8-1.2
3	10 or (10% PVA to 3% CS)	16-21	0.8-1.2
4	12 or (12% PVA to 3% CS)	16-21	0.8-1.2

2.2.1.1 In situ blends.

PVA, PVADBP, and PVAEXT with PVA percentages of 6, 7, 8, 9, 10, 11, and 12% were by dissolving 6, 7, 8, 9, 10, 11, and 12gm of PVA into deionized water, distilled *Bidens pilosa*, and crude extract *Bidens pilosa* respectively. Nanofibers from these three categories were then obtained by adjusting the applied voltage from 16 to 21 and feed rate of between 0.8 and 1.2.

2.2.1.2 In-situ/Ex-situ blends

PVA, PVADBP PVAEXT solutions were mixed with Chitosan at ratios ranging from 3 to 1 up to 5:1 while the rest of the parameters were adjusted as in category 1 above.

2.2.1.3 Ex-situ composites.

Purely ex-situ mixtures included the following: Two component blends (PVA:CS, PVA:DBP, PVA:EXT), and Triplicate blends (PVA:DBP:CS, and PVA:EXT:CS) which were prepared by mixing PVA with either Chitosan or *Bidens pilosa* extracts at a ratio ranging from 3:1 to 5:1 for the two component blends and 4:1:1 to 6:1:1 for the triplicate blends. The rest of the parameters were adjusted as in the category 1.

The resulting ex situ and In situ composite solutions were loaded into 5ml syringes readied for electrospinning process. The loaded syringe was connected to pump that monitors the flow rate, then connected to the nozzle by the silicon tube. The nozzle was connected to the spinneret which was then attached to the crocodile tip connected to high voltage direct current.

2.3 Characterization.

Characterization of the resulting nanofibers were carried out by the following instruments.

2.3.1 Scanning Electron Microscope (SEM).

2.3.1.1 Background

Electron microscope operation is based on the use of electron beams to obtain the image of an object which cannot be obtained by other microscopic techniques like the electromagnetic fields. Electron microscope has got a superior resolving charges (200 times higher) compared to the light microscope. The reason for this is explained by the fact that the smaller the wavelength the stronger the resolving charges (73). Take for example the wavelength of green light is (0.55 μ) is 1 which is 10000 times stronger than electron beam (0.000005 μ or 0.05 Å; 1 μ = 10,000 Å). So regardless of the small numerical aperture, electron microscope can resolve an object which is 0.001 μ compared to the light microscope whose limit is 0.2 μ . There are three

types of Electron microscopes i.e. Transmission electron microscope (TEM), Scanning Transmission electron microscope, (STM), and Scanning electron microscope (SEM) (73).

2.3.1.2 Theoretical background of SEM

In Scanning Electron microscope, a narrow beam of electrons is generated from an electron gun and processed by magnetic lenses and then focused on to a specimen whose surface is rapidly scanned by the beam. This process leads to the release of secondary electrons and other radiations from the surface of the specimen and their intensity is dependent on the chemical characteristics and shape of the specimen. These electrons are then collected by a detector and electronic signals are created. The signal are scanned to produce an image just in the same manner television system operates. Images are produced on a cathode ray tube (CRT) as shown in Figure 2.1 (73)

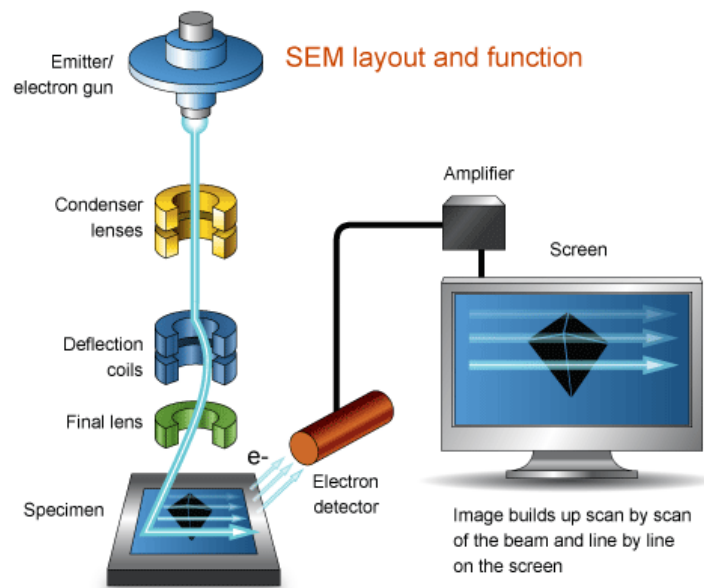


Figure 2.1 Scheme showing the working principle of SEM (73)

2.3.1.3 Preparation of samples for SEM tests.

In this characterization, Zeiss supra 40 FESEM machine modal 196040579 was employed to determine the morphological characteristics of the nanofibers. Samples for imaging were prepared by cutting 2 square centimeters of the aluminum foil containing the fibers and put of

the stage for the SEM imaging. The FESEM was operated at a working distance of 6mm, probe current of 6kv and magnifications of 3000, 18000, 35000, and 70000 x.

2.3.2 Fourier Transformation Infra-Red Spectroscopy

2.3.2.1 Background

All the internal energy of a given molecule at first can be resolved in terms of vibrational, rotational or electronic energy level. So Infrared Spectroscopy is the study and analysis of interactions between a given matter and the electromagnetic fields in the infra-red region. In the infra-red region electromagnetic waves combine with molecular vibrations thus a material can be excited to higher vibration level. The probability of a given Infra-red frequency to be absorbed is dependent on the interaction of that frequency and the molecule. This probability will be higher if the photon and vibrational energy of the molecule coincide (74).

FTIR is a very important technique to give us the compositional information of a given material and is an essential equipment in almost all research labs.

Generally in spectroscopy, information on both absorbed and non-absorbed frequencies is paramount. This therefore requires that radiation covers a broad range of the spectrum and all frequencies are analyzed. This is the case in the dispersive spectroscopy where light is dispersed into individual frequencies by a prism or a grating. However in the FTIR spectroscopy a totally different approach is employed (74).

2.3.2.2 Operation principle of FTIR Spectrometers.

An FTIR set up as shown in Figure 2.2 consists of the following components; a source, interferometer, sample compartment, detector, amplifier, A/D convertor, and a computer. The radiation generated from the source passes through the sample and then through the interferometer until it reaches the detector. The signal is amplified by the amplifier, and converted to digital format through the analog to digital converter as shown in Figure 2.2. The Fourier transformations ensues as soon as the computer picks up the digital signal (74).

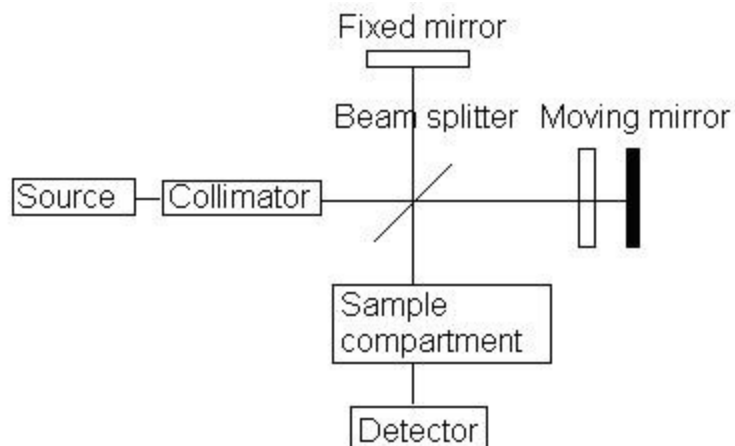


Figure 2.2 FTIR Spectroscope (74).

The Fourier transform derives its name from Jean Baptiste Joseph Fourier who described the Fourier transform in equation 1.

$$f(\omega) = \int_0^{\infty} e^{i\omega t} f(t) dt$$

Equation 1: Fourier transform

Where t is time, and i is the square root of -1. The method converts a function into a new function (74).

2.3.2.3 Preparation of samples for FTIR.

Samples used in the FTIR analysis included both powder and the nanofibers forms. A sample of both cases was mixed with KBr and ground. The ground mixture at a ratio of 1: 0.2 for KBr: sample respectively because KBr is already thick and it's required that a small amount of sample is added (Beer's law). The samples were then compressed to form discs. The discs were placed in the FTIR and analyzed. All nanofibers that contained chitosan were chemically cross linked using glutaldehyde. Nanofibers were placed above glutaldehyde solution in a petri dish in a desiccator. Fibers were left to absorb the evaporating glutaldehyde for 2hrs before being transferred to a vacuum oven which was heated to 70 °C for 24hrs. Physical cross linking was done by exposing the fibers to heat of 100 °C in vacuum for 30 minutes (75).

2.3.4 Swelling and weight loss tests

Both cross-linked and non-cross-linked fibers were used in these test to determine:

The ability of the fiber to absorb exudates and other fluids from wounds as it was reflected in their swelling test results obtained by the following equation. It was generally expected that non cross linked fibers would have a higher degree of swelling since they are not so compacted like in the case of cross linked nanofibers. Weight loss determines degree of degradability and stability of the fibers to determine how long they can withstand during the wound dressing period. It was hypothesized that cross linking of the fibers would help strengthen them and prevent degradability as it would be reflected in the form of lower weight loss compared to the non-cross linked counterparts (76).

2.3.4.1 Test procedure

Nanofibers from the cross linked and non-cross linked nanofibers were immersed in a water bath at 37 °C for 24 hrs. After withdraw from the water, the nano fiber films were rinsed off the surface water using tissue and weighed to get Wt., after they were dried in an oven for 5 hrs at 60 °C and then weighed to get Wd.

2.3.4.2 Calculating degree of swelling

$$\text{Degree of swelling} = (Wt. - W_0) / W_0 \times 100 \quad \text{Equation 2. Degree of swelling}$$

$$\text{Weight loss \%} = (W_0 - W_D) / W_0 \times 100 \quad (76) \quad \text{Equation 3. Weight loss}$$

Where Wt is the weight after immersion in water, W₀ is the dry weight before immersion in water and W_D is the weight after drying the immersed fibers.

2.3.5 Anti-Bacterial tests.

2.3.5.1 Luria Broth liquid media method.

Originally formulated to be used in the culture of E. coli, LB liquid medium is the most commonly used media used for liquid bacteria cultures. The medium is composed of gm./liter Casein enzyme hydrolysate 10.000 Yeast extract 5.000 sodium chloride 5.000 final pH (at 25°C)

7.0±0.2. In general 20gm of LB liquid media powder is dissolved in 1000mL of distilled water. Heat may be required for total dissolution of the powder and sterilization is done by autoclaving for 15 minutes at 15lbs pressure and 121 °C. Luria Broth is a modification of the original formulation by Luria that is most commonly used in molecular and genetic studying due to its simple composition and nutritive value as described by Lennox. Luria broth is a rich media used for easy cultivation of bacteria mostly E. coli due to presence of casein enzyme hydrolysate and yeast extract. The osmotic equilibrium in this medium is maintained by addition of sodium chloride (77).

2.3.4.2 Media preparation

20gm of LB liquid media powder was dissolved in 1 litter of distilled water and stirred by vigorous shaking for a minute. The media was then autoclaved for 15 minutes at 15lbs pressure and after left to cool at room temperature.

2.3.4.3 Bacteria culture.

The two test bacteria used were E. coli (Top 10 MC1061) streptomycin resistant representing the gram negative and S. aureus (MRSA) representing gram positive bacteria Figure 2.3. The two test bacteria are the most predominantly common cause of infections in their respective categories. Gram positive and gram positive bacteria have got characteristic differences in their cell wall structures and thus cell membrane physiology as shown in table 2.2.

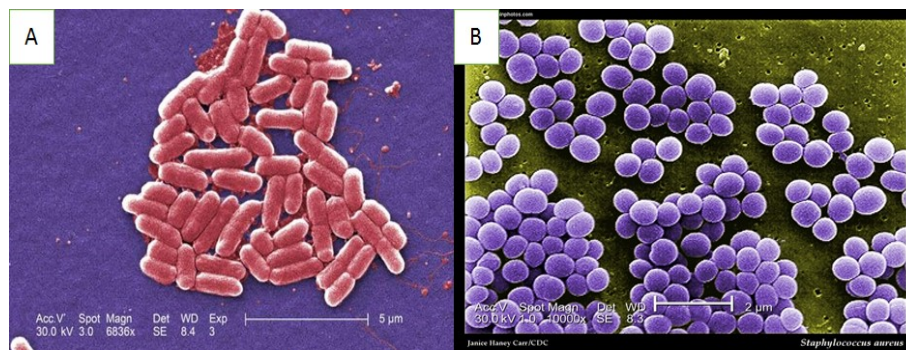


Figure 2.3 Images of E. coli (A) and S. aureus (B) (79).

Table 2.2: Summary of differences between gram positive and gram negative bacteria. (79)

Property of bacteria	Gram Positive	Gram Negative
Thickness of the wall	20-80 nm	10 nm
Number of layers in wall	1	2
Peptidoglycan content	>50%	10-20%
Teichoic acid in wall	+	-
Lipid and Lipoprotein content	0-3%	58%
Protein content	0%	9%
Lipopolysaccharide	0	13%
Sensitivity to penicillin	Yes	Less sensitive
Digested by Lysozyme	Yes	Weakly

2.3.4.4 Preparation of bacteria culture

In a sterile environment in the safe hood, test bacteria from *E. coli* top 10 strain and *S. aureus* were cultured using the steps.

1. Flow hood was sterilized using 70% ethanol
2. Bacteria from both *E. coli* and *S. aureus* from parent stock in eppendoffs were taken out of a refrigerator.
3. LB liquid media was carefully transferred to a falcon tube and closed in a sterile environment.
4. Using a pipette, 5 mL of LB media was put in two sterile falcon tubes.
5. About 0.2mL of Inoculum from the two test bacteria were placed in the two respective falcon tubes and loosely closed.
6. The bacteria culture were transferred to the shaking incubator and fixed there for 24 hrs to be ready for tests.

2.3.4.5 Preparation of the samples.

Samples for anti-bacterial tests (table 2.2) were weighed and standardized at 0.2mg/mL and sterilized by UV lamp for 50 min. The samples were placed in well plates using sterilized pair of forceps, added 2mL of *E.coli* in triplicate and *S.aureus* in triplicates. The two test bacteria were also cultured in triplicates alongside those ones with the test material as illustrated in the scheme 2.1.

The two bacteria bacterial were cultured in LB broth media and incubated for 24 hrs at 37 °C. The inoculum of both *S. aureus* and *E. coli* were diluted and to reduce the optical density to a range of 150 to 170 and then incubated in a shaker incubator for bacterial growth. Bacterial growth and inhibition were studied using the light absorption spectroscopy at absorbance of 600 a.u. 0.2mg/mL of the material was used in this study.

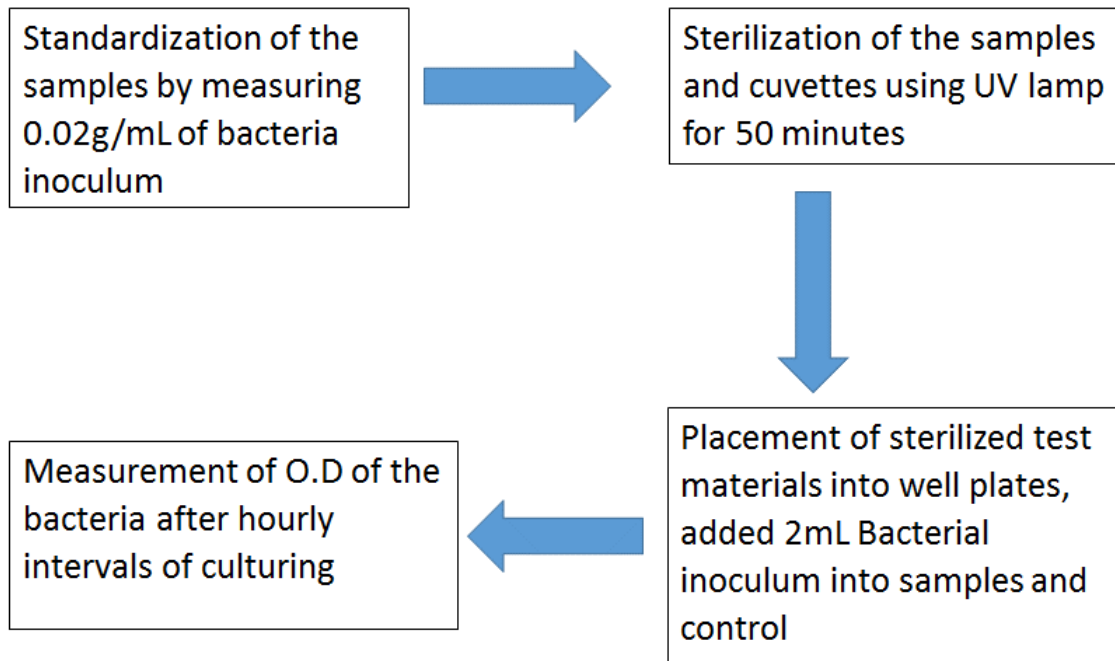


Figure 2.4 A schematic presentation illustrating the sample preparation steps for anti-bacterial tests.

Table 2.3: Samples for anti-bacteria tests are summarized

Sample	Form	Category
Pure DBP	LIQUID	Control
Pure Extract BP	LIQUID	Control
PVA	Nanofibers	Sample
In situ Mixtures	Nanofibers	Sample
PVADBP	Nanofibers	Sample
PVAEXT	Nanofibers	Sample
Ex-situ mixtures	Nanofibers	Sample
PVA: CS	Nanofibers	Sample
PVADBP: CS	Nanofibers	Sample
PVA: DBP: CS	Nanofibers	Sample
PVAEXT: CS	Nanofibers	Sample

Chapter 3

Results and Discussion – Part I

(Preparation and Characterization)

3. RESULTS AND DISCUSSION – Part I

Electrospinning is a relatively simpler technique used in the production of Nanofibers. In the past decade coaxial and multi jet spinning have been popular and with increased research in electrospinning new techniques and parameters will emerge to produce Nanofibers with other properties tailored for enhanced performance in some areas. This development has aided the manufacture of a wide range Nanofibers from various materials over the years.

3.1 SYSTEM VALIDATION.

To ensure that the horizontal electrospinning equipment was in the required standard working conditions, a series of PVA and PVA in distilled Bidens pilosa control solutions were electro spun and studied using the scanning electron microscope (SEM) Figure 3.1. The system readily produced nearly defect free Nanofibers that followed a series of adjustments in the parameters.

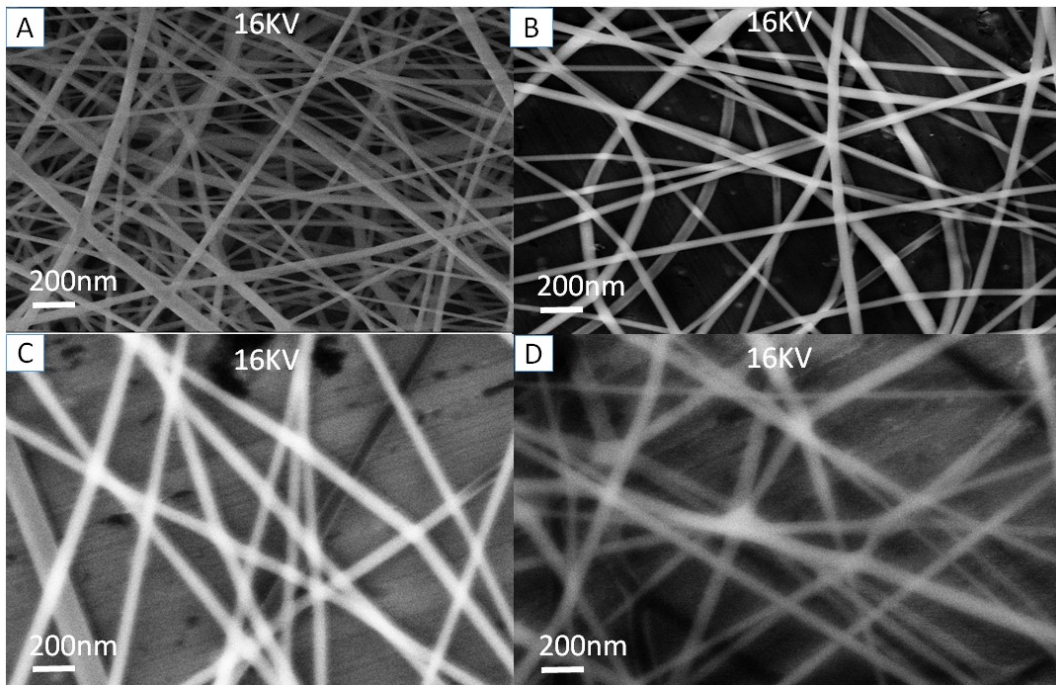


Figure 3.1: SEM Images of (A) PVADBP, (B) PVADBP: CS (C) PVAEXT and (D) PVAEXT: CS Nanofibers at WD6 (x30000 magnification) obtained at a voltage of 16KV, flow rate of 1mL/hr and collector distance of 13cm.

3.2 Composite nanofibers.

Since the turn of the 20th century, interest in developing composite systems has developed tremendously in many fields of science and most especially in materials science. Composite materials take advantage of the properties of individual components and when combined with other materials with either similar or different properties, will yield a material that combines individual characteristics to become much more suited to a specific or multi tasks which individual components wouldn't perform in isolation. This research was premised on the fact that chitosan which is a well studied material from crustaceans, and *Bidens pilosa* a well known and widely used herbal plant in tropical regions are themselves different, but when combined along with a biocompatible and non toxic polymer like PVA could produce a combination of materials that have got better properties for a wide range of applications in both biomedical and agricultural industry as discussed in the aim in this chapter.

3.2.1 Cold extract *Bidens pilosa*, distilled *Bidens pilosa* and Chitosan Nanofibers.

Owing to the fact that *bidens pilosa* were in dilute solution form, it was not possible to electrospun them into nanofibers. Attempt to spin them resulted in mainly droppings. This is due to the diverse materials comprising of *Bidens pilosa* which are mainly short chain polymers. Similarly It was difficult to spun nanofibers from chitosan dissolved in 1% acetic acid.

3.2.2 Insitu Composite mixtures

3.2.2.1 PVA nanofibers.

PVA is known to be highly hydrophilic, biocompatible, nontoxic, and semi crystalline polymer which has got excellent strength, water stability, and gas permeability properties. PVA is available in differing degrees of hydrolysis owing to the fact that its derived from the hydrolysis of polyvinyl acetate, its properties are therefore largely controlled by hydrolysis. As such PVA of hydrolysis of 98 to 99% hydrolysis has got superior mechanical and chemical properties as compared to the 87 to 89% PVA. This property eventually affects the interaction of PVA with other materials especially polar polymers. Electrospinning PVA nanofibers has picked up

momentum in recent years since it can produce fibers with the scale of nano meters to a few micrometers and it is less costly and convenient as opposed to other methods. The dissolution of PVA largely depends on a number of factors which include, the nature of the solvent, the temperature of dissolution, and the extent of polymer dissolution. So nanofibers produced by PVA solution are largely dependent on the rheological characteristics of the solution. In this research PVA was dissolved in de ionised water and temperature used was 80 °C for 4 hrs. The solution at different concentrations was electrospun and results as discussed in the solution parameters were obtained. One important note to make was the fact that PVA dissolved with ease, produced relatively beadless fibers see SEM image a in Figure 3.2 with limited droppings as compared to other combinations at the concentration of 8%.

3.2.2.2 PVA dissolved in Distilled *Bidens pilosa* (PVADBP) nanofibers.

This category of nanofibers provided good fibers and had the most minimum of challenges as it was characterised with near zero droppings, fewer bead formation and smoothness of nano fiber synthesis see SEM image c in Figure 3.2. The only parameter differences came from the solution parameters as discussed later in this chapter. This could have resulted from the fact that distilled *Bidens pilosa* had some bonds broken during the distillation process and thus reaction with PVA polymer chains resulted in reduction of charged groups on the surface of the composite which facilitated the electrostatic forces to overcome the charges and thus easy spinning.

3.2.2.3 PVA in extract *Bidens pilosa* (PVAEXT) nanofibers.

Fibers from PVA in cold extract *Bidens pilosa* were generally generated with ease and there were very few instances of bead formation as can be revealed in SEM micrograph e in Figure 3.2

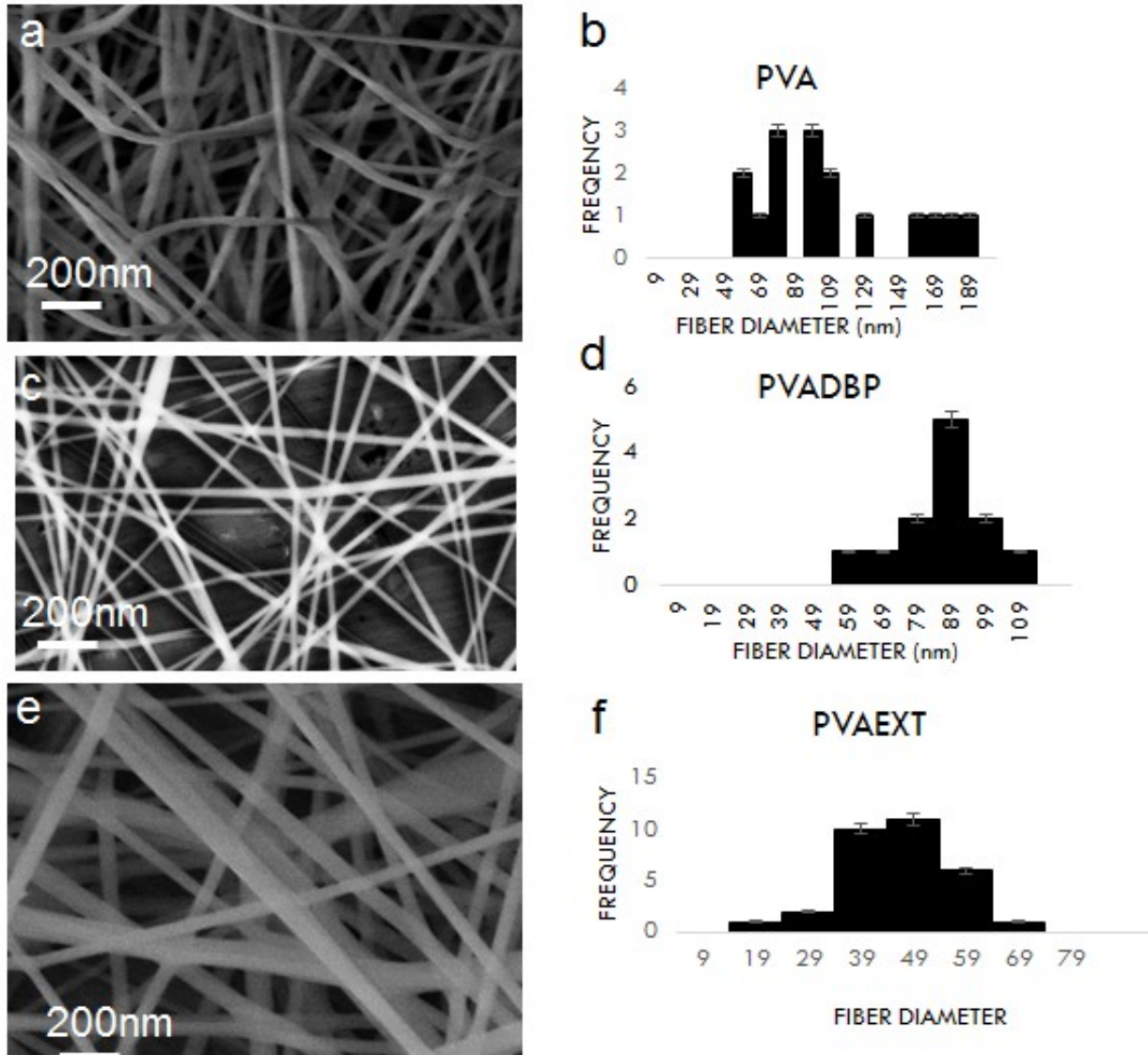


Figure 3.2 SEM images of PVA (a), PVADBP (b) and PVAEXT (c) at WD6, (x30000 magnification), and their histograms (d), (e), and (f) at 16kv, 1mL/hr and 13cm collector distance.

The fiber were uniform in their diameter distribution when the parameters reached ideal level as results revealed high levels of uniformity.

3.2.3 In-situ mixtures with Chitosan

3.2.3.1 PVA and Chitosan.

PVA and Chitosan were prepared by dissolving chitosan in 1% acetic acid and then adding to PVA dissolved in de ionised water at varying ratios. The result were obtained and these were largely controlled by the molecular weight of the chitosan, ratio adjustments and the voltage as discussed later in this chapter. At a high ratio of PVA:CS, nearly beady fibers were formed and this masked all the other factors that were at play. However at as the ratio of PVA in the mixture lowered, difficulties in electrospinning observed and dropping from the needle tip increased. This was more in the mixture containing the medium molecular weight chitosan Figure 3.2. than that having the higher molecular weight chitosan provided the concentration of chitosan was maintained at 3% Figure 3.3.

3.2.3.2 PVA in distilled *Bidens pilosa* and Chitosan PVADBP: CS.

In this category PVA was dissolved in distilled *Bidens pilosa* and then resulting mixture mixed with chitosan at ratios ranging fom 3:1 to 4:1. The chitosan used here was both the heavy molecular weight chiosan (HMWC) (SEM micrographs in Figure 3.3) and medium molecular weight chitosan (MMWC) (SEM micrographs in Figure 3.4).

3.2.3.3 PVA in cold extract *Bidens pilosa* and Chitosan PVAEXT: CS.

This combination was probably the most difficult to electrospin of the composites studied in this research. There was a problem with dropping both on the collector and on the ground surface. The fibers formed however were relatively less beaded howeverthe collection insufficient. Although literature does not have any documented research on *Bidens pilosa* based nanofibers, the reasons are certainly the chemical properties of chitosan and cold extract of *Bidens pilosa* had a role to play. Its is likely that the two components were both highly charged with the same kind of charge and were therefore not able interract well making the surface charges charge high and unable to be overcome by the voltage and thus the electrostatic forces generated were not sufficient to overcome the charges for the fibers to be electrospun and thus fibers formed were riddled with beads as can be seen in Figure 3.3.

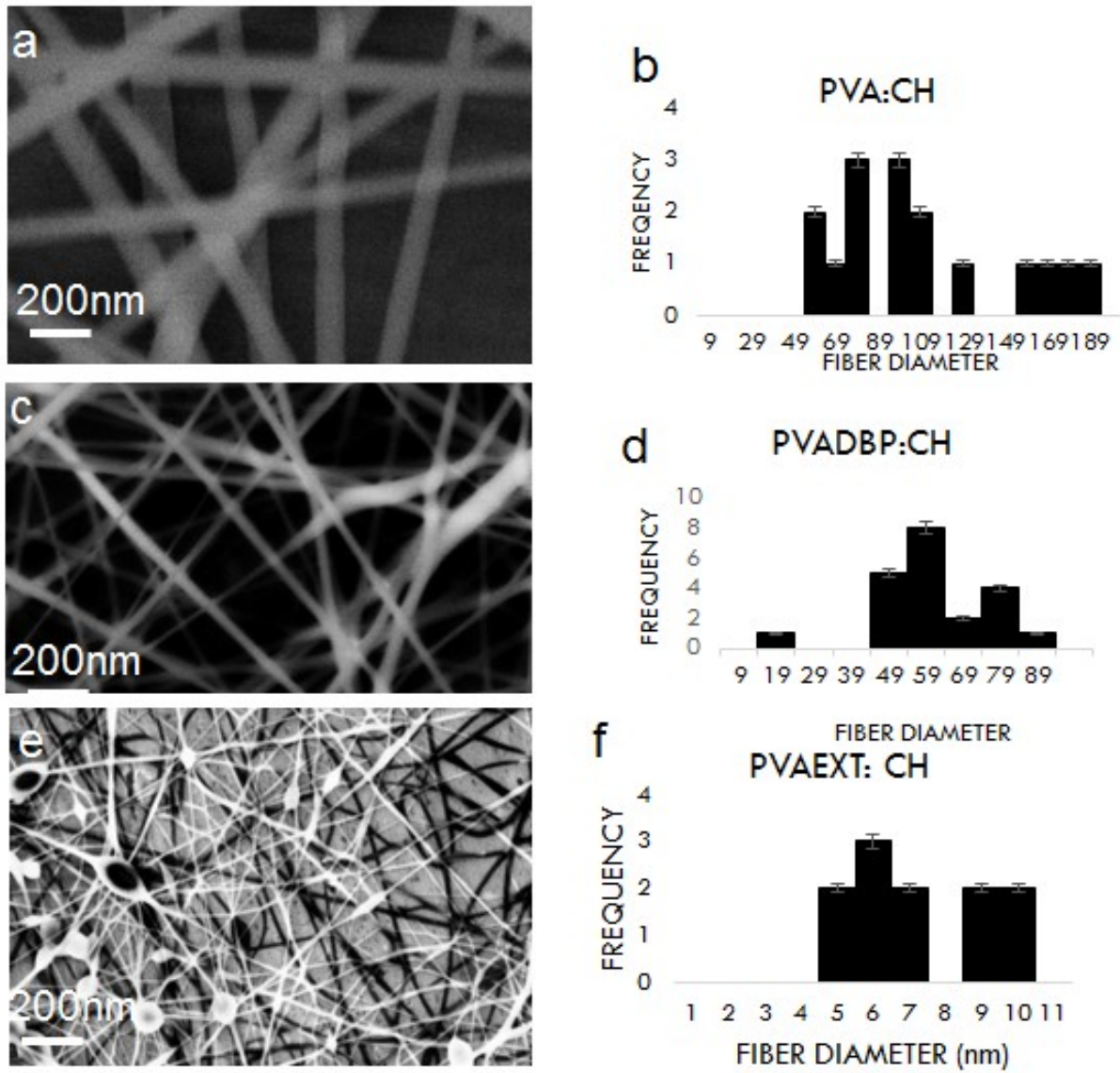


Figure 3.3 SEM images of PVA: CS (a), PVADBP: CS (b) and PVAEXT: CS (c) nanofibers at WD6, histograms (d), (e) and (f) for fiber diameter distribution, at 4:1 ratio, a flow rate of 1.5mL/hr. and collector distance of 12cm. The arrow in the Figure points to the formed beads.

3.2.4 Ex-situ mixtures

3.2.4 .1 Polyvinyl alcohol and distilled *Bidens pilosa* PVA: DBP

PVA:DBP nanofibers were prepared by mixing PVA dissolved in deionised water with fresh liquid extract of distilled *Bidens pilosa* at ratios that ranged from 3:1 to 5:1. It was generally performed with ease as compared with the PVA:CS nanofibers however the problem of beading

somewhat affected the results. These nanofibers were generally synthesized with limited dropping from the needle tip. The ratios also had an impact on the electrospinning process in that higher ratios (4:1 and 5:1) produced better fibers and minimal droppings as compared with the 3:1 ratio. These results were heavily dependent on the other parameters such as applied voltage, feed rate, and time taken to dissolve the PVA solution and also the combined solution.

Nanofibers formed at ideal parameters show non tendency to form beads and also near uniform fiber diameter distribution as revealed by SEM micrograph A in Figure 3.5

3.2.4 .2 PVA and Cold extract *Bidens pilosa* (PVA: EXT).

Polvinyl alcohol : Crude extract *Bidens pilosa* (PVA:EXT) were produced by combining PVA and cold extract solution of *Bidens pilosa* at ratios ranging from 3:1 to 5:1. At lower electrospinning these nanofibers was difficult. This however was not solely linked to the ratios but also to the flow rate and voltage.

To achieve good fiber formation a combination of all these factors had to be altered and thus enable the mixture to produce better nanofibers as can be seen in the SEM micrograph B in Figure 3.4. One notable challenge with this combination was the dropping of the solution and failure to form a stable tailor cone and this was mainly controlled with the ratio adjustment and flow rate regulation.

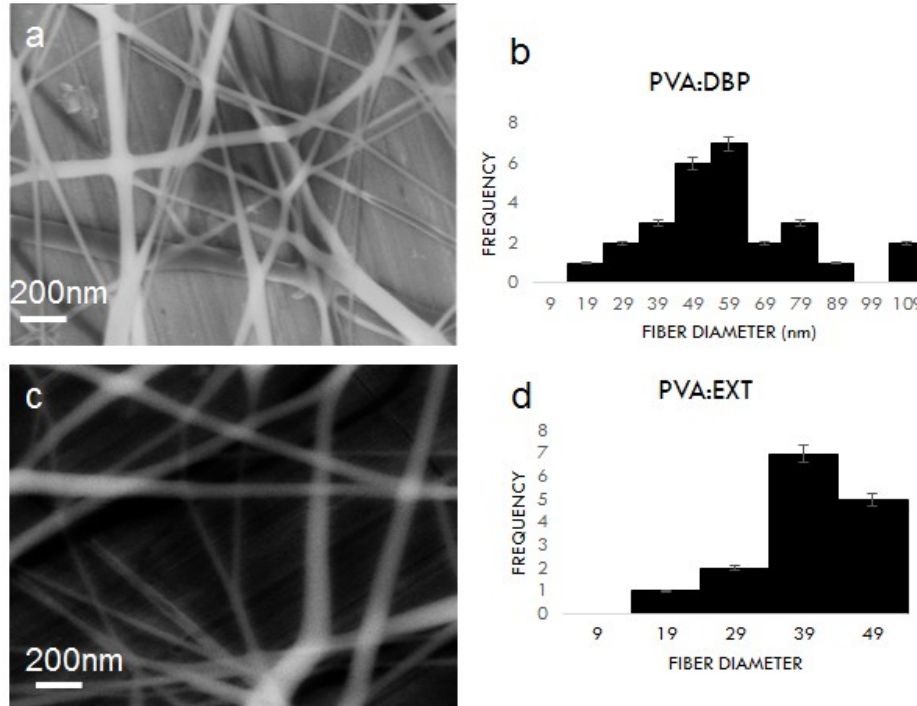


Figure 3.4 SEM images of PVA: DBP (a) and PVA: EXT (b) nanofibers at WD6, (x30000 magnification) with their fiber diameter distribution histograms (c) and (d) obtained at a voltage of 16KV and 1mL/hr. of flow rate.

3.2.5 Ex-situ mixtures with Chitosan

3.2.5.1 PVA, Distilled Bidens pilosa and Chitosan nanofibers (PVA: DBP: CS).

This triplicate composite was prepared by combining PVA , Distilled Bidens pilosa and chitosan at the ratios that ranged from 4:1:1 up to 6:1:1. The nanofibers shown in SEM micrograph A in Figure 3.6 generally indicate better fibers with better properties than the two composite systems tried with PVA:DBP and PVA:EXT. The fibers were generally smooth and were easy to generate with minor challenges of droppings and beading. Higher ratios were also observed to produce relatively less beaded fibers compared to lower ratios. The properties of the fibers also largely depended on the solution parameters during the electrospinning process.

At a ratio of PVA lower than 4, there were difficulties in obtaining nanofibers on the collector foil even when all paramaters were adjusted. Improved nano fiber formation started to form as

the PVA ratio approached and exceeded 4. Further increase in PVA ratio ensured good morphology of nanofibers coupled with near zero bead formation see SEM image A in Figure 3.6.

3.2.5.2 PVA, Cold extract *Bidens pilosa* and Chitosan (PVA: EXT: CS).

In comparison to the PVA:DBP:CS nanofibers, PVA:EXT: CS were replete with difficulties involving the electrospinning process and there was a high problem of dropping. However in comparison to the PVA:EXT and PVAEXT:CS these nano fibers were better in both aspects. They were relatively smooth and less beaded as compared to PVAEXT: CS composite counterparts (see SEM micrograph B in Figure 3.5).

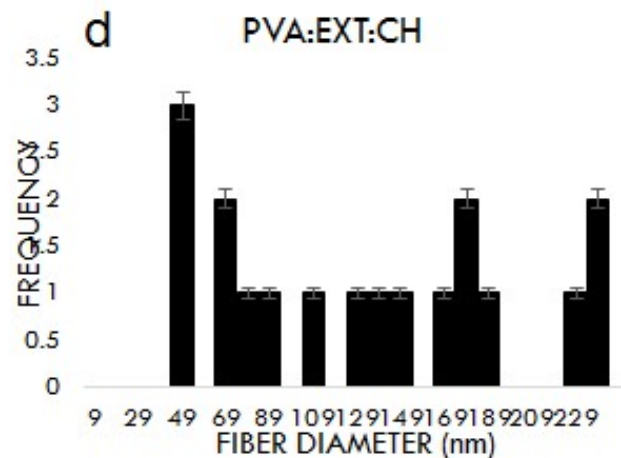
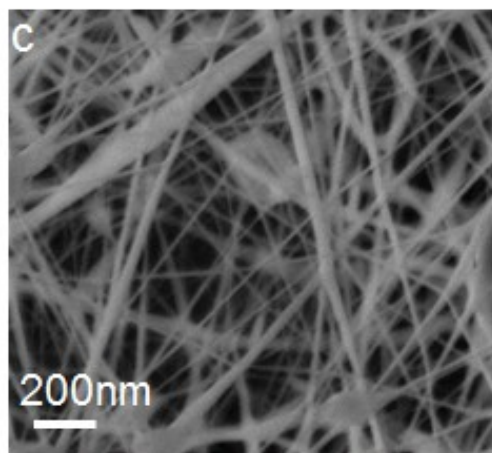
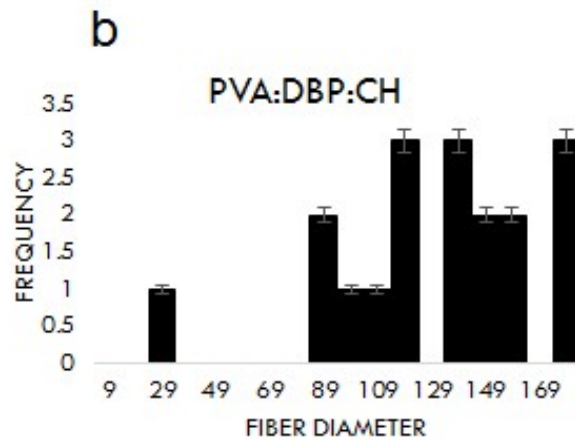
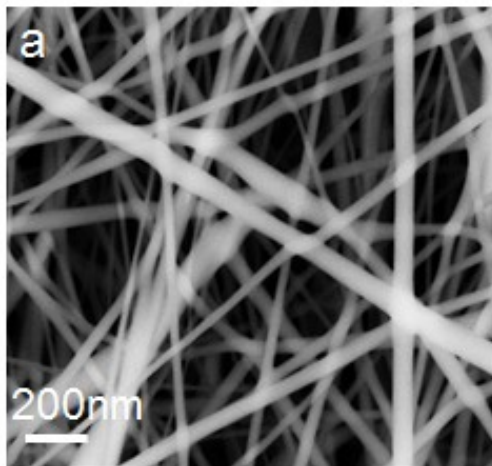


Figure 3.5 SEM images of PVA: DBP (a) and PVA: EXT (b) nanofibers with Chitosan of concentration 3% at WD6 (x30000 magnification) with their fiber diameter distribution histograms (c) and (d) obtained at a voltage of 16KV and 1mL/hr. of flow rate.

3.3 Effect of working parameters on the morphology of Nanofibers

3.3.1 Effect of Voltage on In situ mixtures.

Voltage was the single most important driving force for the electrospinning process and as such its effect on fiber morphology was evident. To be able to spin the solution in the syringe to obtain fibers, a certain optimum amount of current is required to eject and sequester the liquid material into fibers that are then collected on the collector plate. In order to study the effect of voltage on the nanofiber characteristics, a concentration of 8% of the following solutions PVA solution, PVADBP and PVAEXT was prepared and a range of spinning voltage ranging from 16kv to 21kv as shown in SEM images in Figure 3.7. At the voltage of 16 nanofibers of PVADBP studied were formed with a few challenges as can be seen in SEM images in Figures 3.7. The voltage was ideal for fiber formation in all categories of material combination. PVAEXT and PVADBP at the same parameters produced smooth beadles and non-entangled nanofibers with nearly similar diameter range distribution.

The diameter of the nanofibers in both PVADBP and PVAEXT ranged between 10 to 80nm and there was narrow diameter distribution. As the voltage was increased to 18, these properties changed see SEM micrograph B in Figure 3.6. At 18kv, whereas incidences of bead formation were observed, nanofibers formed generally suffered fiber diameter inconsistency as well as increase in average fiber diameter. This challenge was exhibited in both PVADBP and PVAEXT (see SEM image B in Figure 3.7). The range of nanofiber diameter in both cases at 18kv was between 26 to 179nm which was nearly double the voltage of 16kv. As the voltage was increased to 21kv (SEM micrograph C in Figure 3.6), the fiber diameter was increased and there was a problem of wide diameter distribution as well as incidences of electric discharge.

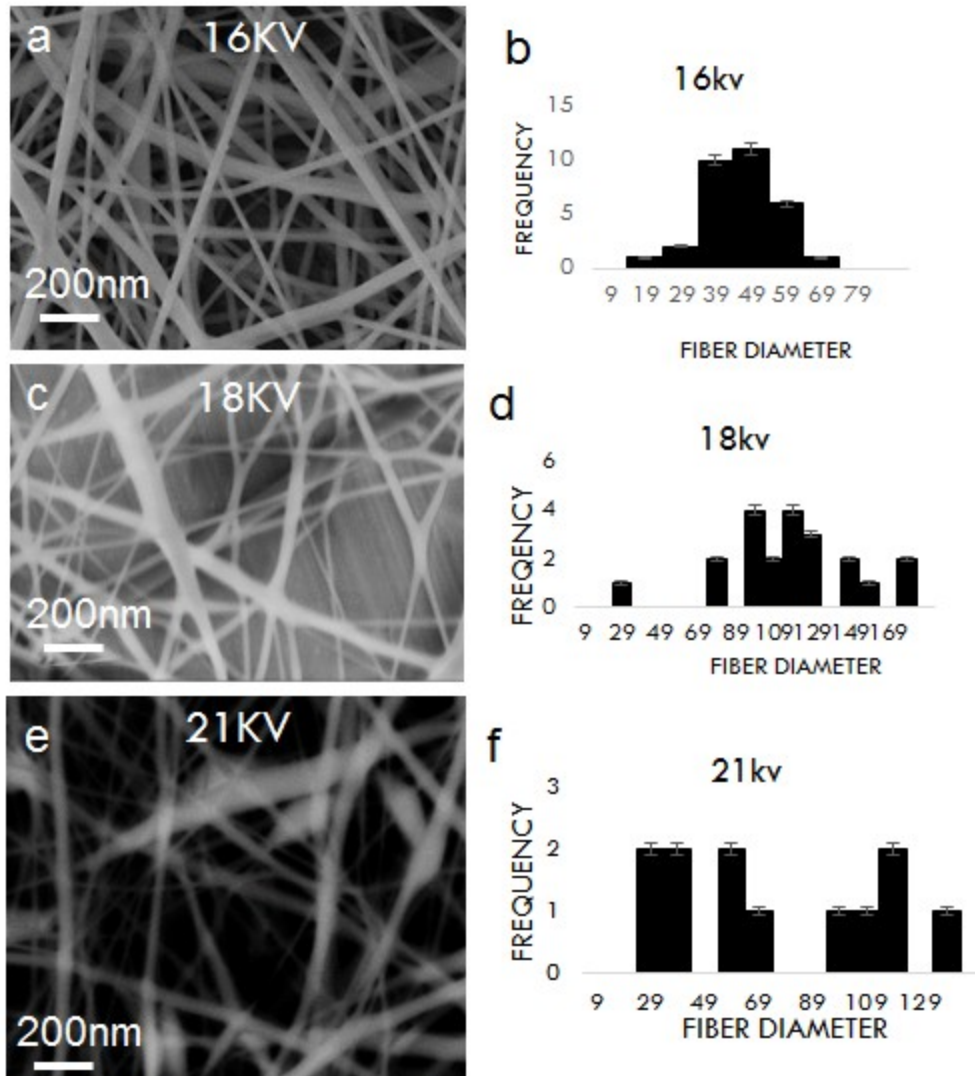


Figure 3.6 SEM images of PVADBP nanofibers with effect of voltage (a) (16kv), (b) (18kv) and (c) (21kv) on 8% at WD6 (x30000 magnification), flow rate 1mL/hr., distance of 12cm with their histogram (d), (e) and (f) for fiber diameter distribution.

3.3.2 Effect of flow rate on nanofiber morphology.

The flow rate of the solution had remarkable impact on the morphology of nanofibers formed. It was largely responsible for bead formation. Composites of PVAEXT, PVADBP and PVADBP:CS were prepared as explained before and were subjected to a constant voltage of 16kv and distance of 12cm while adjusting the flow rate from 0.8 to 1.2mL/hr. SEM images Figure 3.8 reveals the extent of impact that a slight change in flow rate had on the formed nanofibers. The

effect of flow rate was similar. In both cases of PVADBP and PVAEXT, at the voltage of 1mL/hr., fiber formation was uninterrupted, and smooth with negligible levels of dropping as can be evidenced in SEM image b in Figures 3.8. When the flow rate was reduced to 0.8, there was a shift in fiber properties as can be seen in SEM image (a) in Figure 3.8. The two materials studied in this case produced properties that were common for example fiber inconsistency and bead formation in both cases. On the other hand when the flow rate was raised above 1mL/hr., there were challenges similar to those associated with low flow rate see SEM micrograph c in Figure 3.8. At the flow rate of 1.2mL/hr. (see SEM image c in Figure 3.7) the fiber diameter were widely distributed and beading problem too was observed. The diameter of the fibers was however smaller than those at lower flow rates.

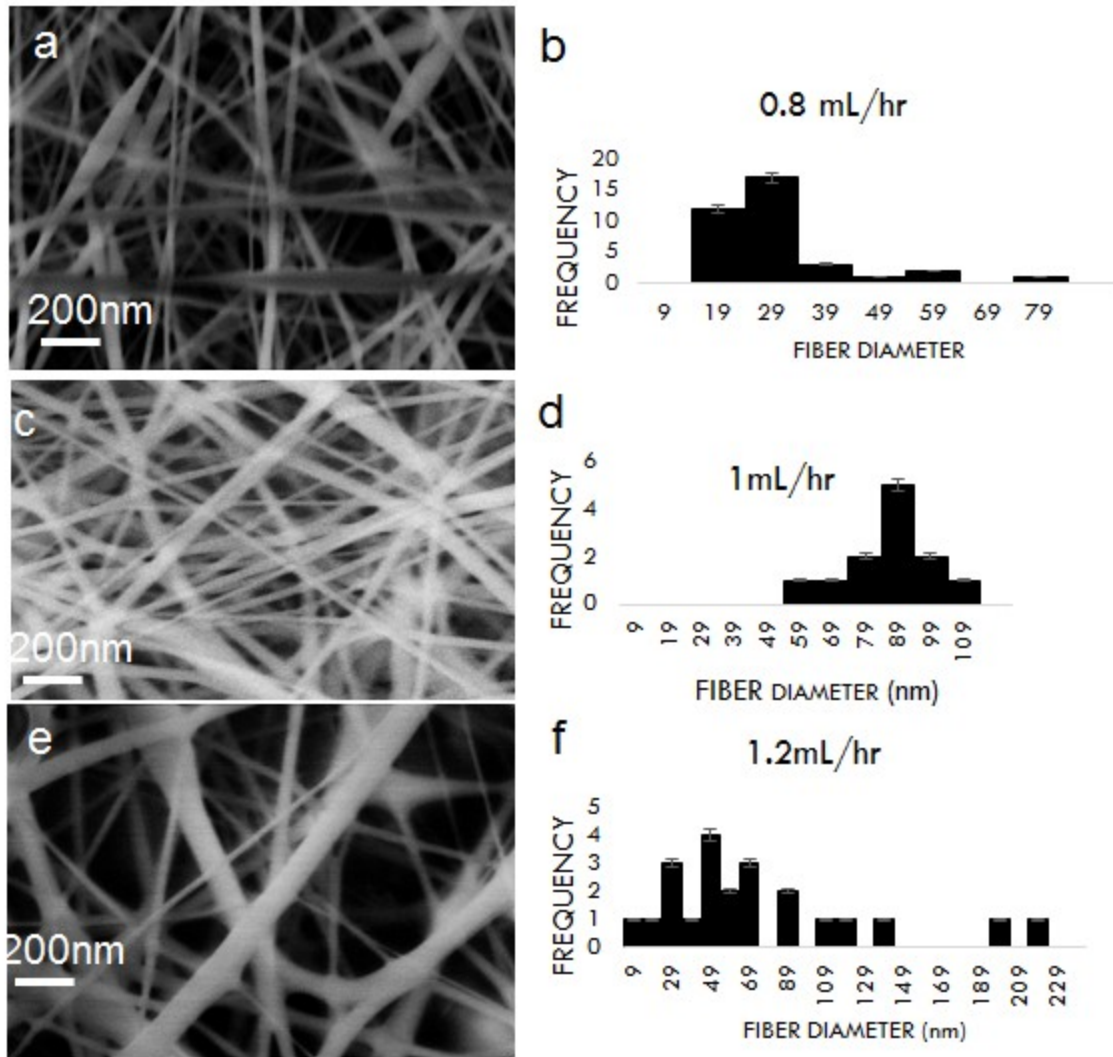


Figure 3.7 SEM images of PVADBP nanofibers with effect of flow rate (a) (0.8mL/hr), (b) (1mL/hr) and (c) (1.2mL/hr) on 8% at WD6, (x30000 magnification), obtained at 16KV and collector distance of 12cm with their histogram (d), (e) and (f) for fiber diameter distribution.

It was observed that at higher flow rate there, is wide distribution of nanofibers covering between 8 to 150 nm. Also dominating the fiber diameter were narrow fibers with diameter less than 50nm.

3.3.3 Effect of collector distance on Nano fiber properties

Just like flow rate, the effect of collector distance on both in situ and ex-situ mixtures was similar. To study the effect of collector distance on the morphology of nanofibers formed, the other two parameters of voltage and flow rate had to be fixed at 16kv and 1mL/hr. respectively. A series of experiments were run on PVA: DBP: CS, PVADBP, and PVADBP: CS, PVA, and PVA: CS, PVAEXT and PVA: EXT were run and exhibited characteristics were obtained by the SEM micrographs in Figure 3.9. At the distance of 12cm at a constant flow rate and voltage, nanofibers were formed with minimal challenges and the resulting nanofibers were smooth and nearly beadless the main undoing of this distance was fiber diameter inconsistency with a range of between 29 to 179 nm for the case of PVA:DBP:CS. At 13 cm however there was a noticeable decrease in the range of fiber diameter distribution. Further increase in collector distance did not yield very good results as fiber diameter distribution increased tremendously SEM micrographs in Figure 3.8.

As the distance was increased from 12 to 13cm there was a reduction in fiber diameter distribution while further increase from 13 to 14cm yielded mixed results.

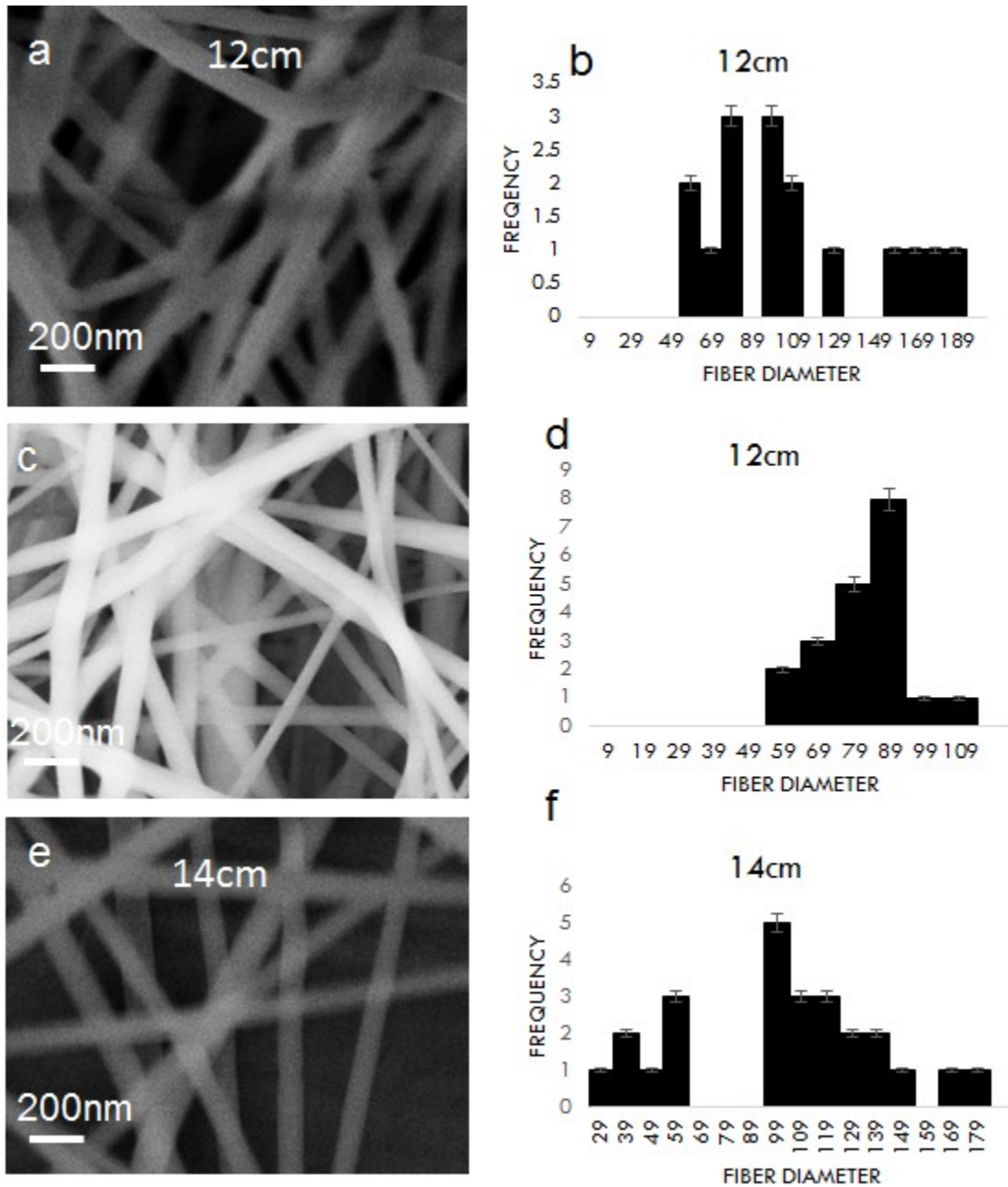


Figure 3.8 SEM images of Insitu composite nanofibers investigating effect of collector distance (a) 12cm, (b) 13cm and (c) 14cm at WD6, (x30000 magnification), with histograms (d), (e), and (f) for fiber diameter distribution at voltage of 16kv.

3.3.4 Effect of solution concentration.

Concentration of the solution is one of the key factors that determine the type of fibers that can be obtained by electrospinning. In order to study the influence of concentration on nano fiber formation, different solutions (PVADBP, PVAEXT, PVADBP:CS, PVAEXT:CS) as shown in SEM images in Figure 3.9. It was observed that the formation of smooth beadless fibers increases with increase in the concentration. At concentration of 6% of PVADBP, PVAEXT, PVADBP:CS and PVAEXT:CS fiber breaks along with beads were observed see image a in Figure 3.9, this however improved to smooth beadless fibers at 8% see SEM image b in Figure 3.9. As the concentration increased to 10% (SEM image c in Figure 3.9), fiber entanglement was observed and ribbon like structures were produced at the concentration of 14% as shown in SEM micrograph d in Figure 3.10.

The effect of concentration on in-situ mixture was eminent and a slight change in concentration led to clearly noticeable differences. On the other hand effect of collector distance on the in situ mixture was not as severe. In ex-situ mixtures low concentration was associated with beads and as it was increased, beadless fibers started forming. Unlike in situ mixtures, at the concentration of 12% , fibers were still clear without ribbon like formations.

Lower concentration of the polymer was insufficient to maintain a stable jet from the Taylor cone to the collector and the breaks that result lead to formation of beads SEM micrographs A for PVADBP and PVADBP:CS. This low concentration is associated with increased surface tension which can not be overcome by the electrostatic forces largely because of the low chain entanglement in the solution and high solvent ratio in the solution. Researchers including Yuan et,al attributed this scenario to the lower viscosity and conductivity of the material at lower concentration as compared to higher concentrations. Lowered conductivity was the main factor suggested to be associated with bead formation (3).

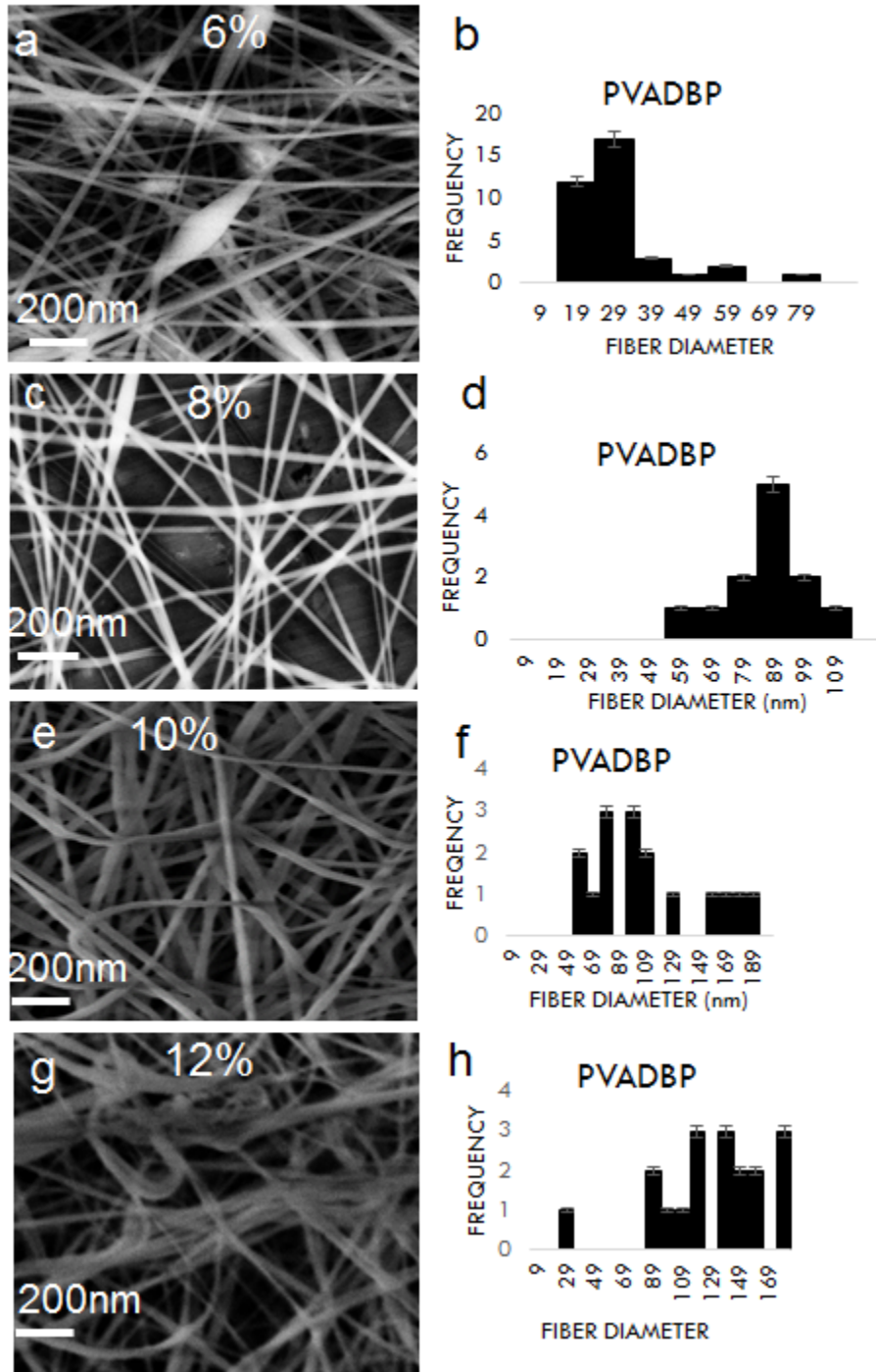


Figure 3.9 SEM images of PVADBP nanofibers electrospun at WD6, (x30000 magnification), flow rate 1mL/min and voltage 16kv from PVA solutions concentration (w/w): (a) 6%, (b) 8%, (c) 10%, and (d) 12%, (w/w), respectively.

Table 3.1 and subsequent Figure 3.10 shows the viscosity values of PVADBP in mini pass (which is the measure of resistance of the solution to the L4 probe rotation) increase with increasing concentration from 6% up to 12% of PVADBP. It was observed that viscosity of a solution increases the disappearance of beads in higher concentration was a direct result of improving the level of fiber entanglement, lowered solvent ratio and increased conductivity SEM micrographs B for both PVADBP and PVADBP:CS. High concentration of the material led to increase in fiber diameter.

Table 3.1 Shows the viscosity of the PVADBP solution at different concentrations

Concentration %	Viscosity in mPass
6	112
8	320
10	1190
12	2980

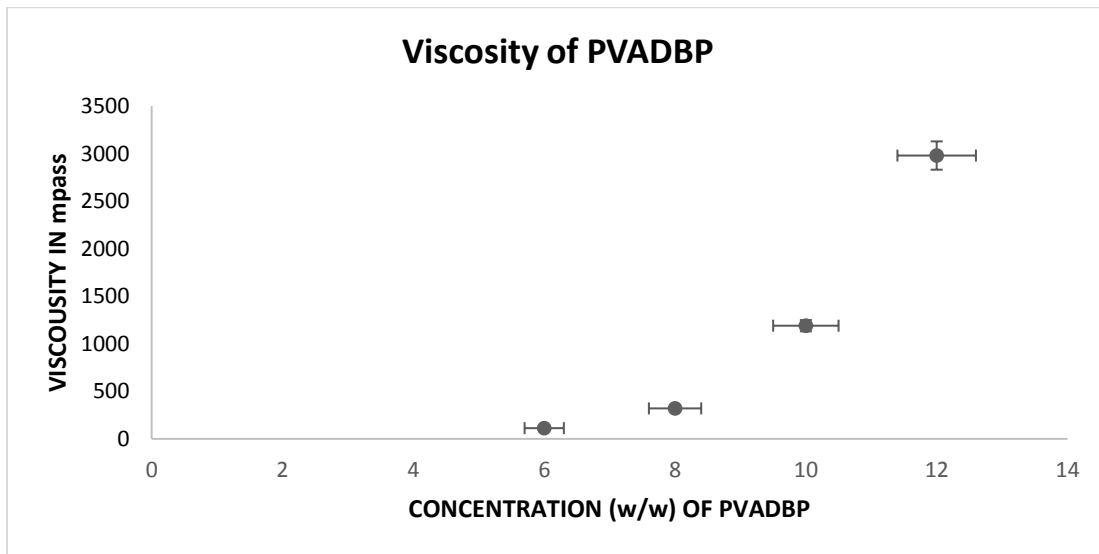


Figure 3.10. Changes in viscosity with Change in concentration of PVADBP.

3.3.5 Effect of ratio adjustments.

For the preparation of PVA:CS, PVA:DBP, PVA:EXT, PVADBP:CS, PVAEXT:CS, PVA:DBP:CS, PVA:EXT:CS nanofibers, adjustments in the ratios of the constituting components had to be

adjusted until an optimum ratio was achieved. Lower ratios of PVA in the mixture led to challenges in even getting the electrospinning process to begin, as the amount of PVA was increased, spinning of fibers started improving however with significant level of beading. When the amount of PVA reached an optimum value, smooth fibers with less beading was achieved. These ratios ranged from 3:1 of PVA : CS/EXT/DBP 4:1:1 for the case until 5:1 for the former and 6:1:1 for the later and the results are revealed in the SEM micrgraphs in Figures 3.11.

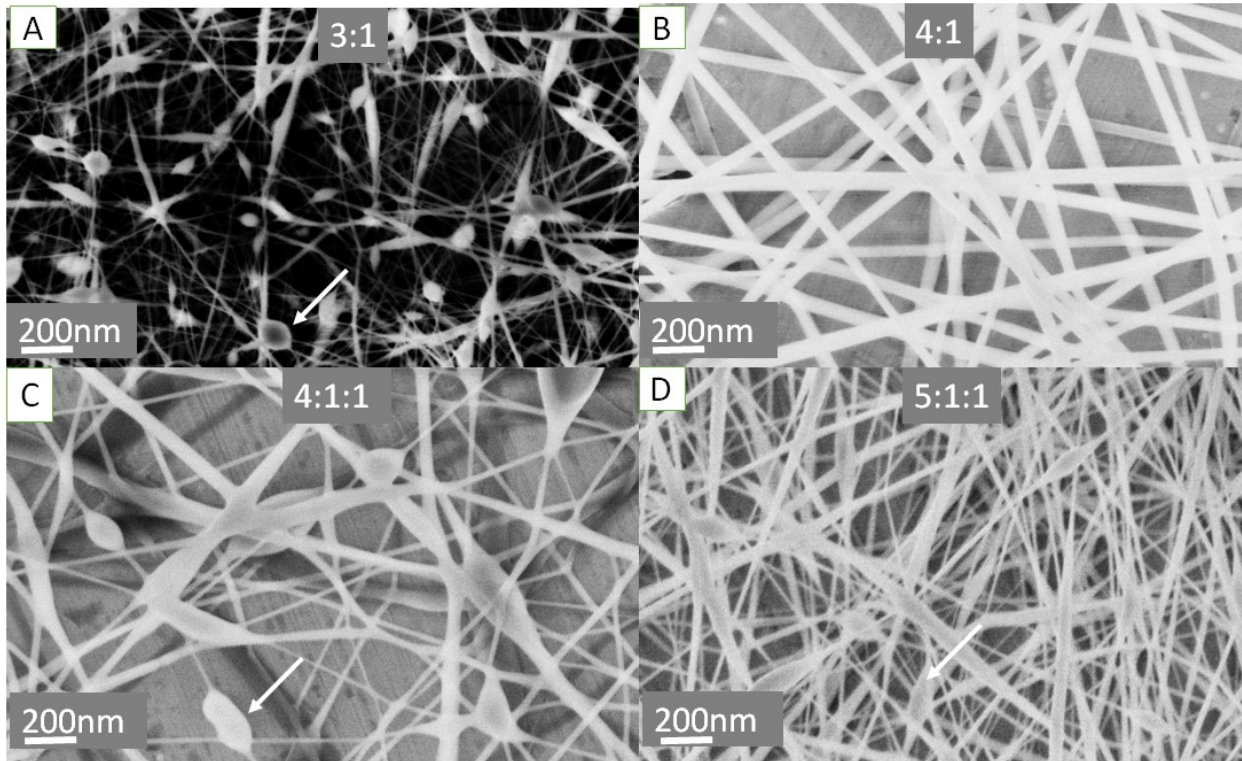


Figure 3.11 SEM images showing the Effect of solution Ratio for PVA: CS ((A) 3:1, (B) 4:1) and PVA: DBP: CS ((C) 4:1:1, (D) 5:1:1) nanofibers at WD6, voltage of 16kv, flow rate of 1mL/h and collector distance of 13cm.

3.3.6 Effect of differences in the molecular weight of Chitosan.

The molecular weight of chitosan had a notable impact on the viscosity of chitosan and the composite solution in general. Three molecular weights of chitosan were investigated in these experiments in order to determine which of the three was most suitable for electrospinning and could form fibers consistent with the requirements for the intended application. The molecular weights of chitosan used were, High molecular weight (HMWC 1600), medium molecular weight chitosan (MMWC 400) and low molecular weight chitosan (LMWC 110). Solutions from each of the three categories of chitosan were dissolved in 1% acetic acid solution then added to the PVA, PVADBP, and PVAEXT at different ratios ranging from 3:1 up to 5:1. Results indicated that High molecular weight chitosan (HMWC) produced more viscous solutions as compared to the medium and low molecular weight chitosan and the least viscous solution was produced by the low molecular weight chitosan as can be seen in the Figure 3.40. High molecular weight chitosan was too viscous to spin at 4% and had to be lowered to 2% while the medium required an increment from 2 to 3%.

The low molecular weight was best spun at 4%. SEM micrographs were obtained for the three categories of molecular weight at a concentration of 3% and results indicated that at the low concentration, High molecular weight chitosan produce more stable and beadless fibers and the trend was more beads were produced as the molecular weight was reversed. However at higher concentration, it was not only difficult to stir the high molecular weight chitosan, but it was also hard to spin even at the high voltage. This is because the viscosity too high for the electric field to overcome in order to spin the fibers. The conclusion derived from this experiment was that at low concentration it, was worthwhile using high molecular weight but if it required high concentration of chitosan, low molecular weight chitosan would be more suitable (Figure 3.12).

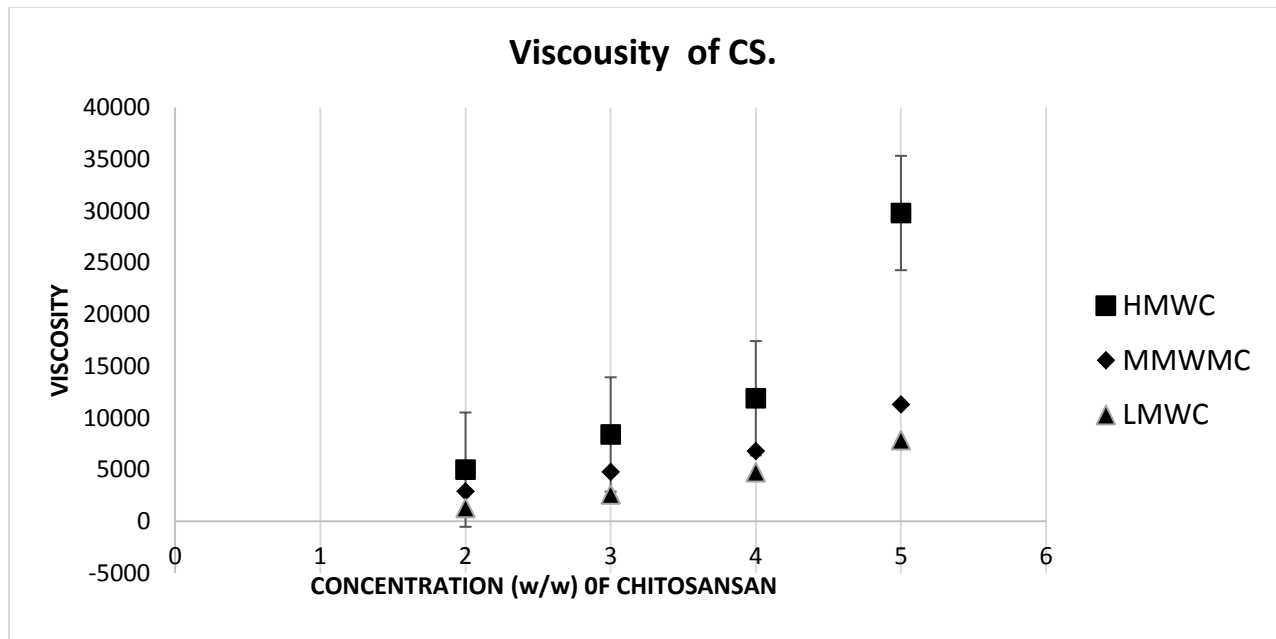


Figure 3.12 Viscosity of the different molecular weights of Chitosan.

3.4 Discussion.

The finding in this research pertaining to effect of voltage on nanofiber morphology is well in line with the findings in literature. Li *et, al* studied the effect of voltage on the formation of PVA fibers and found out that diameter of the fibers increased with increase in voltage (3). The same results were obtained by Zhang *et, al* (72). They studied the effect of different parameters on the formation of polyurethane nanofibers and discovered an increase in fiber diameter at higher voltages as compared with the low voltage. Khan Z *et, al* studied the effect of applied voltage on the nanofiber morphology and observed the same trend (Figure 3.13) (81).

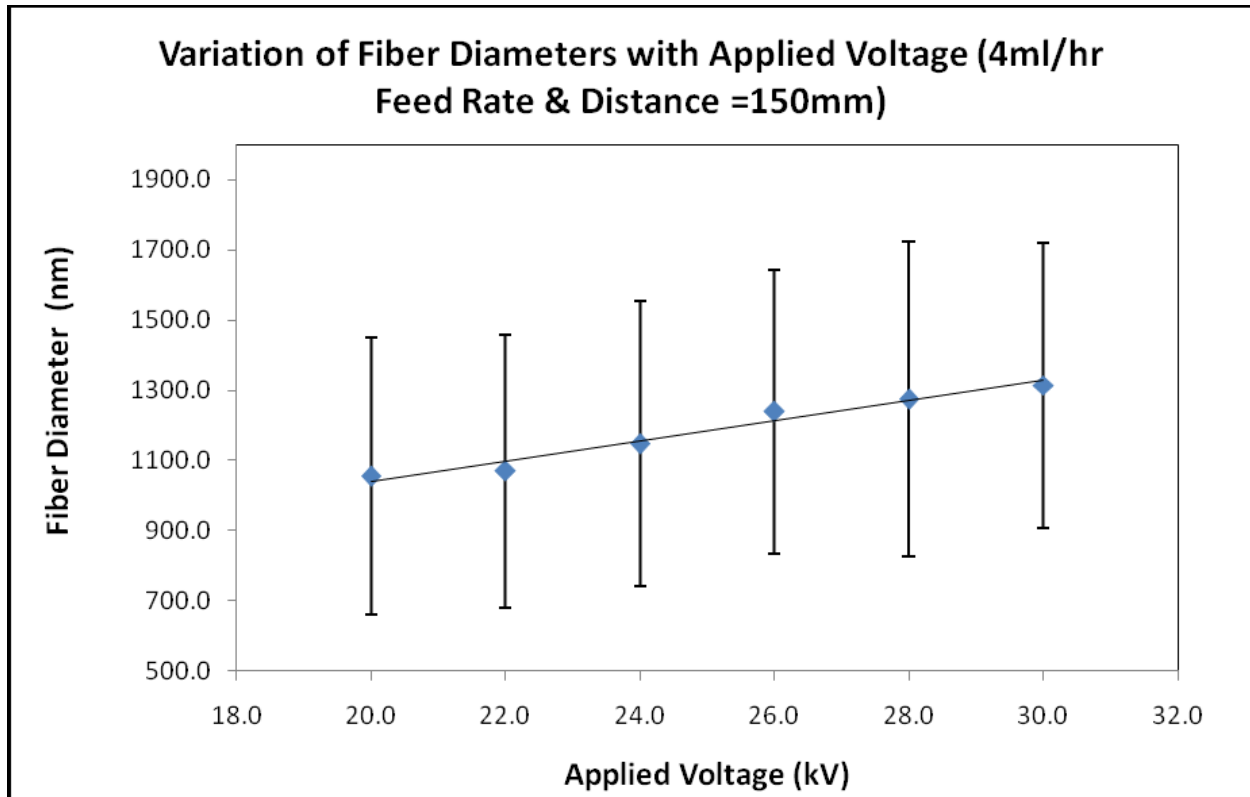


Figure 3.13 Effect of voltage on nanofiber diameter on Polysulfone nanofibers at a fixed flow rate of 4mL/hr. and distance of 150mm. (81)

The feed rate refers to the amount of solution availed at the needle to be electrospun. This parameter is very important as it is directly linked to the tailor cone stabilization. The finding here in were supported by literature. Khan K *et, al* studied the effect of feeding rate on the formation of polysulfone nanofibers and reported an increase in diameter of nanofibers at higher flow rates than low flow rates Figure 3.14 (81). They attributed this effect to the lesser time available for the material to reach the needle tip and lesser time available to form the tailor cone and hence lesser time for the solvent to evaporate and thus leading to formation of thicker fibers. The fiber diameter at lower feed rate is similarly attributed to the fact that little amount of solvent is available at a particular time for electrospinning. This causes the jet to be unstable and interrupted thus affecting the continuity of the ejected solution. This in turn leads to increase in surface tension of the solvent resulting in the formation of beaded fibers (72, 81, 82).

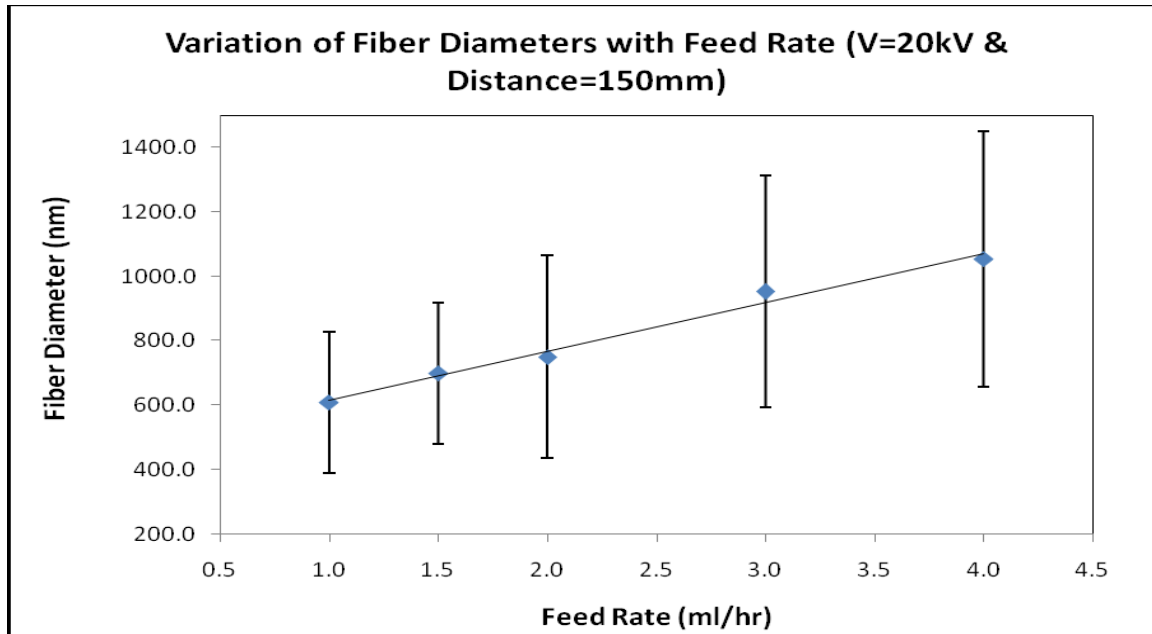


Figure 3.14 Effect of feed rate on Polysulfone nanofibers morphology obtained at a fixed voltage of 20KV and collector distance of 150mm (81)

The effect of collector distance influences two important factors: jet travelling time that is associated with the solvent evaporation time, and the field strength which is the voltage over a given distance. Shorter distance are normally associated with larger fiber diameters. This is explained by the fact that the shorter the distance, the shorter is the time taken for the fibers to reach the collector and in turn the shorter the time available for the solution to fully evaporate and thus larger diameters. Long distances allow ample time for the solution to evaporate and thus allow the fibers to become thinner before landing on the collector.

The other observed property was the wide range of fiber diameters associated with either too short distance or too long distances. This observation was well in line with the established research findings in literature. Li *et, al* (43) observed that while lower collector distances increase the fiber diameter, some other research teams including Megelski *et, al* (6) suggested that the effect of collector distance on fiber morphology is not as pronounced though influences to a fiber diameter but other solution parameters are largely responsible for the significant changes in fiber diameters. Whereas some findings in literature associate collector distances with bead formation, findings in this research did not point to that. Huang *et, al* in

their examination of fiber properties with changes in collector distances similarly indicated that collector distance did not influence bead formation and attributed bead formation to the solution parameters (81, 82).

For the ratio adjustments the results are similar to those found in literature is well corresponding to the findings in this research.

Research done by Khan *et, al* (5) and Demir *et,al* (4) on polysulfone and polysterene reported that for smooth nanofibers to be obtained higher ratios of the polysulfone, and polysterene were required in their repective composites. Nitanan *et, al* studying the effect of solution parameters on the morphology of polysterene nanofibers reported increase diameter with increase in the ratio of polysterene in the mixture (81).

Jamnongkan *et, al* who studied effect of PVA to chitosan ratios on the morphology of the formed nanofibers reported the following: At 100:0 ratio of PVA:CS, ideal fibers were formed. These fibers were smooth, beadles and nearly uniform in diameter. At a higher ratio of PVA to CS (9 :1) nearly ideal fibers were obtained. This trend continued continued with depreciating quality of the nanofibers until it was down to 50 at which point nanofibers failed to form see SEM mages in Figure 3.15.

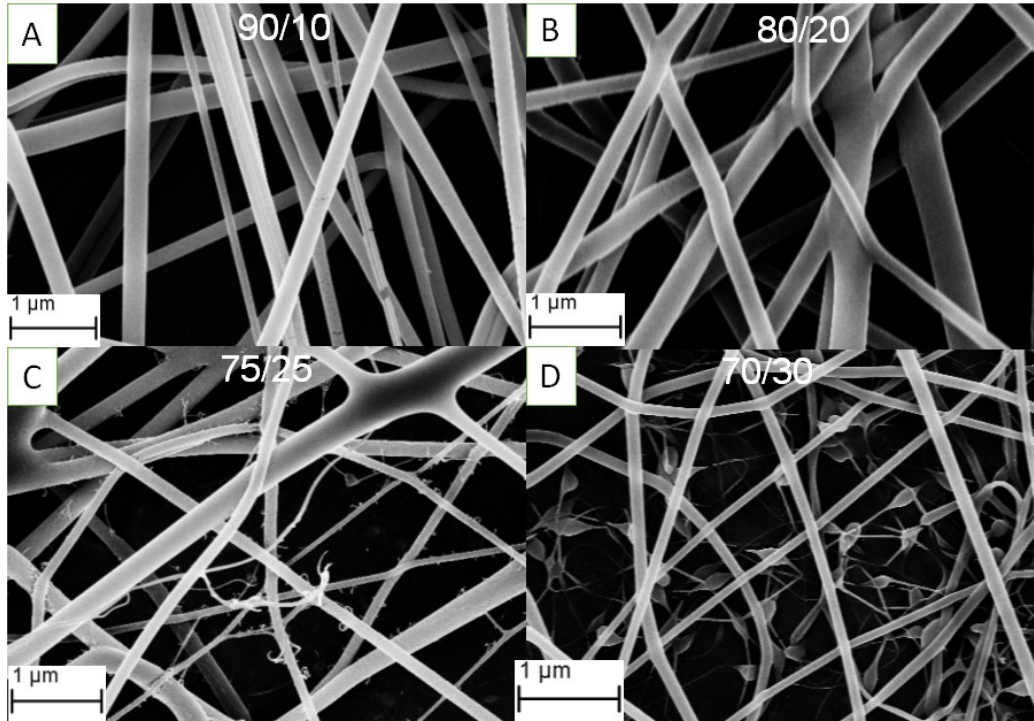


Figure 3.15 SEM images of PVA and Chitosan blend electrospun nanofibers with different weight at varying ratios of PVA/CS; (A) 90/10, (B) 80/20, (C) 75/25, and (D) 70/30 (83) obtained at a constant voltage of 15KV (81).

They attributed this effect to the fact that chitosan is ionic polyelectrolyte with a higher charge density on the surface which requires strong elongation forces to overcome the resistance and form fibers. As the chitosan ratio increases in the blend, the over surface tension which largely depends on the repulsion of the excess charges on the formed jet increases which leads to failure to form nanofibers. Just as in the case of Nitanan *et, al*, Jamnongkan *et, al* also observed increase in fiber diameter with increase in the ratio of polymer i.e. PVA to chitosan see Figure 3.16.

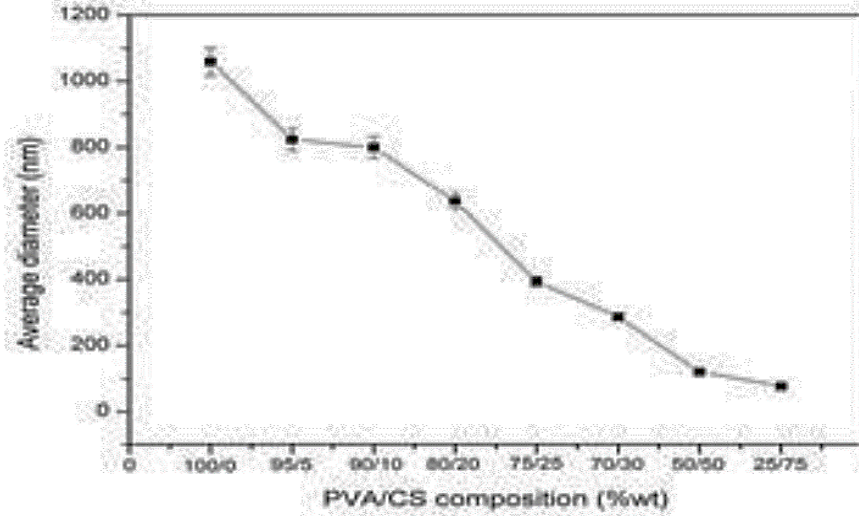


Figure 3.16 Average diameter of the electrospun PVA and Chitosan nanofibers as a function of the weight ratio (PVA/CS) (84).

The effect of concentration has been reported multiple times in literature and findings in this research were largely similar to those in literature. Khan *et, al*, and Demir *et, al* (4) reported that increase on concentration of a polymer gives equal difficulty like decrease in concentration thus a balance must be achieved to arrive at a moderate concentration that creates beadless and uniform fibers (72, 81). Study carried by Deitzel J.M *et, al* also revealed that increase in concentration not only increase fiber diameter, but also leads to formation of a wide range of fiber diameter distribution as in Figure 3.17 (84).

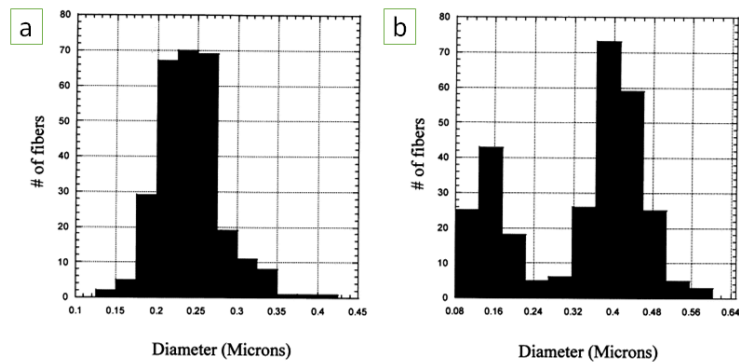


Figure 3.17 Size distribution of diameters in nanofibers electrospun from polyethylene oxide PEO/water solutions: (a) 7 wt%; and (b) 10 wt% (84).

3.5 Water Immersion tests.

The weights were then taken and calculations for weight loss and degree of swelling were made according to the procedure outline in the previous chapter. Results were then tabulated and analysed according to the Figure 3.18.

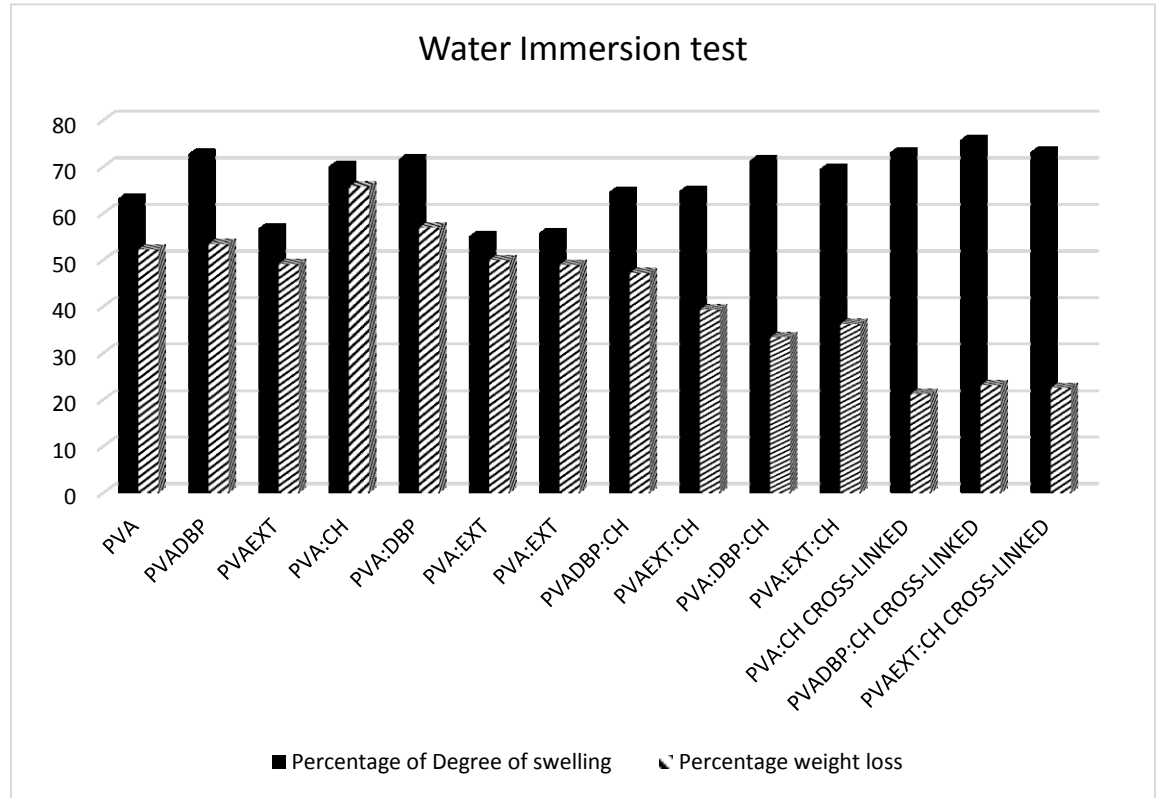


Figure 3.18 Water Immersion test for weight loss and swelling capacity of the nanofibers.

The results obtained shown that the nanofibers formed had higher water absorbing caopacity coupled with a lower weight loss. The swelling in the case of the cross linked fibers was not as much, however the loss of weight was significantly greater than the no no crosslinked category. The principle of weight loss and sweling ability is very important for the nanofibers whose purposed application involves absorption of molecules while maintaining their intergrity. This is the case for this research as the intended application is to enhance the nanofibers' ability to

absorb exudates and also maintain a stable structure. The fiber category with the highest swelling ability are highlighted in table 3.2

Table 3.1: Results of the water immersion test.

Sample	Weight (gm) before immersion	Weight (gm) immediately after immersion	weight (gm) after immersion and drying	Percentage of Degree of swelling	Percentage weight loss
PVA	0.1332	0.3615	0.0636	63.15	52.2
PVADBP	0.131	0.48	0.061	72.708	53.4
PVAEXT	0.0865	0.2	0.044	56.75	49.1
PVA:CS	0.0484	0.1615	0.0166	70.03	65.7
PVA:DBP	0.1387	0.489	0.0597	71.6	56.95
PVA:EXT	0.012	0.0267	0.006	55.056	50
PVA:EXT	0.0823	0.186	0.042	55.75	48.96
PVADBP:CS	0.142	0.401	0.075	64.5	47.18
PVAEXT:CS	0.0088	0.025	0.00534	64.8	39.31
PVA:DBP:CS	0.078	0.272	0.052	71.32	33.33
PVA:EXT:CS	0.061	0.2	0.0389	69.5	36.22
PVA:CS CROSS-LINKED	0.033	0.1226	0.026	73.08	21.21
PVADBP:CS CROSS-LINKED	0.0182	0.075	0.014	75.73	23.076
PVAEXT:CS CROSS-LINKED	0.08	0.298	0.062	73.15	22.5

3.6 Fourier transform infra-red spectroscopy.

FTIR test were carried out to determine the chemical changes that occurred due either was done in 3 combinatorial phases changes in chemical reactions during preparation of the composite blends which

- 1- Blends that involved polyvinyl alcohol and chitosan at a ratio of 4:1 respectively as shown in the spectral charts in Figure 3.19 for their individual sp

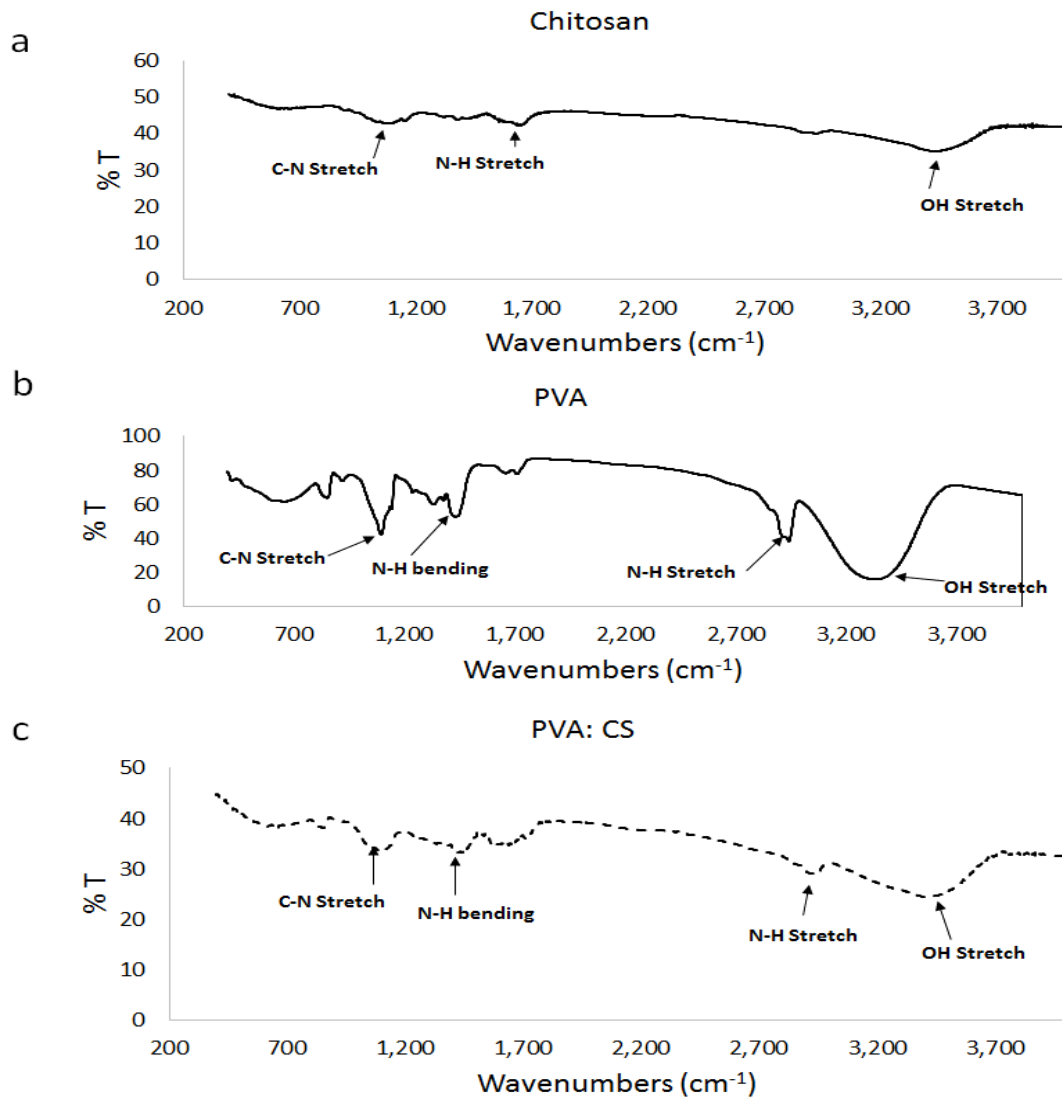


Figure 3.19 FTIR Charts for (a) Chitosan (b) PVA and (c) PVA: CS blend at a ratio of 4:1.

- 2- It was also used to determine the fundamental differences in chemical groups between the different components of the *Bidens pilosa* plant extracts (distilled and crude) as showed in the individual spectra in Figure 3.20.

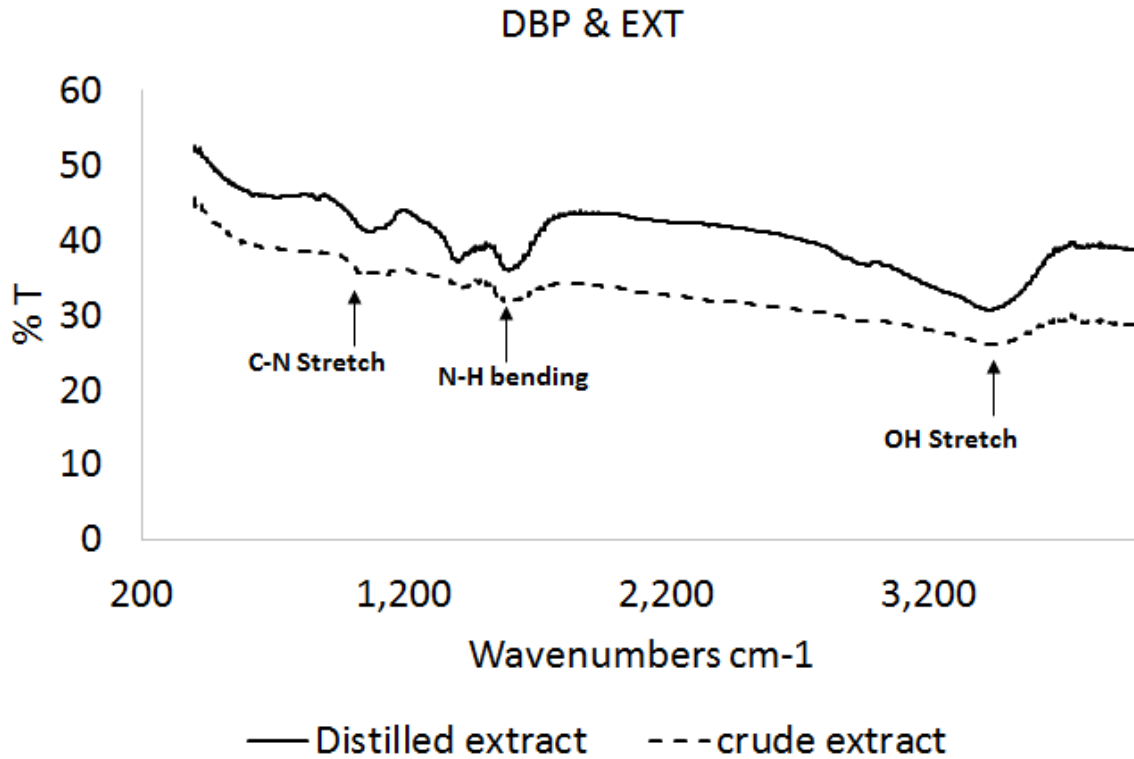


Figure 3.20. FTIR Charts for crude extract and distilled extract *Bidens pilosa* showing detailed composition of their individual functional groups

- 3- FTIR spectra were also used to ascertain chemical changes that occurred when plant extract was combined with PVA as showed in the individual spectra in Figure 3.21
- 4- Finally the FTIR technique was used to study chemical differences that would occur if the PVADBP solution was blended with chitosan at a ratio of 4:1 respectively to form nanofibers and the results indicated in Figure 3.21 (c).

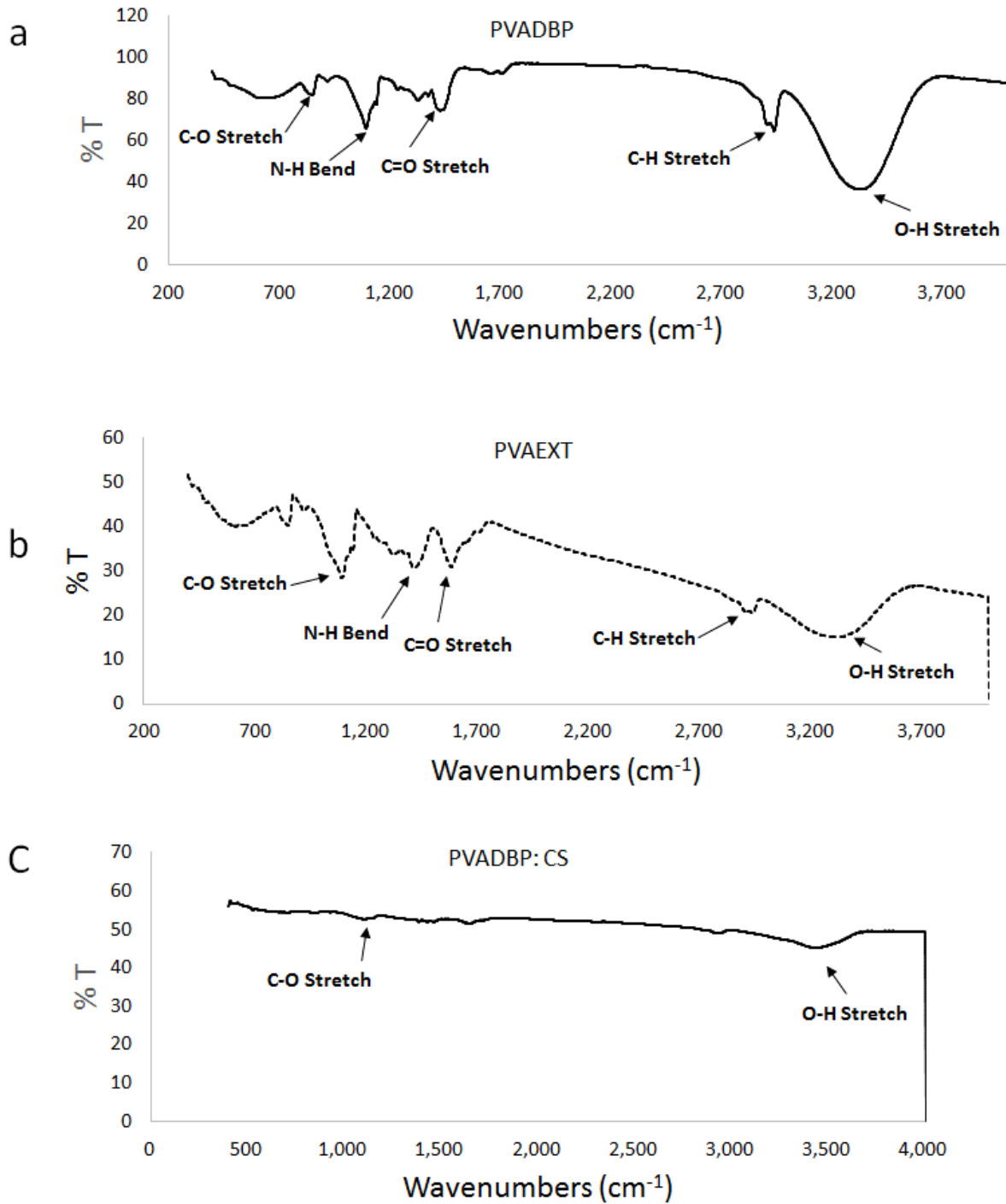


Figure 3.21. FTIR Charts for Crude extract (a) distilled *Bidens pilosa* in PVA nanofibers (PVADBP), (b) crude extract *Bidens pilosa* in PVA nanofibers (PVAEXT) Showing changes that occur in their blends and (c) distilled *Bidens pilosa* in PVA nanofibers and Chitosan.

DISCUSSION

It was observed that significant chemical changes occur to PVA when it was dissolved in either distilled or cold extract of *Bidens pilosa* as shown in Figure 3.21. One such notable observation was changes in OH bonds. OH bonds were very pronounced in the PVA alone, when combined with extract *Bidens pilosa* however, the intensity of OH groups were reduced. On combining with distilled *Bidens pilosa* however, the O-H bonds intensification resurfaced as shown in the comparative chart in Figure 3.19 and Figure 3.21 (a) and (b).

There was a clearly marked chemical difference between the distilled and cold extract of *Bidens pilosa* as shown in Figure 3.20. This meant that distillation had a chemical effect on the composition of the distilled *bidens pilosa*. *Bidens pilosa* extract contains a variety of chemical groups including volatile oils which distillation process destroyed by breaking the bonds and this was proven by presence of an extra peak in the distilled extract that did not exist in the distillate. Another notable observation was chemical interaction between the C-N groups after dissolution and nanofiber synthesis with PVA. While this interaction was limited in the case of distilled *Bidens pilosa*, it was more imminent with the cold extract *Bidens pilosa* pointing again to the effect of distillation on the chemical integrity of the *Bidens pilosa* extract. Addition of chitosan to the PVADBP shown chemical property changes by the notable shifts in OH interactions, CN, NH and C-X groups as shown in Figure 3.21 (c). The normal spectra for chitosan according to literature has got characteristic peaks of OH, CN, and N-H stretches. However after combination with PVADBP these chemical interaction lead to significant changes in these peaks.

The chemical interactions lead to unveiling of new chemical groups which have got enhanced capabilities for applications in various fields.

When PVA was mixed with chitosan there was a shift in peaks especially in the OH stretches region there is also a shift NH region and intensification at the region of O-H bonds and C-O stretches as shown in the Figure 3.19. Intensification of OH C-S and NH stretching were

observed. This means bond breakages exposed these functional groups. Just as the pure extract solutions behave so does the mixture with polyvinyl alcohol for both categories.

Chapter 4

Results and Discussion – Part II

(Antibacterial Tests)

4. Anti-bacterial tests results.

To study anti-bacterial properties of nanofibers generated from PVA, chitosan, distilled and crude extract *Bidens pilosa* composite blends, two species of bacteria, *S. aureus* representing gram positive and *E. coli* top 10 strain representing gram negative were used. The samples tested in this experiment are summarized in table 4.1.

Table 4.1: Materials tested against *E.coli* and *S. aureus*.

Sample	Description
PVA	Control
EXT	Control
DBP	Control
PVADBP	Sample
PVAEXT	Sample
PVA:CS	Sample
PVA : DBP	Sample
PVA: EXT	Sample
PVADBP: CS	Sample
PVAEXT:CS	Sample
PVA: DBP: CS	Sample

Nanofibers developed from the composite samples, control PVA and the raw materials were sterilized and exposed to the bacteria and Bacterial growth curves were obtained by plotting the OD values against the time during which measurements were done.

4.1 Effect of PVA nanofibers on test bacteria

Polyvinyl alcohol although with no known antibacterial effect as a polymer, shown some limited effect against mainly *E. coli* with limited effect on *S. aureus* as shown in Figure 4.1.

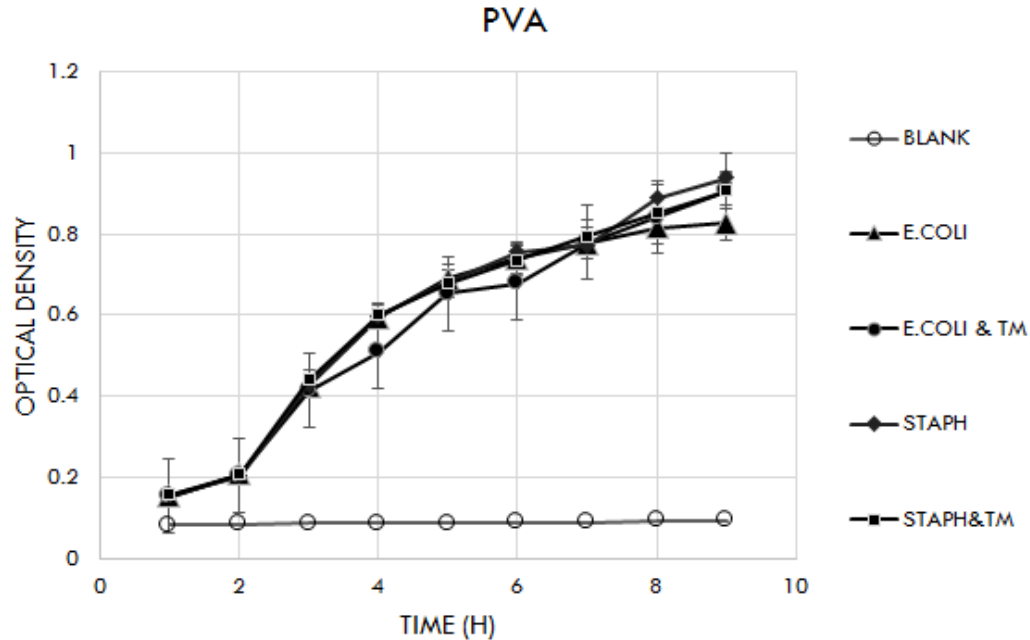


Figure 4.1. Growth curves for *E. coli* and *S. aureus* with PVA nanofibers

The limited effect of PVA nanofibers is attributed to the chemical properties of PVA polymer in that it lacks active surface groups that interacts with the bacteria cells walls thus disrupting the normal physiology of the of the bacteria.

4.2 Effect of Pure extract and Pure distilled *Bidens pilosa* on test bacteria

There was a notable effect of crude extract of *Bidens pilosa* on the two test bacteria although in all cases the growth followed a constant trend with lower intensity in the case with the test material until the fourth hour when it started dropping in the case of extract presence as shown in Figure 4.2 (a). This lowered growth in both test bacteria when exposed to the extract is attributed to the natural chemical compounds contained in the material that interact with the bacteria and thus affecting their growth. Results also indicated that while two bacteria responded in similar pattern, *E. coli* was more sensitive to the presence of extract in the initial stages of culturing.

Pure distilled *Bidens pilosa* shown the weakest effect on the bacterial growth on both *E. coli* and *S. aureus* as shown in Figure 4.2 (b). The slight effect inhibition in bacterial growth was

nearly equal in both types of bacteria investigated. This result could be attributed to the fact that distillation could have destroyed some functional bonds whose integrity was required to effect the interaction between the material and the bacterial cell walls

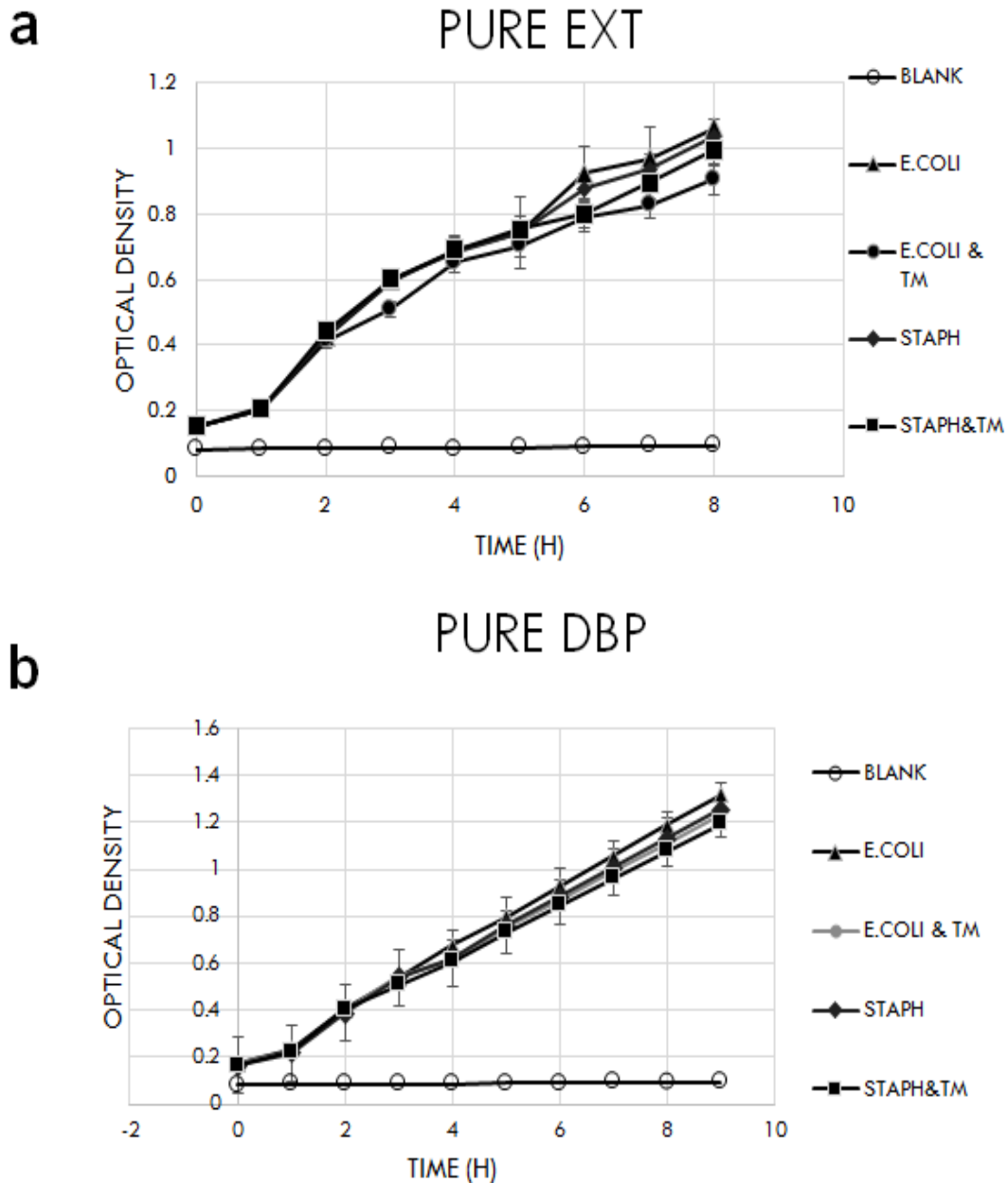


Figure 4.2. Growth curves for *E. coli* and *S. aureus* with (a) pure extract *Bidens pilosa* nanofibers (EXT), and (b) Distilled *Bidens pilosa* nanofibers (DBP).

4.3 Effect of PVADBP and PVAEXT nanofibers on test bacteria.

Distilled *Bidens pilosa* nanofibers obtained by dissolving PVA into the DPB while producing very good fibers did not translate it into the anti-bacterial effects. Results generally show limited inhibition of both *S. aureus* and *E. coli* as shown in Figure 4.3 (b). There was equal response of both *E. coli* and *S. aureus* when exposed to PVADBP nanofibers. While both cases had slightly lower O.D values when exposed to the PVADBP nanofibers, increase in growth with time followed a similar trend. Crude extract nanofibers obtained by dissolving PVA into fresh extract of *Bidens pilosa* shown remarkable effect on the two test bacteria as seen in Figure 4.3 (a).

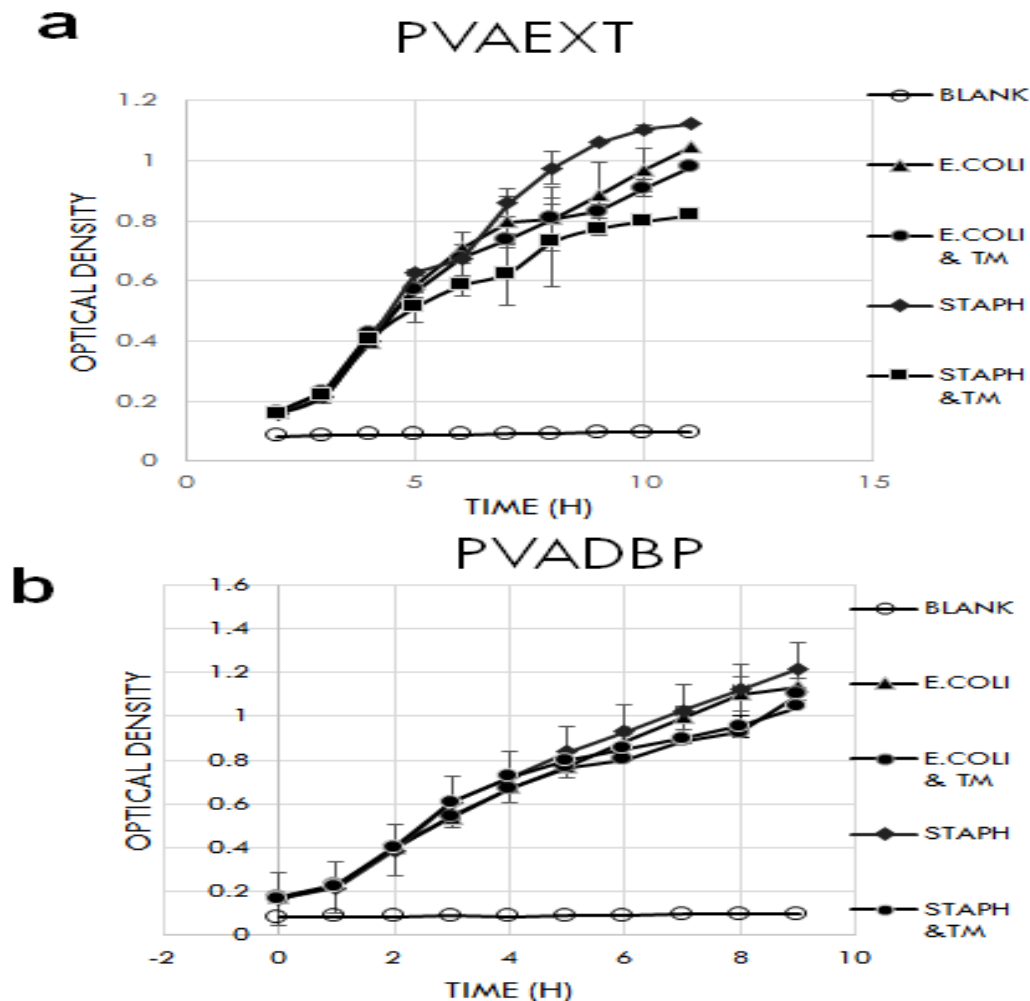


Figure 4.3. Growth curves for *E. coli* and *S. aureus* with (a) PVA dissolved in extract *Bidens pilosa* nanofibers (PVAEXT), and (b) PVA dissolved in distilled *Bidens pilosa* nanofibers (PVADBP).

Although both *E. coli* and *S. aureus* shown remarkable effect when exposed to pure extract Nanofibers, the greatest effect were observed with the staphylococci. This bacteria being gram positive with a thin peptidoglycan could be easily targeted by the active groups in the extract than for the *E. coli* which has got a thick peptidoglycan.

4.4 Effect of PVA: CS and PVA: DBP: CS nanofibers on test bacteria

PVA and Chitosan were combined at an optimum ratio and their nanofibers were the most effective against both test bacteria in this research as shown in Figure 4.4 (a). This enhanced anti-bacterial effect is attributed to the presence of chitosan whose surface groups on interaction with bacteria cell surface the charged groups interfere with the physiology of the bacteria and thus causing their death. The anti-bacterial effect of PVA: CS although strong in both *S. aureus* and *E. coli*, it was more resounding in the former. In both cases, the optical density remained constant just after 5 hrs. A combination involving PVA, chitosan, and distilled *Bidens pilosa* at a ratio provided nanofibers that shown remarkable anti bacterial activity on both *E. coli* and *S. aureus* as shown in Figure 4.4 (b). The effect was lower to that exhibited by the PVADBP:CS. The lowered effect of PVA:DBP:CS was not due to the lowering of the DPB ratio in the mixture but rather largely to the lower ratio of Chitosan in the mixture although DBP its self shown limited inhibition of bacterial growth.

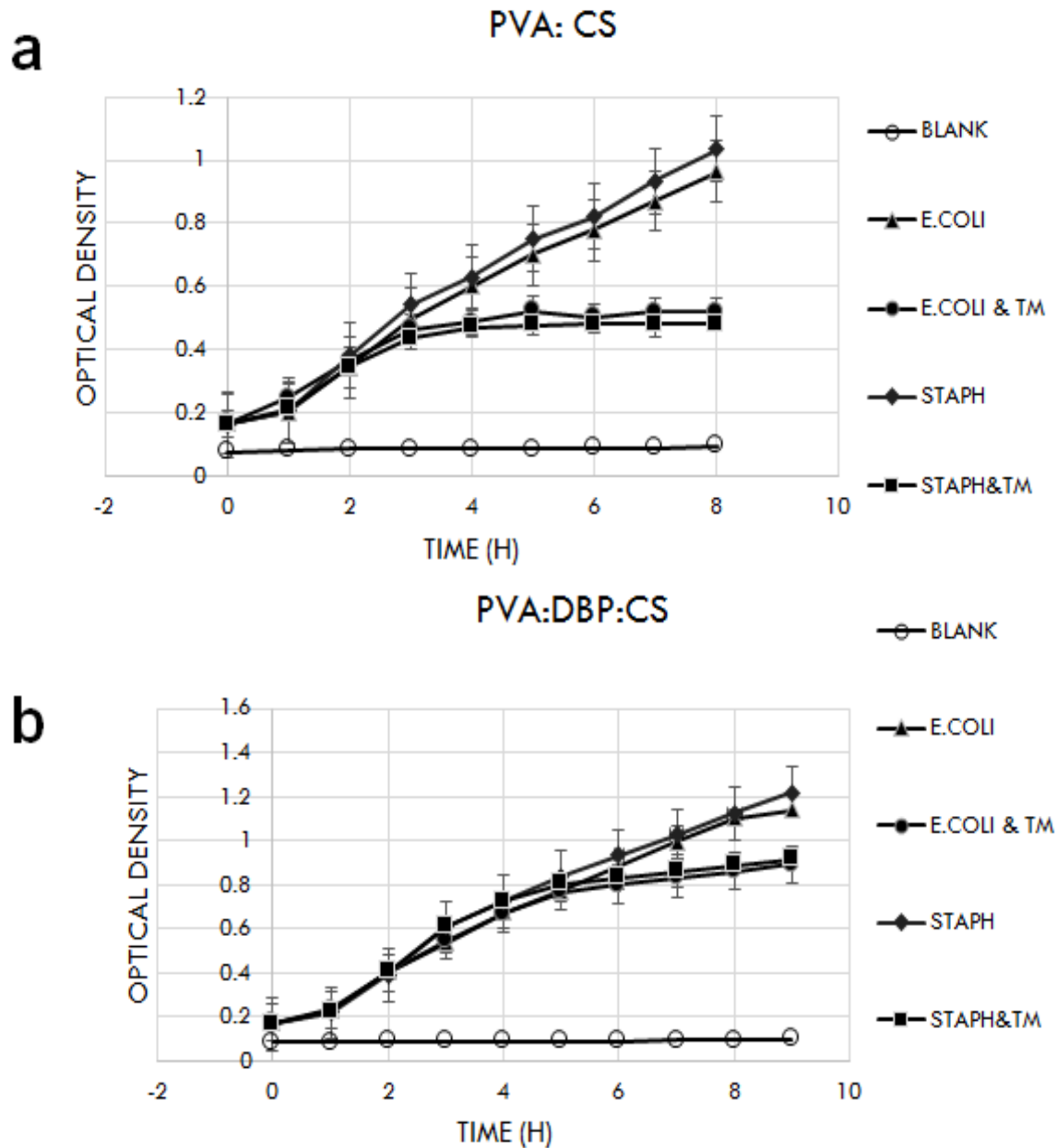


Figure 4.4. Growth curves for *E. coli* and *S. aureus* with (a) PVA and chitosan nanofibers, (b) PVA, Distilled *Bidens pilosa*, and Chitosan

4.5 Effect of PVADBP: CS, and PVAEXT: CS nanofibers on test bacteria

While PVADBP Nanofibers did not show notable effect on the two test bacteria, combination with chitosan produced remarkable effect on both *E. coli* and *S. aureus* as shown in Figure 4.5

(a). The effect was nearly equal in both bacteria although *S. aureus* responded quite strongly of the two. Just like in the case of PVA and chitosan, the drastic shift in the antibacterial properties is attributed by the presence of chitosan.

It was expected that PVAEXT: CS combination would probably be the most effective in antibacterial action against both *E. coli*, and *S. aureus* owing to the strong effect of PVAEXT and PVA: CS. However due poor spinnability of the PVAEXT: CS composite it was difficult to obtain Nanofibers that would have the two materials in combination. The cause of poor fiber formation is explained in Chapter 3, the two polymers were both polyelectrolytes and combining them resulted in increased charges on the surface and increased surface tension with the voltage being too weak to overcome these charges no nanofibers would form. The effect of PVAEXT: CS nanofibers as shown in Figure 4.5 (b).

There was very limited effect of the PVAEXT: CS nanofibers on the two test bacteria. This was probably due to the fact that there were almost no fibers formed in this combination.

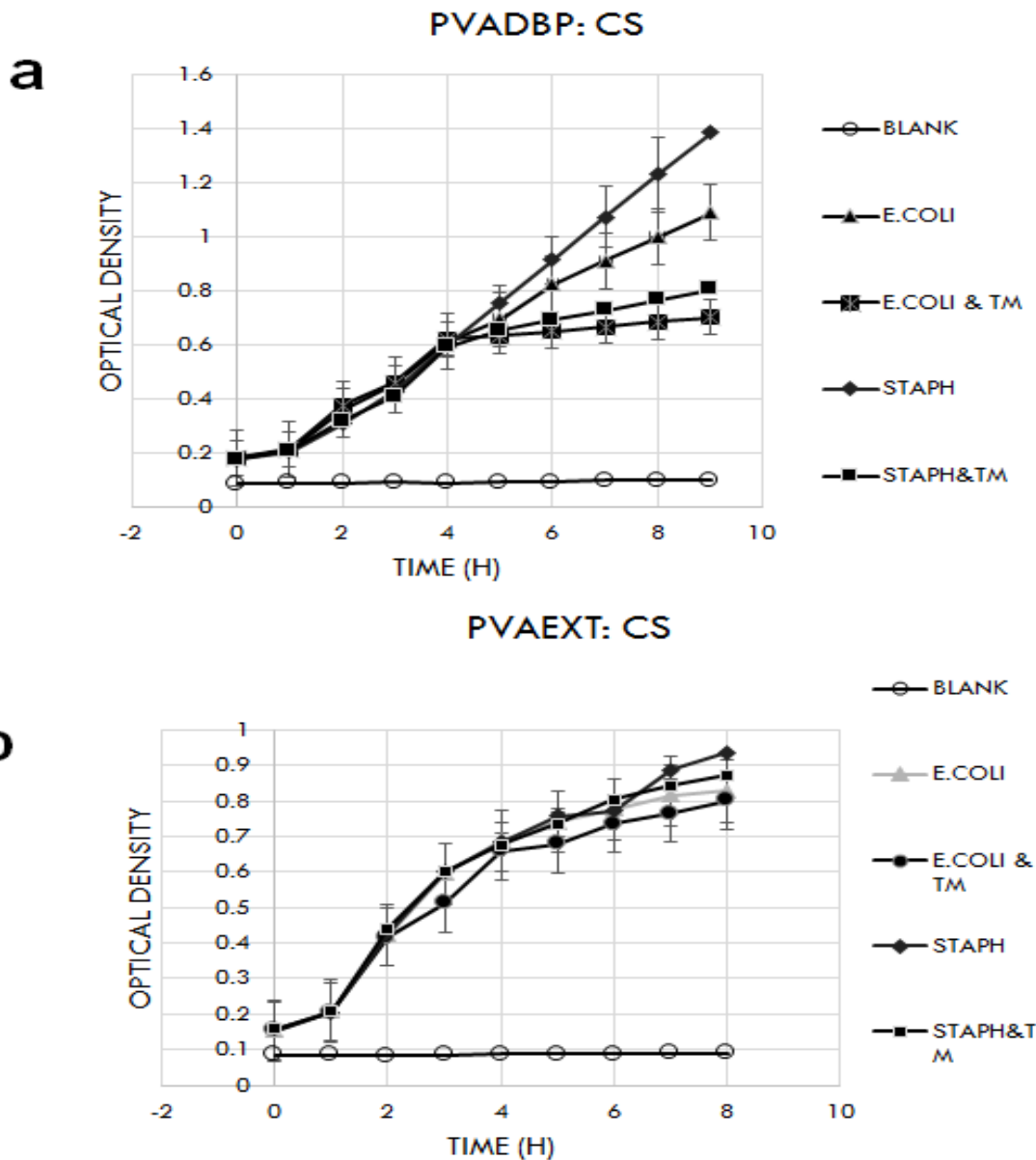


Figure 4.5. Growth curves for *E. coli* and *S. aureus* with (a) PVA dissolved in distilled *Bidens pilosa* and chitosan Nanofibers, and (b) PVA dissolved in crude extract and chitosan nanofibers.

4.6 Discussion

The focus of anti-bacterial research has shifted from traditional anti-biotics into possible plant remedies due to the rampant anti biotic resistance developed by human pathogenic microorganism. This antibiotic resistance develops as a result of excessive use of commercial

synthetic drugs. Alternatives presented in the natural plant extracts have been extensively tested and proven potent in the quest to replace synthetic drugs. To ascertain if a given plant extract contains anti-microbial properties, several invitro screening tests to evaluate them are necessary and this is the first step towards the development of a new eco-friendly and more effective drug against pathogenic microbes. In this research a similar attempt to investigate the effect of *Bidens pilosa* plant extract on two test bacteria *E.coli* and *S. aureus* was made. *Bidens pilosa* is widely known for various medicinal applications including anti septic and ant bacterial roles owing to the rich Chemical composition contained in this plant. Crude extract of *Bidens pilosa* inhibited the two test bacteria by over 40% at 0.2mg/mL while insignificant inhibition was revealed for the case of distilled *Bidens pilosa* at the same concentration. Nanofibers developed from cold extract *Bidens pilosa* exhibited over 50% inhibition of bacterial growth in the case of *E. coli* while revealing over 60% in the case *S. aureus*. The rich chemical compounds found in *Bidens pilosa* include among them quercetin and kaempferol which are known to have anti-bacterial properties. These compounds do this by penetrating the bacterial cell walls and interfering with the physiology of the bacteria. Greater effect against *S. aureus* is due to the fact that gram positive bacteria have a thinner wall which can easily be penetrated by the active compounds. At nanoscale these compounds are made much readily available to interact with bacterial cell wall since there is increased surface area of the material and this exposure of active groups which diffuse through bacterial porins and thus affect enzymes which control bacterial virulence and survival thus resulting in cell lysis. Non pathogenic bacteria which do not have such virulence and survival enzymes are not affected in this mode of action.

Chitosan which shown very high anti-bacterial property derives its properties from the chemical groups contained in the chitosan molecule. Compounds containing chitosan inhibited bacterial growth by over 70% at a concentration of 0.2mg/mL. Chitosan kills bacteria by damaging their cell membranes through the interaction of NH_3^+ with phospholipids and thus creating leakage channels on the cell wall of bacteria which kills the bacteria.

Chapter 5

Conclusion and Future Work

CONCLUSION & FUTURE WORK

Pure chitosan nanofibers could not be electrospun from pure chitosan dissolved in 1% acetic acid. This was due to high viscosity and tension created by the poly cationic nature of chitosan. However on adding polyvinyl alcohol, viscosity and surface tension were lowered and formation of nanofibers was enhanced. This is because chitosan interacted with PVA polymers forming H-bonds and thus reducing the polyelectrolyte effect. A blend of PVA-Chitosan at a higher ratio of PVA, produced nearly defect free mesh of nanofibers with fiber diameters ranging from 30 to 150 nm which can be of great importance in the biomedical industry. Similarly *Bidens pilosa* both cold extract and distilled form could not form nanofibers on their own due to the extreme dilution of these materials coupled with polyelectrolyte nature of their components. However on mixing with PVA polymer, nanofibers were formed with a diameter ranging from 25 to 200 nm. These nanofibers can provide a good medium similar to extracellular matrix for tissue culture. The distilled extract when combined with polyvinyl alcohol provided smooth fibers without any problems. Cold extract *Bidens pilosa* although gave some challenges during electrospinning and dissolution of polyvinyl alcohol, provided the smoothest nanofibers of the two categories. Composite of either crude extract or distilled *Bidens pilosa* on combination with chitosan produced mixed results. While it was easier to form electrospun nanofibers with the PVADBP: CS, it practically difficult to get any substantial fibers with PVAEXT: CS. In the cases where combinations with chitosan yielded fibers, the ratio of Polymer PVA in the mixture played a crucial role. Increasing the ratio of PVA in the mixture reduces the formation of beads and thus produce smooth fibers. Blended solutions were best electrospun within 24 hrs of mixture to achieve smooth fiber formation. PVADBP and PVAEXT nanofibers were easily collected from the aluminum foil unlike blends that contained chitosan and this challenge was overcome by increasing the ratio of PVA ratio in the blend. When these different blends of composites were tested against *E. coli* and *S. aureus*, it was discovered that some combinations (PVA: CS, PVADBP, PVADBP: CS, and PVA: DBP: CS) showed remarkable anti-bacterial properties, whereas (PVA, pure DBP, and PVAEXT: CS) did not have any notable anti-bacterial effect. PVAEXT nanofibers showed moderate anti-bacterial against *S. aureus* and its pure form cold extract shown mild to negligible anti-bacterial effect.

The main goal of this research which was to successfully produce defect free nanofibers from a blend of natural materials which improved anti-bacterial properties was achieved to a certain extent with combinations that involved chitosan. For the nanofibers to be used in biomedical industry, there is need to assess their cytotoxicity and cell regenerative properties. In doing this there will be need for further characterization of these nanofibers to ascertain the porosity properties, and mechanical properties. These nanofibers could also be suitable for drug delivery applications and for that to come to effect, a series of experiments tailored to investigate their drug uptake and release properties need to be carried out.

Future remains to carry out further investigations into how best the blend of PVAEXT BP and chitosan can be combined to produce defect free nanofibers through addition of salts to reduce the over charged surfaces and also employ some surfactants to reduce on the surface tension of the blend. More studies into the quantity of acetic acid needed to facilitate chitosan dissolution and improve its viscosity are needed for the three different molecular weight chitosan.

More work need to be done on understanding the exact mechanism of anti-bacterial properties of chitosan nanofibers and also expand the research into potential application in anti-viral properties against some of the most deadly viruses that are causing anxiety and fear among the scientific community. To harness the benefits of natural biomaterials for biomedical applications, further studies involving a combination of different plant extracts known to possess some medical effect while increasing the ratio of chitosan in the blend and developing defect free nanofibers from this combination would enhance their properties in anti-microbial and enhance cell regeneration.

Chapter 6

References

References

- 1- BBC. Superbugs to kill 'more than cancer by 2050 <http://www.bbc.com/news/health-30416844> (accessed Jan 2016)
- 2- World Health Organization. Plaques. <http://www.who.int/mediacentre/factsheets/fs267/en/> (Accessed July 2015)
- 3-National Geographic. Ebola epidemic: <http://news.nationalgeographic.com/news/2014/10/141025-ebola-epidemic-perspective-history-pandemic/> (Accessed 2015)
- 4- Spellberg, B.; Guidos, R.; Gilbert, D.; Bradley, J.; Boucher, H.W.; Scheld, W.M.; Bartlett, J.G.; Edwards, J. The Epidemic of Antibiotic-Resistant Infections: A Call to Action for the Medical Community from the Infectious Diseases Society of America. *J. Clinical Infectious Diseases* **2008**; *46*, 155–64.
- 5- Woodford, N.; Livermore, D.M. Infections caused by Gram-positive bacteria: a review of the global Challenge. *J. Infection*, **2009**, *59*, 4-16.
- 6- Högberg, L.D.; Cars, A.H.O.; The global need for effective antibiotics: Challenges and recent advances. *J. trends in pharmaceutical sciences*, **2010**, *31*, 509–515.
- 7- Davies, J.; Davies, D. Origins and Evolution of Antibiotic Resistance. *J. American Society for Microbiology*, **2010**, *74*, 417-433.
- 8- Suzanne humphries. Antibiotics, <http://drsuzanne.net/dr-suzanne-humphries-antibiotics-antivirals-antifungals/> (Accessed Jan 2016).
- 9- Kranthi K.; Rao, R. R. D.V.M.V.S.V.; Manasa.; D.; CS, G.S. A Study on Bacterial Pathogens in Wound Infections at Ganni Subba Lakshmi Medical College. *J. Inter Health Sci & Res*, **2013**, 2249-9571.
- 10- Guo, S.; DiPietro, L.A. Factors Affecting Wound Healing. *J. Dent Res*, **2010**, *89*, 219-229.
- 11- James, G.A.; Swogger, E.; Wolcott, R.; Pulcini, E.d.; Secor, P.; Sestrich, J.; Costerton, J.W.; Stewart, P. Biofilms in Chronic wounds. *J. Wound Rep Reg*, **2008**, *16*, 37–44.

- 12- Ayoade, K.O.; Dominguez, A.R. Bacterial Skin Infections. *J. Springer* **2014**, *177*, 1-5
- 13- Steinberg, N.; Kolodkin-Gal, L. The Matrix Reloaded: How Sensing the Extracellular Matrix Synchronizes Bacterial Communities. *J. Bacteriology*, **2015**, *197*, 1-12.
- 14- Valle, J.; Solano, C.; Garcí'a, B.; Toledo-Arana, T.; Lasa, I. Biofilm switch and immune response determinants at early stages of infection. *J. Trends in Microbiology*. **2013**, *21*, 364-371.
- 15- Bouwstra, J.A.; Ponc H.N.M. Structure of the skin barrier and its modulation by vesicular formulations. *J. prog Lipid Res*, **2003**, *42*, 1-36.
- 16- Pharmaceris. Structure of the skin: <http://www.pharmaceris.pl/en/skin-structure/125> (Accessed July 2015).
- 17- Zhong, P.S.; Zhang Y.z.; Lim, C.T.; Tissue scaffolds for skin wound healing and dermal reconstruction. *J. Nanomed & Nanobiotech*, **2010**, *2*, 510-526.
- 18- The British Museum. Lycurgus Cup:
http://www.britishmuseum.org/research/collection_online/collection_object_details.aspx?objectId=61219&partId=1&searCSText=Lycurgus%20Cup (Accessed July 2015)
- 19- Nature nanotechnology | VOL 4 | DECEMBER 2009 |
<http://www.nature.com/nnano/journal/v4/n12/pdf/nnano.2009.356.pdf>
- 20- Hardman, R. A. Toxicological Review of Quantum Dots: Toxicity Depends on PhysicoChemical and Environmental Factors. *J. Environmental Health Perspectives*, **2006**, *114*, 165–172.
- 21-Audy G.; Whitman, Lambert, P.J.; Dyson, O.F.; Akula, S.M.; Applications of Nanotechnology in the Biomedical Sciences: Small Materials, Big Impacts, and Unknown Consequences. *J. Springer sci*, **2008**, 1-14.
- 22- Roco, M. C. Government Nanotechnology Funding: An International Outlook. National Nanotechnology Initiative. Senate of the United States (January 16, 2003). 21st century Nanotechnology Research and Development Act. (**2002**).
(http://www.nano.gov/intpersp_roco.html)

- 23- Glasgow, J. N.; Everts, M.; Curiel, D. T. Transductional Targeting of Adenovirus Vectors for Gene Therapy. *J. Cancer Gene Therapy*, **2006**, *13*, 830–834.
- 24- Langer, R. Drug Delivery and Targeting. *J. Nature*, **1998**, *392*(6679 Suppl), 5–10.
- Lee, J. H.; Kang, M.; Choung, S. J.; Ogino, K.; Miyata, S.; Kim, M. S.; Park, J. Y.; & Kim, J. B. The Preparation of TiO₂ Nm Photocatalyst Film by a Hydrothermal Method and its Sterilization Performance for Giardia Lamblia. *J. Water Research*, **2004**, *38*, 713–719.
- 25- Smith, R. A. J., Porteous, C. M., Gane, A. M., & Murphy, M. P. Delivery of Bioactive Molecules to Mitochondria InVivo. *Proceedings of the National Academy of Sciences of the United States of America*, **2003**, *100*, 5407–5412.
- 26- Perkel, J. M. The Ups and Downs of Nanobiotech. *J. The Scientist*, **2004**, *18*, 14.
- 27- Yamaguchi, Y.; & Igarashi, R. Nanotechnology for Therapy of Type 2 Diabetes. *J. Nippon Rinsho*, **2006**, *64*, 295–300.
- 28- Cao, Y., & Lam, L. Projections for Insulin Treatment for Diabetics. *J. Drugs Today (Barc)*, **2002**, *38*, 419–427.
- 29- Baba, Y. Nanotechnology in Medicine. *J. Nippon Rinsho*, **2006**, *64*, 189–198.
- 30- Weinberg, R. A. How Cancer Arises. *J. Scientific American*, **1996**, *275*, 62–70.
- 31- Jotterand, 2008 F Emerging Conceptual, Ethical and Policy Issues in Bionanotechnology. J springer.
- 32- Kobayashi, T.; Kan, K.; Nishida, K.; Yamato, M.; Okano, T.; Corneal regeneration by transplantation of corneal epithelial cell sheets fabricated with automated cell culture system in rabbit model. *J. Biomaterials*, **2013**, *34*, 9010-7.
- 33- Emerich, D.F.; Thanos, C.G. Nanotechnology and medicine. *Expert Opin Biol Ther.* **2003**, *3*(4), 655-63.
- 33- National Nanotechnology initiative <http://www.nano.gov/nanoteCS-101/special> (Accessed Nov 2015).

34- Andersen, E.S.; Dong, M.; Nielsen, M.M.; Jahn, K.; Subramani, R.; Mamdouh, W.; Golas, M.M.; Sander, B.; Stark, H.; Oliveira, C.L.P.; Pedersen, J.S.; Birkedal, V.; Besenbacher, F.; Gothelf, K.V.; Kjems, J. Self-assembly of a nanoscale DNA box with a controllable lid. *J. nature*, **2009**, 459.

35- Smart Nanobox Built Out of DNA Origami

http://www.medgadget.com/2009/05/smart_nanobox_built_out_of_dna_origami.html

36- Nanotechnology today. <http://www.nano.gov/nanotech-101/special> (Accessed 2015)

38- Kim, J.S.; Kuk, E.; Yu, K.N.; Kim, J.H.; Park, S.J.; Lee, H.J.; Kim, S.H.; Park, Y.K.; Park, Y.H.; Hwang, C.Y.; Kim, Y.K.; Lee, Y.S.; Jeong, D.H.; Cho, M.H. Antimicrobial effects of silver NPs Nano medicine: Nanotechnology. *Biology and Medicine* **2007**, 3, 95–101.

39- Chaloupka, K.; Malam, Y.; Seifalian, A.M. Nanosilver as a new generation of nanoproduct in biomedical applications. *J. Trends in Biotechnology*, **2010**, 28, 580-589.

40- Prabhu, S.; Poulouse, E.K. Silver NPs: mechanism of antimicrobial action, synthesis, medical applications, and Toxicity effects, *International Nano Letters* 2012, 2:32.

41- Kumari, M.; Ferina, P.N.; Amirulhusni, A.N.; Zain, Z.M.; Ping, L.J.; Durairaj, R. Antibiofilm properties of Chemically synthesized silver NPs found against *Pseudomonas aeruginosa*, *J Nanobiotech*, **2014**, 12, 2.

42- Silver Knight, Silver Nano, 2012 available at

<http://www.hirshfields.com/designresource/flooring/silverknight.html>

43- Li, C.; Fu, L.; Yu, C.; Li, Z.; Guan, H.; Hu, D.; Zhao, D.; Lu, L. Silver nanoparticle/Chitosan oligosaccharide/poly(vinyl alcohol) nanofibers as wound dressings. *Inter. J. of Nano medicine*. **2013**, 8, 4131–4145.

44- Vimala¹, K.; Mohan, Y.M.; Varaprasad¹, K.; Redd, N.N.; Ravindra, S.; Naidu³, N.S.; Raju, K.M. Fabrication of Curcumin Encapsulated Chitosan-PVA Silver Nanocomposite Films for Improved Antimicrobial Activity. *J. Biomaterials and Nanobiotech*, **2011**, 2, 55-64.

45- Paladini, F.; Simone, D.S.; Sannino, A.; Pollini, M. Antibacterial and Antifungal Dressings Obtained by Photochemical Deposition of Silver NPs, *J Appl polymer science*, 2013, DOI: 10.1002/app.40326

46- Kim, J.S.; Kuk, E.; Yu, K.N.; Kim, J.H.; Park, S.J.; Lee, H.J.; Kim, S.H.; Park, Y.K.; Park, Y.H.; Hwang, C.Y.; Kim, Y.K.; Lee, Y.S.; Jeong, D.H.; Cho, M.H. Antimicrobial effects of silver NPs Nanomedicine: Nanotechnology. *Biology and Medicine* **2007**, *3*, 95–101.

47- Kumari, M.; Ferina, P.N.; Amirulhusni, A.N.; Zain, Z.M.; Ping, L.J.; Durairaj, R. Antibiofilm properties of Chemically synthesized silver NPs found against *Pseudomonas aeruginosa*, *J Nanobiotech*, **2014**, *12*, 2.

48- Regiel, A.; Irusta, S.; Kyzio, A.; Arruebo, M.; Santamaria, J. Preparation and Characterization of Chitosan–silver nanocomposite films and their antibacterial activity against *Staphylococcus sp*, *J Nano*, **2013**, *24*, 015101 (13pp) doi:10.1088/0957-4484/24/1/015101.

49- Shameli, K.; Ahmad, A.; Zargar, Z.; Yunus, W.; Ibrahim, N.A.; Shabanzadeh, P.; Moghaddam, G.J. Synthesis and Characterization of silver/montmorillonite/Chitosan bionanocomposites by Chemical reduction method and their antibacterial activity. *Inter. J. Nano medicine*. **2011**, *6*, 271–284.

50- Lee, S.J.; Heo, D.N.; Moon, J.H.; Ko, W.K.; Lee, B.K.; Bae, M.S.; Park, S.W.; Kim, J.E.; Lee, D.H.; Kim, E.C.; Lee, C.H.; Kwon, H. Electrospun Chitosan nanofibers with controlled levels of silver NPs. Preparation, Characterization and antibacterial activity. *J. Carbohydrate Polymers* **2014**, *111*, 530–537.

51- Fouda, M.M.G.; El-Aassar, M.R.; Al-Deyab, S.S. Antimicrobial activity of carboxymethyl Chitosan/polyethylene oxide nanofibers embedded silver NPs. *J. Carbohydrate Polymers*. **2013**, *92*, 1012–1017.

52- Zhao, Y.; Zhou, Y.; Wu, X.; Wang, L.; Xua, L.; Wei, S. A facile method for electrospinning of Ag NPs/poly (vinylalcohol)/carboxymethyl-Chitosan nanofibers. *J. Appl Surf Sci*. **2012**, *258*, 8867–8873.

53- Silver Knight. Silver Nano:

<http://www.hirshfields.com/designresource/flooring/silverknight.html> (Accessed Dec 2015)

54- Camargo, P.H.C.; Satyanarayana, K.G.; Wypych, F. Nanocomposites: Synthesis, Structure, Properties and New Application Opportunities. *J. Materials Research*, **2009**, *12*, 1-39.

55- Subbiah, T.; Bhat, G. S.; Tock, R. W.; Parameswaran, S.; Ramkumar, S. S. Electrospinning of nanofibers. *J. Appl Pol Sci*, **2005**, *96*, 557–569.

56- Sill, T. J. Horst, A. R. Electrospinning: Applications in drug delivery and tissue engineering. *J. Biomaterials*, **2008**, *29* 1989–2006.

57- Goldberg, M.; Langer, R.; Jia, X. Nanostructured materials for applications in drug delivery and tissue engineering. *J. Biomaterials Sci*, **2007**, *18*, 241-268.

58- Smith, L.A. Ma, P.X. Nano-fibrous scaffolds for tissue engineering. *J. Colloids and Surfaces*, **2004**, *39*, 125–131.

59- Deepa, B.; Abraham, E.; Cherian, B.M.; Bismarck, A.; Blaker, J.J.; Pothan, L.A.L.; Leao, A.L.; Souza, S.F.; Kottaisamy, M. Structure, morphology and thermal characteristics of banana nanofibers obtained by steam explosion. *J. Bioresource Tech*, **2011**, *102*, 1988–1997.

60- Subbiah, T., Bhat, G. S., Tock, R. W., Parameswaran, S., Ramkumar, S. S. Electrospinning of nanofibers. *J. Appl. Polym. Sci.*, **2005**, *96*, 557-569.

61- Xu, J.; Zhang, J.; Gao, W.; Liang, H.; Wang, H.; Li, J. Preparation of Chitosan/PLA blend micro/nanofibers by electrospinning, *J Materials Letters*, **2009**, *63*, 658–660.

62- Liu, H.; Ding, X.; Zhou, G.; Li, P.; Wei, X.; Fan, Y. Electrospinning of Nanofibers for Tissue Engineering Applications. *J. Nanomaterials*, **2013**, 1-12 available

at <http://dx.doi.org/10.1155/2013/495708>

63- Encyclopædia Britannica. Polyvinyl alcohol (PVA):

<http://www.britannica.com/science/polyvinyl-alcohol> (Accessed Aug 2015)

64- Sparks, R. Electrospinning nano-water Channels for super-absorption composites - <http://blogs.flinders.edu.au/nano-news/2014/09/04/electrospinning-nano-water-Channels-for-super-absorption-composites/#sthash.E2xTv7do.dpuf> (Accessed Dec 2015)

- 65- Santos, C.; Silva, C.J.; Guimarães, R.; Büttel, Z.; Tamagnin, P.; Zille, A. Fabrication and Characterization of PVA, PVA/Chitosan and PVA/cyanobacterial exopolysaccharide nanofibrous composite nanofiltration membranes prepared by Electrospinning. *J American Chemical Society*, **2014**, *245*, 1-2.
- 66- Susana, P.; Castro, M.; Paulín, E.G.L. Is Chitosan a New Panacea? Areas of Application. *J Intek open sci minds*. <http://dx.doi.org/10.5772/51200>
- 67- Raafat, D.; Bargaen, K.; Haas, A.; Sahl, H.G. Insights into the Mode of Action of Chitosan as an Antibacterial Compound. *Appl. Environ. Microbiol*, **2008**, *74*, 3764-3773
- 68- Shelma R.; Paul,w.; Sharma, C.P. Chitin Nanofibre Reinforced Thin Chitosan Films for Wound Healing Application. *J. Trends Biomater. Artif. Organs*. **2008**, *22*, 111-115.
- 69- Nascimento¹, G.G.F.; Locatelli¹, J.; Freitas, P.C.; Silva. G.L. ANTI-BACTERIAL ACTIVITY OF PLANT EXTRACTS AND PHYTOCHEMICALS ON ANTIBIOTIC RESISTANT BACTERIA. *Brazilian J. Microbiology*, **2000**, *31*, 247-256
- 70- Bartolome, A.P.; Villaseñor, I.M.; Yang, W. *Bidens pilosa* L. (Asteraceae): Botanical Properties, Traditional Uses, Photochemistry, and Pharmacology. *J. Evidence-Based Complementary and Alternative Medicine*. **2013**, 1-50, doi.org/10.1155/2013/340215.
- 71- Li, z.; Wang, c. one dimensional nanostructures, electrospinning technique and unique fibers. *J. springer*, **2013** *11*, 141-145.
- 72- Zhang, Li.; Wang, C. One-Dimensional Nanostructures. *J Springer Briefs in Materials*, **2013**, DOI: 10.1007/978-3-642-36427-3_2.
- 73- My scope training for advanced research
<http://www.ammr.org.au/myscope/sem/practice/principles/magnification.php> (Accessed Dec 2015).
- 74- Chemwicks, How an FTIR Spectrometer Operates.
http://Chemwiki.ucdavis.edu/Physical_CSemistry/Spectroscopy/Vibrational_Spectroscopy/Infrared_Spectroscopy/How_an_FTIR_Spectrometer_Operates (Accessed Dec 2015).

- 75- Jessica D.; Schiffman; Schauer, C.L. Cross-Linking Chitosan Nanofibers. *J. Biomacromolecules* **2007**, *8*, 594-601.
- 76- Zahedi, P.; Jafari, S.H.; Karami, Z. Preparation and release properties of electrospun poly (vinyl alcohol)/poly(ϵ -caprolactone) hybrid nanofibers: Optimization of process parameters via D-optimal design method. *J. Macromolecular Research*, **2013**, *21*, 649-659.
- 78- Thermofischer scientific. LB Broth and LB Agar:
<https://www.thermofisher.com/eg/en/home/life-science/cell-culture/microbiological-culture/bacterial-growth-media/lb-broth-and-lb-agar.html> (Accessed Dec 2015)
- 79- Aryal s. bacteriology: <http://www.microbiologyinfo.com/differences-between-gram-positive-and-gram-negative-bacteria/> (Accessed Jan 2016).
- 80- Nitanan, T.; Akkaramongkolporn, P. Effects of Solution Parameters on Morphology and Diameter of Electrospun Polystyrene Nanofibers. *Advanced Materials Research Vols.* **2011**, *194*, 629-632.
- 81- Khan, Z.; Kafiah, F.M. Preparation of Polysulfone Electrospun Nanofibers. King Fahd University
https://www.academia.edu/16840322/Preparation_of_Polysulfone_Electrospun_Nanofibers_Effect_of_Electrospinning_and_Solution_Parameters (Accessed Jan 2016)
- 82- Queen, H. ELECTROSPINNING CHITOSAN-BASED NANOFIBERS FOR BIOMEDICAL APPLICATIONS, Master thesis North Carolina State University 2006.
- 83- Jamnongkan, T.; Shiota, R.; Sukumaran, S.K.; Sugimoto, M.; Koyama, K. Controlling diameter of fibers for antibacterial dressings. 2013 Society of Plastics Engineers (SPE).
- 84- Deitzel, J.M.; Kleinmeyer, J.; Harris, D.; Tan, N.C.B. The effect of processing variables on the morphology of electrospun nanofibers and textiles. *J. Polymer*, **2001**, *142*, 261–272.
- 85- Vitali, L.; Justi, K.C.; Laranjeira, M.C.M.; Fávere, V.T. Impregnation of chelating agent 3,3-bis-N,N bis-(carboxymethyl)aminomethyl-o-cresolsulfonephthalein in biopolymer Chitosan. Adsorption equilibrium of Cu (II) in aqueous medium. *J. Polímeros*, **2006**, *16*, 1678-5169.